STUDIES ON

THERMAL STRUCTURE IN THE SEAS AROUND INDIA

Thesis submitted to the
Cochin University of Science and Technology
For the Degree
of

DOCTOR OF PHILOSOPHY
IN
PHYSICAL OCEANOGRAPHY

UNDER FACULTY OF MARINE SCIENCES

By
P. G. K. MURTHY, M.Sc. (Tech.)

NAVAL PHYSICAL AND OCEANOGRAPHIC LABORATORY
COCHIN - 682004

OCTOBER 1986

CERTIFICATE

This is to certify that this Thesis is an authentic record of research work carried out by Sri. P.G.K. Murthy, M.Sc(Tech.) under my superivision and guidance in Naval Physical and Oceanographic Laboratory, Cochin, for the Ph.D. Degree of the Cochin University of Science and Technology and no part of it has previously formed the basis for the award of any other degree in any other University.

Dr. G. S. SHARMA
(Supervising Teacher)
Professor in Physical Oceanography
School of Marine Sciences
Cochin University of Science and Technology

Cochin 682 016,
October, 1986.

ACKNOWLEDGEMENT

I am highly indebted to Dr G.S.Sharma, Professor in Physical Oceanography, School of Marine Sciences, Cochin University of Science and Technology, for his excellent guidance, critical scientific treatment, and several authoritative discussions during the progress of this work. I am grateful to him, particularly for sacrificing his personal commitments at various phases of the work.

I am grateful to Dr V.K. Aatre, Director, Naval Physical and Oceanographic Laboratory, Cochin for extending the facilities for my work, for his encouragement and constant persuasion during this work, which enabled the completion of my thesis.

I am thankful to Dr R.R.Rao, my colleague, for his lucid and interesting discussions on several occasions and permitting me to use a part of his unpublished work.

The computer programming assistance from my colleagues S/Shri M.X. Joseph and G.R.K.Murty and the help from several colleagues, particularly Dr. Basil Mathew and S/Shri C.K.B.Kurup and M.P. Ajaikumar are appreciated. I acknowledge Shri P. Suseelan for typing the thesis and Shri John P. Varghese for draughting the diagrams.

I express thanks to my wife Smt. P. Sita Devy for her help in data handling and bearing the brunt of domestic management all alone during this work.

CONTENTS

PREFACE

The North Indian Ocean is unique in its land-locked nature and exposure to regular reversing monsoons and associated circulation regimes compared to any other part of the tropical oceans. The thermal variability in the upper layers of the North Indian Ocean is governed by these unique features. In turn, the thermal structure controls the atmospheric and oceanic circulations. Therefore, a sound knowledge of regional nature of seasonal and short-term variability in the thermal conditions can be applied for the monsoon prediction, Ocean Thermal Energy Conversion (OTEC), underwater surveillance, fishery exploration, offshore drilling operations etc. Some studies were made in the recent past to document the scales of this variability. But, these studies mostly suffer from either coarse spatial resolution or inadequate data. Further, greater interest was shown in the western Arabian Sea compared to the eastern Arabian Sea and Bay of Bengal. In addition, the information on the short-term variability in these regions is meagre. Hence, an attempt is made in this study to document the observed variability of thermal structure, both on seasonal and short-term scales, in the eastern Arabian Sea and southwestern Bay of Bengal, from the spatial and time series data sets from a reasonably strong data base.

The thesis consists of six chapters with further subdivisions.

The first chapter is divided into two sections dealing with introduction in section-I and analysis and presentation of material in section-II.

In the second chapter, thermal structures for representative areas are presented and their seasonal variability is analysed in the light of various controlling mechanisms.

The seasonal characteristics of the surface mixed layer are discussed in the third chapter.

The fourth chapter deals with the distribution of thermal anomaly at different depths and its seasonal changes are discussed in relation to the physical and dynamical processes.

The characteristics of internal waves are presented in the fifth chapter, from the time series data sets and their probable generating mechanisms are discussed.

A summary of the results and conclusions of this study constitutes the sixth chapter.

LIST OF FIGURES

CHAPTER I

CHAPTER I

SECTION I

INTRODUCTION

The oceans derive heat energy mainly from the sun, through visible band of the electro-magnetic spectrum. The one-dimensional heat exchange processes at the air-sea interface produce surplus of heat energy in the tropics and a deficit in the extratropics, maintaining a balance around 35°N/S. Such differential energy on the earth is redistributed from the tropics to the extratropics by the oceans and the atmosphere, through current and wind regimes. Although on an annual cycle the land-sea-atmosphere system maintains an equilibrium in temperature, the zonal pattern of mean sea surface temperature (SST) from 60°S-70°N suggest a bell-shaped distribution (Pickard and Emery , 1982).

1.1.2 Thermal structure in the sea.

The net heat energy at the air-sea boundary propagates into the subsurface layer of the sea with exponential decay and its absorption within this layer creates a negative temperature gradient with depth. However, the winds, waves and currents cause mixing in the top layer through turbulent and convective processes. This layer, with a nearly homogeneous temperature is normally termed as 'mixed layer'. The warm waters in the mixed layer is connected to the cold

waters below by a transition region of sharp decrease in temperature, commonly known as 'thermocline'.

The characteristics of the thermal structure in the upper layers of the sea, such as the Sea Surface Temperature (SST), temperature and depth of the mixed layer and the thickness and strength of the thermocline exhibit three dimensional variability in space and time domains. In the tropics and middle latitudes, the top of the thermocline extends into the lower portion of the mixed layer during some part of the year. Beneath the thermocline, the temperatures are low with weak vertical thermal gradients, usually unaffected by seasonal changes.

The variability of thermal structure in the time domain at a region in the sea constitutes long-term, seasonal and short-term variations with time scales varying from a few years to a few seconds. Normally, the short-term variability of the temperature superimposes over the seasonal and long-term signals. The temporal effects of these components extend to considerable depths in the sea. Long-term variability of the temperature is not contemplated in this investigation.

1.1.3 Seasonal variability of thermal structure

Seasonal variation of the thermal conditions in the sea, having time scales of 2-3 months, is governed by a variety of physical and dynamical processes. Some of them, along with their effects on thermal conditions, are outlined below.

During summer, the surplus heat energy at the sea surface warms up the surface layer and reduces the thickness of the mixed layer. On the other hand, the heat loss from the sea surface during winter decreases the temperature of the surface layer and through buoyant motions produces a deep mixed layer.

The monsoons and associated reversals in circulation have significant impact on the thermal conditions in the North Indian Ocean. The extensive cloud cover during the southwest monsoon and net heat loss at the sea surface create a prominent cooling in the surface layer. The turbulent motions associated with strong winds, swift currents, large surface waves and heat losses at the sea surface deepen the mixed layer substantially. The water column in the upper 150-300 m is influenced by the monsoon (Duing, 1970). Below the mixed layer, the temperature shows a rise upto 200 m depth during the active period of southwest monsoon. (Ramam et al., 1979 and subsequent works). Besides, the Ekman transport produced by the strong winds creates intense upwelling and sinking regions, during southwest monsoon, along the coastal belts. Upwelling and sinking zones can also be produced by baroclinic currents depending on the direction of transports. Upwelling/divergence reduces the temperatures at the affected depths, shoals the mixed layer and causes an uplift of isotherms in thermocline, while the opposite conditions prevail during sinking/convergence Meso-scale currents also modify the temperatures depening on whether they flow from hot or cold regions. The local temperatures in the sea are also modulated by the flow of characteristic water masses.

The propagation of Rossby/Kelvin waves modify the thermocline characteristics, particularly in the equatorial areas.

1.1.4 Short-term variability of thermal structure

Short-term temperature variability in the upper layers of the sea is characterized by time scales from a few seconds to a few days and governed by several mechanisms. The net heat energy fluxes at the sea surface on a diurnal scale influence the thermal conditions in the sea. Internal gravity waves are waves found in the interior of the oceans. They induce prominent rhythmic oscillations in the thermal structure at the subsurface levels, with periods varying from a few minutes to a few days. The heat and salt exchanges at the boundary between warm, more saline water overlying cold, less saline water change the temperature and salinity of these layers through double diffusion, on time scales of a few days. The meteorological disturbances, like depressions and cyclones produce low temperatures in the upper layers of the sea at the eye of the storm, strong lateral temperature gradients, and deeper mixed layers. After the passage of the disturbance, the waters revert to pre-storm conditions within 2-3 weeks (Rao etal., 1983; Murty et al., 1983; Ramesh Babu and Sastry, 1984). Occasionally, frontal zones are associated with large fluctuation in lateral temperature gradients over time scales of a few days. Although, all these processes control short-term temperature variability, the present study is confined to the influence of the internal gravity waves on it.

The ocean medium contains stratified waters in the thermocline region with density discontinuity surface generally coinciding with the top of the thermocline. When the stratified waters get disturbed, they tend to revert to the predisturbed state through sinusoidal oscillations, known as internal (gravity) waves. The disturbing forces comprise (i) external forces like tidal forces, sudden changes of atmospheric pressure, wind stress and swells, (ii) internal forces such as shears developed in the heterogeneous current structure, or across the interface of two water masses (Perry and Schimke, 1965), and (iii) shears in the flow pattern over an irregular bottom topography (Defant, 1961). Besides them, minor mechanisms like the collapse of a submarine wake in the stratified medium, motion of a ship through a thin layer of fresh water capping the sea water, and wave to wave interaction of long-period (period $>$ 12 hours) internal waves trigger short-period (period $<$ 12 hours) internal waves (Roberts (1975). In the actual environment, many of these mechanisms simultaneously or individually generate the internal waves (Roberts, 1975).

The internal wave field is generally bounded by the inertial freqency ($\frac{\text{Sin } \phi}{12}$, where ϕ represents the latitude of the place) as the lower limit, and Brunt-Vaisala Frequency as the upper limit. The amplitude of the internal waves at any depth is governed by the energy received from the generating mechanism and the density gradient at that depth. Near coasts, they move shoreward, but their directions vary in the open ocean. The internal waves have a wide spectrum of

characteristics. Their periods range from a few minutes to a few days and amplitudes from a couple of metres to about 100 m, velocities upto 3.0 m/s and wavelengths from a few hundreds of metres to a few hundreds of kilometers (Roberts, 1975). These waves break in the thermocline region after becoming unstable, producing step structures in the thermal profile (Woods and Wiley, 1972; Federov, 1978).

A variety of techniques to measure internal wave parameters are adopted, considering time variations of the conservative properties on synoptic scales. At a stationary position in the field, the operations of bathythermograph, Salinity-Temperature-Depth (STD) recorder is repeated at close time intervals to monitor internal waves. Various sensors fixed at different levels to a FLIP (Floating Instrument Platform) measure the time history of ocean parameters to derive the internal wave field. A neutrally buoyant float, designed to float at a specified density level, a thermistor chain or an array of current meters attached to a moored buoy, measure the internal waves. Radars, aircrafts and satellites (John et al., 1975) are employed to follow the positions of slicks at the sea surface to obtain the internal wave parameters (except 'amplitudes') . The sonar can also be used to map the internal waves upto a depth of 1200 m (Robert , 1981).

1.1.5 Importance of thermal structure

A knowledge of the ocean thermal structure has direct bearing on the following fields.

The North Indian Ocean feeds heat and moisture to the overlying atmosphere for the development of monsoons. The response of the Indian seas to the monsoonal forcing is already described. Thus, in these interwoven processes, the SST along with subsurface temperature conditions indicate the intensity of their interaction. Hence, for a proper understanding of this air-sea coupling, a comprehensive knowledge of the thermal structure in the upper layers of the Arabian Sea and Bay of Bengal is essential. Such a knowledge eventually leads to improved prediction of the monsoon system. Besides, the information on the heat fluxes across the sea surface and the heat content in the mixed layer improve the weather forecast. Further, the mixed layer determines the characteristics of the sound duct, a layer in which the underwater objects can be detected from farther distances. It also governs the catch and mobility of fish. The thermal conditions in the deep water influence the characteristics of deep sound channel, used for long-range underwater communication.

A precise knowledge on the short-term variations of temperature at the subsurface levels is useful in a wide range of applications like Ocean Thermal Energy Conversion (OTEC), underwater surveillance, catch potential of certain type (herring) of fish (Levastu and Hela, 1970), offshore drilling operations, sediment transport (La Fond, 1961) and disposal of pollutants.

1.1.6 Typical thermal features of the North Indian Ocean

The thermal structure in the North Indian Ocean shows typical deviations in certain respects compared to other tropical oceans. The ocean, bounded by the Asian continent on the three sides reflects the effect of continentality on the thermal conditions of the upper layer. The annual cycle of SST over large parts of the ocean shows a strong bimodal signal. Large meridional and zonal temperature gradients exist at the surface and subsurface levels. The monsoons and depressions are typical meteorological features over the North Indian Ocean, to which, the oceanic thermal structure reacts sharply. The heat losses at the sea surface, entrainment, and upwelling produce mid-summer cooling - a typical feature in the Arabian Sea and Bay of Bengal - during southwest monsoon and each one of these mechanisms dominates differently in different regions. The winter cooling in the northern regions and the progressive warming of the waters during monsoon transition periods reflect the corresponding changes in the subsurface thermal conditions. The circulation regimes associated with currents and winds produce strong upwelling in the coastal waters and simultaneous offshore downwelling during summer and vice versa during winter.

The equatorial Indian Ocean is characterized by the propagation of Rossby waves of periods 1-3 months and Kelvin waves of about 6 months (McPhaden, 1982a; Luyten and Roemmich, 1982), which affect the thermocline structure.

1.1.7 Literature survey

Although innumerable studies are carried out on the thermal structure in the world oceans, in view of the space and scope of the present investigation, the literature survey is confined only to the area covered in the present investigation. The mean monthly thermal conditions, along with surface winds and currents for this area are illustrated in several atlases. The early atlases were published by the Scripps Institution of Oceanography (Anon. 1944), on the SSTs of the world oceans by the US Navy Hydrographic Office (Anon. 1950), on the surface currents and mean monthly SSTs in the Indian Ocean, and by the Koninklijk Nederlands Meteorologisch Instituut (Anon. 1952) presenting meteorological and oceanographic properties. Subsequent atlases by Wooster et al. (1967) for the Arabian Sea, Wyrtki (1971), and Hasternath and Lamb (1979) for the Indian Ocean, and Robinson et al. (1979) for the North Atlantic and Indian Oceans present the detailed distribution of oceanographic parameters, winds and currents, together with the distribution of derived parameters. The Russian atlas (Anon. 1978) gives a detailed distribution of oceanographic and meteorological parameters for the Atlantic and Indian Oceans.

Galle (1924) presents the currents and mean temperatures in two degree quadrangles for the entire Indian Ocean. La Fond (1954b) gives a detailed account on the environmental factors governing the thermal structure in the sea. Working out the mean monthly temperatures off Bombay and Saurashtra, Jayaraman and Gogate (1957) suggest a fall of SST towards north. From a similar study, Ramasastry and

Myrland (1959) indicate a bimodal oscillation for the annual cycle of SST along the southwest coast of India. Noble (1968) supports the bimodal signal along north Canara coast with primary and secondary maxima in May and November, and corresponding minima in August and January respectively. Subsequent works (Sharma, 1968 ; Lonkar, 1971; Colborn, 1975; Anjneyulu, 1980; Narayana Pillai et al., 1980) confirm the occurrence of this feature with a lag of one month in different regions in the Arabian Sea and Bay of Bengal. Patil and Ranamirtham (1962) infer a change of 0.5°C in SST in winter, around Laccadive Islands. Panikkar and Jayaraman (1966) review the contrastive hydrographic features of the Arabian Sea and Bay of Bengal. Sastry and D'Souza (1970) report increasing SSTs from west to east and strong temperature gradients at a depth of 100 m due to the presence of warm and cold eddies during summer monsoon in the Arabian Sea. Rao et al. (1974) describe the effect of winter cooling and seasonal heating on the thermal conditions off Karwar and Vengurla. Colborn (1975) classifies the Indian Ocean into different areas and documents the response of thermal structure in the upper 500 m in relation to seasonal climatic changes and dynamical processes. Ramesh Babu et al. (1976) attribute the drop of 1-2°C in SST off Saurashtra during southwest monsoon to the strong winds. Further works by Ramam et al.(1979) and Anjaneyulu (1980) share the same view. Duing and Leetma (1980) examine this cooling in relation to heat fluxes, advection across the equator and upwelling over the Arabian Sea and conclude that it is mainly due to upwelling. Rao et al. (1981, 1983) and Rao (1986) investigate the surface layer cooling in seas around India from the Monsoon Experiment data sets and attribute it to heat losses from the sea and upwelling, while

Ramesh Babu and Sastry (1984) suggest this cooling to be due to entrainment also. Reveiwing the SST pattern for some regions in the Arabian Sea, Sastry and Ramesh Babu (1985) attribute the initial fall of SST in June to the heat losses from the sea and further cooling to entrainment. Joseph and Pillai (1986) observe the surface cooling over the Arabian Sea and Bay of Bengal and suggest the SST anomaly as an indicator of the strength of the monsoon.

Ramesh Babu et al. (1980) and Varma et al. (1980) report a southward fall of SST in the northeastern Arabian Sea during February to April, owing to seasonal heating. Narayana Pillai et al. (1980) notice three maxima (in March, June and October) and two minima (in Septmber and December/January) for the SST annual cycle off Ratnagiri and report 10°C as the annual range of SST off Karwar. Basil Mathew (1982) indicates a similar annual range off Cochin. Qasim (1982) reports slightly lower SST range of 6°C north of Goa with a maximum seasonal change of 12°C due to monsoonal cooling and upwelling, during the southwest monsoon. McPhaden (1982b) explains the seasonal variability of the thermal conditions in the upper 200 m at Gana Island,based on heat energy exchanges.

The investigations on the thermal conditions in the Bay of Bengal started earlier compared to those in the Arabian Sea. Sewell (1929) reports two maxima in November and February, and a minimum in December/January for the annual cycle of SST in the Bay of Bengal. In the subsequent works (Chacko, 1956 ; Rao and Rao, 1962; Ramasastry, 1963 ; Anjaneyulu, 1980), two maxima and two minima are reported to occur about May and September/October, and July/August and December/

January respectively. Ganapati and Murty (1954) observe warmer waters in February and March and cooler waters in October and December off Waltair and explain their occurrence in relation to heat exchanges and circulation. Chacko (1956) indicates an annual range of 4 - 5°C for SST off Madras. La Fond (1958), and Rao and Rao (1962) also find similar ranges, fluctuating by about 1°C from this range, at a few places in the western Bay. Ramamsastry (1963) documents the seasonal variability of the thermal conditions along the east coast of India, in relation to circulation pattern. Rao and Jayaraman (1968a) indicate SST variation of 1°C in the southern and central Bay waters from February to March, increasing southward. Anjaneyulu (1980) and Joseph and Pillai (1986) report the lowest SST values during the southwest monsoon in the Bay of Bengal and Arabian Sea due to large amounts of heat loss from the sea and upwelling, and correlate the intensity of the monsoon to the SST anomalies. Basil Mathew (1982) notices annual ranges of SST, of 4°C off Waltair, and 3°C off Madras.

La Fond and Purnachandra Rao (1954) considers mixed layer depth (MLD) as the depth to the top of the main seasonal thermocline, which can be followed from day-to-day. Defant (1961) limits the mixed layer to a depth of 1°C fall from SST, and this was adopted in several investigations (Sastry and D'Souza, 1970; Rao et al., 1976; Qasim, 1982; Varma et al., 1980) in the Arabian Sea and Bay of Bengal. Wyrtki (1971) restricts it to a depth, at which the vertical line from SST intersects the line joining the shallowest layer of 5 m thickness with a temperature change of 0.5°C. Colborn (1975) concludes that the criteria suggested by Defant and Wyrtki closely agree for the data sets in

the Indian Ocean. In some of the works (Sharma, 1968; Ramesh Babu et al., 1976, Robinson et al., 1979), the top of the thermocline, based on slightly different criteria, is mapped over the Indian Ocean.

Although several investigations contain qualitative statements on surface mixed layer, very few works concentrate on its variability in a comprehensive manner.

Patil and Ramamirtham (1962) indicate a mixed layer depth (MLD) of 65-80 m during December around Laccadive Islands. Patil et al. (1964) mention low (20-30 m) MLDs off Veraval during January to May. Reviewing the contrastive hydrographic features over the Arabian Sea and Bay of Bengal, Panikkar and Jayaraman (1966) relate higher range of MLD in the Arabian Sea to upwelling. Considering the top of the thermocline as indicator of upwelling, Sharma (1966) links its seasonal march between Cape Comorin and Mangalore to upwelling and sinking. Sharma (1968) discusses the seasonal variations of thermal structure in the coastal waters between Kolachel and Mangalore in relation to coastal dynamical processes. Rao and Jayaraman (1968b) report east-west changes of mixed layer in the North Equatorial Indian Ocean. Sastry and D'Souza (1970) attribute the spatial variability of mixed layer in the eastern region and central regions of the Arabian Sea during southwest monsoon to the circulation. Ramesh Babu et al. (1976) attribute deepening (15-40 m) of top of thermocline north of Bombay during May-July to strong monsoon winds. Rao et al. (1976) report the same feature in the Arabian Sea east of 60°E for the area between 10-15°N. Further works also observe a cooling (by about

2°C) of the mixed layer in the Arabian Sea and Bay of Bengal during the southwest monsoon, and relate it to various mechanisms like prevailing meteorological conditions (Ramam et al., 1979 ; Anjaneyulu, 1980 ; Joseph and Pillai, 1986), heat losses from the sea and current shear (Rao et al., 1981, 1983; Ramesh Babu and Sastry, 1984) and entrainment(Sastry and Ramesh Babu, 1985).

Ramesh Babu et al. (1980) report a progressive fall in the mixed layer thickness of the northeastern Arabian Sea, during March. In the northern Arabian Sea, during January to May, Varma et al. (1980) propose winter cooling for deepening of the mixed layer, and eddy flows along 64°E for its southward shoaling. Narayana Pillai et al. (1980) attribute the large variability of the top of thermocline between Tuticorin and Ratnagiri to the seasonal changes and coastal processes. Qasim (1982) reports that north of Goa, the Arabian Sea, in general, exhibits large mixed layer in deep waters compared to shallow waters. Basil Mathew (1982) explains the seasonal variability of the mixed layer along west and east coasts of India in relation to upwelling and sinking.

Rao and Jayaraman (1968a) report deep mixed layer in the western and central Bay of Bengal during February to March. Basil Mathew (1982) relates the seasonal march of mixed layer off Waltair and Madras to upwelling and sinking. Rao et al. (1983) attribute the deepening of mixed layer during southwest monsoon at some positions in the Bay of Bengal to the heat transport from the sea.

Fridtjof Nansen was the first to observe the internal waves, when his ship 'Fram' got stuck up by the 'dead water phenomenon', which Ekman (1904) explained to be due to the action of internal waves against ship's motion. Very few investigations are available on the short-term variability in the Arabian Sea and Bay of Bengal. A beginning of such studies was made in the Bay of Bengal in mid-fifties, but subsequently it progressed very little due to lack of time series data. However, with the advent of MONEX program, the activity in this field is revived.

Rao and Jayaraman (1968b) refer the wavy pattern of the thermal structure in the North Equatorial Indian Ocean during February to March, to the internal waves and speculate standing internal waves (along 76° 20'E). Ramesh Babu et al. (1976) interpret the layer of weak temperature gradient in the thermocline off Saurashtra coast during southwest monsoon to be due to internal wave breaking. Ramam et al. (1979) identify internal tides off Mahe during May and July and document the internal wave characteristics.

La Fond and Poornachandra Rao (1954) reveal the internal tides off the central east coast of India and account for a phase lag of 4-5 hours between internal waves and tides. Perry and Schimke (1965) reveal short-period internal waves with large amplitudes off Saurashtra, and relate them to the shear developed between two contrastrive watermasses. La Fond and La Fond (1968) report internal tides off Andhra coast and short-period internal waves off Calcutta and

Thailand, and analyse their characteristics. Rao and Jayaraman (1968a) interpret the wavy nature of the thermal structure during February to March in the southern and central Bay of Bengal to the internal waves. Rao et al. (1983) attribute the oscillatory nature of thermal fields during southwest monsoon period in the central Bay to internal waves. From a 13 hour record of temperature, salinity, and current in the western Bay of Bengal, Antony et al. (1985) document short-period internal waves and link them to interaction of tidal current against a submarine obstacale. Briscoe (1975a) and Levine (1983) provide excellent reviews on the wide spectrum of global investigations on the internal waves. It may be appropriate to quote the words of Walter Munk (1981). ' Forty years ago, internal waves played the role of an attractive nuisance : attractive for their analytical elegance and their accessibility to a variety of experimental methods, a nuisance for their interference with what was then considered the principal task of physical oceanography, namely, charting the "mean" density field. Twenty years from now I expect that internal waves will be recognised as being intimately involved with the vertical fluxes of heat, salt, and momentum, and so to provide a vital link in the understanding of the mean fields of mass and motion in the oceans.'

Many of the past investigations on the temperature variation in the Indian seas were made from the synoptic data sets confining to a few cruise tracks over a limited area. Hence, regional features from these studies seldom represent the gross features of the Arabian Sea/Bay of Bengal. Besides, they might have been vitiated by the internal waves. Nevertheless, some studies attempted to document the regional behaviour of thermal variability on seasonal scales,

suffered from coarse spatial resolution and insufficient data density. Further, the knowledge on the short-term temperature variations in these regions is scanty. Hence, an attempt is made in this investigation to study the seasonal and short-term variations of thermal structure in the upper layer of the seas around India,from a reasonably strong data base.

SECTION II

MATERIAL AND METHODS

1.2.1 Material

(a) Seasonal variability :- The Arabian Sea and Bay of Bengal cover a huge area of 78,48,000 km^2 and 22,00,000 km^2 respectively. Considering the scope of the study, the area was restricted to 5-24°N, 65-90°E. The MBT data collected for several years over this area were compiled from the following sources.

(i) National Oceanographic Data Centre (NODC), Washington
(ii) Andhra University field programs, Waltair
(iii) Pelagic fishery survey programs, Cochin
(iv) Darshak Expedition (1973-74)
(v) Monsoon Experiments (MONEX)
(vi) Indo-Polish Expedition (1977)

The temperature values, extracted at depth interval of 5 m, are grouped monthwise in each two degree quadrangle. These temperatures are screened through a test before analysis. For a minimum of five BT profiles in a month, the mean temperature (T) and standard deviation (σ) were computed for each depth, and the temperatures falling outside ($T \pm 2\sigma$) limits are rejected. For the months with less than five BT profiles, simple averaging is done. The distribution of such accepted BT data for the area under investigation is presented in Fig.1. The areas 5 - 10°N and 65-70°E in the Arabian Sea, and 10-22°N and 80-90°E in the Bay of Bengal are not covered in this study, due to wide gaps in data. Since the individual BT profiles in a month may terminate at different depths, the mean BT profile is expected to contain artificial positive and negative temperature gradients at these depths. In such cases, the mean of the temperature gradients in the 10 m water columns above and below such depths is assumed to represent the actual average condition.

(b) Internal waves :- The studies on internal waves are based on time-series measurements of MBT profiles at five stationary positions in the Arabian Sea and Bay of Bengal (Fig.1). MBT operations were carried out as a part of the field programme/expeditions and the details of their coverage are given in Table 1.

The sampling interval of $\geq$ 10 minutes enabled BT operations upto 270 m. The surface marine meteorological data were recorded at the sampling intervals, for the stations T3-T5. The salinity data

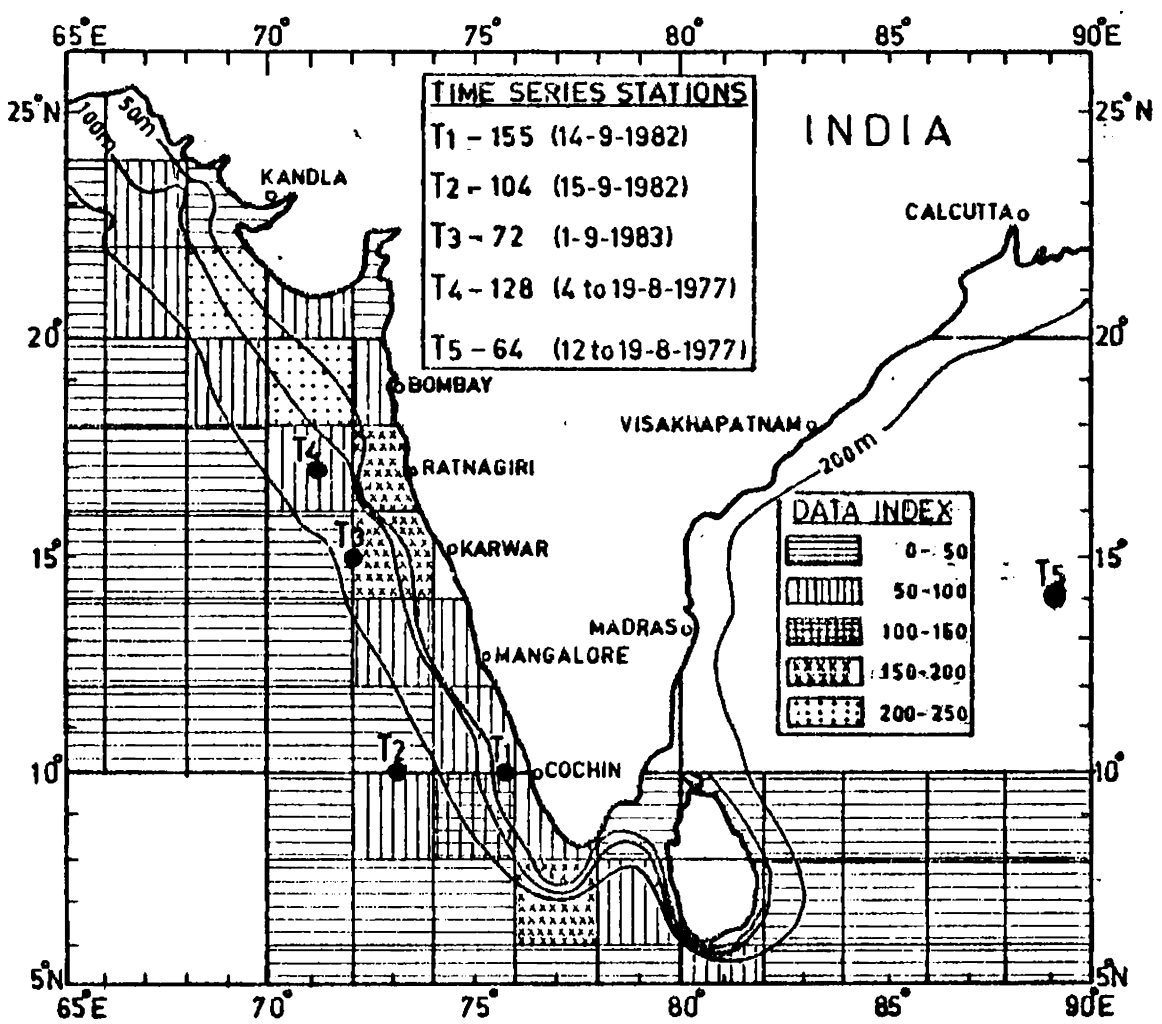

FIG.1 COVERAGE OF THE DATA

Figures in the legends represent the number of BT operations

TABLE 1

Station	Station position with date	Bottom Depth (m)	Ship	Programme	Sampling interval (minutes)	Duration	Nature of Analysis
T_1	10°N,75°50'E 14 Sep 82	61	MT Prashikshani	NPOL field experiment	5	1/2 day	Short-period internal waves
T_2	10°N,73°E 15 Sep 82	2000	"	"	5	1/2 day	
T_3	15°N,72°E 01 Sep 83	2000	ORV Sagarkanya	First Indian cruise of DOD	10	1/2 day	
T_4	17°N,71°E 04-19 Aug 77	2500	INS Betwa	Monsoon-77	180	16 days	Long-period internal waves
T_5	14°N,89°E 12-19 Aug 77	3000	INS Beas	Monsoon-77	180	8 days	

were also collected at synoptic hours at these stations. The ship was anchored at station T1, while it maintained position, with occasional manoeuvres, at other stations. The ship's drift during the operations was within 15 km. All the ships were provided with satellite navigation systems for position fixing.

1.2.2 Analysis and presentation

(a) Seasonal thermal structure :- The annual time-depth temperature structures are prepared in each two degree grid having a minimum coverage of eight months. About 50 such structures were prepared for the analysis. But, only a few sections (13 Nos) , representative of the area under study are presented in Figs. 2.1 to 2.6. Nevertheless, the remaining sections are made use of to interpret the results. The temperature-depth fields for the shelf waters are depicted separately to bring out the inshore features clearly. The temperature contours at interval of 1°C are computer plotted and smoothened manually. A two dimensional interpolation is made for months for which data are not available, when the time gap is within two months, and the contouring is done using a dotted line.

b) Mixed layer :- In order to study the regional and seasonal features of the mixed layer, it is to be delineated from the bathythermgrams. The literature suggests a variety of criteria for this purpose (1.1.7). In this analysis, the MLD is demarkated is the depth, where the temperature drops by 1°C from SST. The monthly MLD topography maps, prepared based on the mean monthly temperature profiles for the area under study, are given in Figs.3.1 to 3.6 with isobaths drawn at 10 m interval.

(c) Thermal anomalies :- It is attempted to couple the annual variation of temperature at various depths in the area under study to the seasonal climatic changes and circulation regimes. For this purpose, the mean monthly temperature anomaly for a given depth is evaluated as the difference between monthly and annual mean temperatures. The computations are done only for areas having a minimum coverage of 8 months. The computation of thermal anomalies is restricted to 0, 50 and 100 m depths, because greater depths showed a coverage of less than eight months in several two degree quadrangles. The anomaly maps, which are drawn at a contour interval of 1°C are shown in Figs. 4.1 to 4.3. This method directly gives the annual ranges of the temperature at a depth, for the area under study, which can not be obtained from the conventional isotherm pattern at a depth surface, and from time series vertical temperature section.

The different analyses covered so far can depict the seasonal variation of the thermal conditions in the Arabian Sea and Bay of Bengal, and their response to thermo-dynamical processes. Over time scales of within a few days, the variability of the thermocline is largely governed by internal waves, which normally superimpose over seasonal variability (1.1.4).

(d) Internal waves : - The time series MBT profiles are digitized at 5 m intervals. The analysis for stations T4 and T5 is restricted to a depth of 200 m. The time-depth thermal fields for the stationary positions are presented in Figs.5.1 and 5.2 with

this analysis, the segment length consists of 128 points at the positions T1 and T4, and 64 points at each of the remaining stations. Higher values of n enable a better resolution and the application of FFT analysis on several such segments at a single station provides a higher reliability and consistency of the harmonics.

The depths of the isotherms are smoothened through a 'Hanning Window '. The spectral levels of the harmonics are normalised with respect to its dominant harmonic, which has the maximum spectral level, to compare the different spectra. The spectral levels (normalised) versus frequency/wave period are depicted in Figs.5.3 and 5.4 restricting the presentation to a few typical isotherms for clarity. Normally, the spectral levels are represented by dots on such diagrams but they are joined for identification purpose.

In order to identify the possible generating mechanisms, the FFT analysis is also applied to the surface marine meteorological data, wherever available. The surface wind vectors are resolved into zonal (u) and meridional (v) components before analysis. The diurnal patterns of surface atmospheric pressure and tide resemble each other. Hence, either one of these two is considered in the analysis. As the surface meteorological data at sampling intervals for stations T1 and T2 (off Cochin) are not available, the tide gauge data from Cochin port are considered for FFT analysis, assuming identical trends in tides between Cochin port and stations off Cochin. The normalised spectral levels of these parameters are also included in the same figure (Fig.5.4).

an isotherm interval of 1°C. These structures (except for T1), start from top of the thermocline, as no internal waves exist in the mixed layer. The presentation of the temperature section at station T2 is restricted to seven hours due to frequent interruptions in the operational program after 1400 hours [Fig.5.2 (ii)].

The internal wave period (P) and height are estimated following the isotherms. At all the stationary positions, the MLD was at least three times less than the second layer down below. For a two-layer ocean with the upper layer thickness much less than that of the second layer below, the internal wave speed (C) (Defant, 1961) is given by

$$C = \left(g \; h' \frac{\rho - \rho'}{\rho} \right)^{1/2} \qquad (1)$$

where g = acceleration due to gravity,

h' = thickness of the mixed layer,

ρ' = mean density of the mixed layer

ρ = mean density of the second layer below mixed layer

From the known values of C and P, the wave length (λ) of the internal waves is obtained from $\lambda = \frac{C}{P}$

The Fast Fourier Transform (FFT) technique was applied to the sequential depths of individual isotherms for the respective internal wave fields to obtain the harmonics prevailing in the internal wave spectra. The segment legnth (i.e., number of data points) of the wave spectrum follows 2^n, where n is a positive integer. In

The Brunt-Vaisala frequency (N) for the observed internal wave fields is computed from

$$N = \left(\frac{g}{\rho_{z_i}} \frac{d\rho}{dz} \right)^{1/2} \qquad (2)$$

where ρ_{z_i} = the mean density of the water column between the depths Z_i and Z_{i+1}

$\frac{d\rho}{dz}$ = the density gradient between the depths Z_i and Z_{i+1}

At the positions T1, T2 and T3 the salinities were extracted from the average daily salinity profile for the corresponding depths of isotherms,and the densities were determined for the respective temperature-salinity-depth combinations. The typical Brunt-Vaisala frequency profiles for these stations are given in Fig.5.5.

1.2.3 Limitations

The analysis of the seasonal variability of the thermal structure suffers from various limitations. The heterogeneous sample sizes, based on which the monthly mean temperature profiles are evaluated, can induce deviation from the true variability. The smoothening of the mean profile at certain depths, as mentioned earlier cause some error, particularly on occasions of sudden slump in the sample size. When the mean structure for a month is based on a small number of temperature profiles, it may not represent the true variability due to the influence of internal waves. No attempt is made to isolate the interannual variability of the thermal conditions, due to inadequate data coverage. In areas of strong salinity gradients

the MLD values become over estimates. On the other hand, the shallowness of the shelf areas can restrict the deepening of the mixed layer, apparently under-estimating the MLD values.

The limited duration of the time series data sets can not provide the information on the consistency of the internal wave characteristics. The influence of other generating mechanisms on the observed internal wave characteristics can not be analysed, due to non availability of relevant data sets.

CHAPTER II

CHAPTER II

SEASONAL VARIATION OF THERMAL STRUCTURE

The time-depth temperature field on an annual cycle at a place in the sea documents the seasonal influence on thermal structure. It provides the basic inputs for determining the heat potentials in different depth slabs and the static stability of the water column where salinity changes are insignificant. It indicates the strength of vertical circulation and reveals the presence of Rossby and Kelvin waves. The knowledge of the regional and seasonal thermal features improves the quality of weather and climatic forecasts. It plays a useful role in assessment of the fish potential, underwater surveillance and extraction of energy from the sea.

The mean monthly BT profiles corresponding to a two degree latitude-longitude quadrangle (hereafter referred to as two degree quadrangle/grid for brevity) were subjected to quality checks and smoothing procedure. These temperature profiles were used to depict the seasonal variation of thermal structure in the upper 275 m with an isotherm interval of 1°C. It was not attempted to generate the temperature profile for the months of data missings. For such time gaps within two months, the isotherms were joined by dashed line for continuity. Although, such thermal fields were prepared for a number of two degree quadrangles, the presentation was restricted to a few selected sections representing specific areas in the eastern Arabian Sea and southwest Bay of Bengal. However, the remaining sections were utilised in interpretation of the results. These structures

are separately presented for the inshore (depth $<$ 200 m) and offshore (depth $>$ 200 m)areas for comparison. Two different scales for depth and time are adopted for inshore and offshore thermal structures for documentational convenience.

The monthly vertical temperature sections are shown in Fig.2.1 to 2.4 to document the seasonal variation of thermal structure off Kandla, Bombay, Karwar and Cochin respectively. The region south of peninsular India reflects the influence of the Arabian Sea, Bay of Bengal and equatorial Indian Ocean. To analyse this influence, three sections representing these areas are included in Fig.2.5. The effect of equatorial Indian Ocean water on the southwestern Bay is studied from two sections, which are presented in Fig.2.6. Similar analysis for the remaining areas of Bay of Bengal can not be made due to paucity of data on an annual cycle. The mean temperature profiles are based on heterogeneous sample sizes, distributed unevenly in space and time, and this limitation can not be eliminated. Further, when the sample size is small, the internal waves cannot be filtered from the medium. The variability of the mean temperature of the mixed layer follows closely that of SST and hence it is not separately discussed.

2.1.2 Off Kandla (Fig.2.1)

The shelf region off Kandla is characterized by its shallowness (depths $<$ 100 m) and wide extension (330 km) of the shelf. The section depicting thermal structure in the deep water is located at about 400 km from the coast.

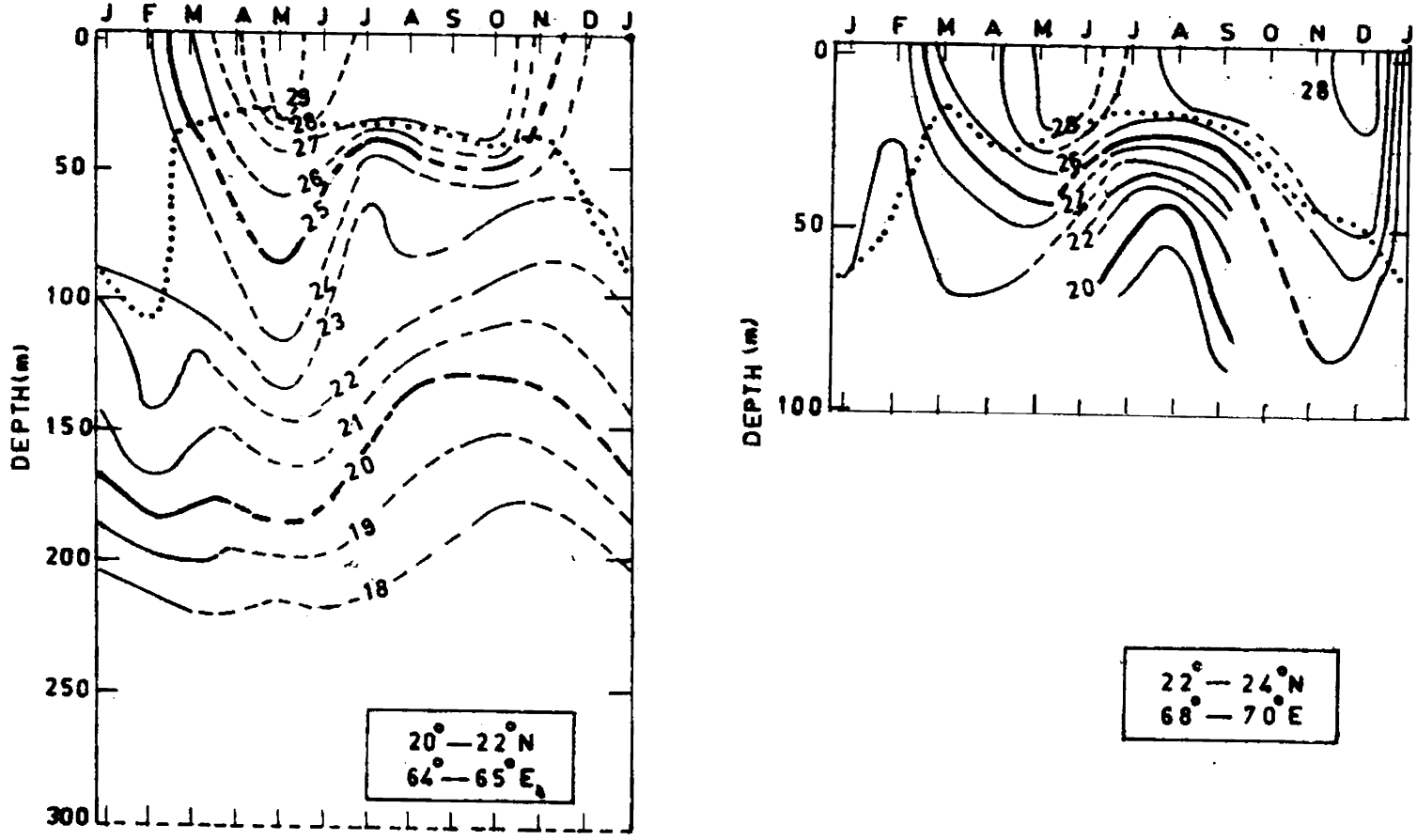

FIG.2.1 SEASONAL VARIATION OF THERMAL STRUCTURE OFF KANDLA

(i) Coastal waters (ii) Deep waters

——— Isotherms (°C) ..... Mixed Layer Depth

The annual range of SST in the coastal waters (4.5°C : 23.5 to 28.0°C) is slightly less compared to offshore waters (5.5°C : 23.5 to 29.0°C). The warmer water in both the regions is confined to May-July. The annual cycle of SST in the shallow waters shows a bimodal oscillation with the maxima in May (28.0°C) and November (28.0°C) and minima in February (23.0°C) and July (27.0°C). On the other hand, it depicts unimodal oscillation in the deep water with maximum (29.0°C) in May and minimum (23.0°C) in January. These temperature maxima emerge out of the pre-monsoon and post-monsoon heating and the minima due to winter and monsoonal cooling. The cold northeast winds and the influence of continentality cool the surface layer of the sea during winter. The net heat residual 40-120 W/m^2 (Hasternath and Lamb, 1979) during March to May and 40-80 W/m^2 during October to November warm the surface layer of the sea (Colborn, 1975). During the southwest monsoon, thick cloud covers reduce the insolation by 80 W/m^2 causing an overall heat loss of 40 W/m^2 (Hasternath and Lamb, 1979) at the sea surface, which decreases the SST. These factors account for the observed seasonal variability of SST.

The seasonal variation of MLD shows the bimodal signal but follows the inverse of SST pattern. In the shelf waters it exhibits maxima in January (60 m) due to winter cooling and the secondary one in May is not so conspicuous, while the minima occur in March (20 m) owing to pre-monsoon heating and August (20 m) because of upwelling, as explained in Chapter IV [Fig.4.2 (ii)]. For deep waters, it displays unimodal oscillation with maximum (105 m) in February and minmum (30 m) in May as a result of winter cooling and pre-summer heating respectively. The deep mixed layers in the shelf (35-60 m) and offshore (40-105 m) regions during November to February are initially caused by sinking as discussed in Chapter IV [Fig.4.1] and later

with an additional influence of intense winter cooling, as dealt in Chapter III [Fig.3.1]. The subsequent shoaling ($\sim$ 30 m) of the mixed layer during March to May is caused by pre-monsoon heating. The clear descent of the isotherms to 50-75 m depths in this region during this period reflects the downward flow of heat (Colborn, 1975). The ascent of isotherms in thermocline in the shelf and deep waters suggests the commencement of upwelling by June at subsurface levels, gradually reaching depths around 20-40 m after a lapse of one or two months. The upwelling appears to cease around August/September in shelf waters but extends to October in deep waters, which are in accordance with the results of thermal anomaly [Fig.4.2 (ii)]. The upwelled waters are restricted to 30-40 m and upwelling rates correspond to about 15-20 m/month. The general pattern of upwelling in the coastal waters and downwelling in the offshore waters, as discussed in Chapter IV [Fig.4.2 (ii)] is not reflected in this region. This may be because that the section considered for deep water is not representative of the offshore conditions. Probably, the offshore downwelling may occur still farther from the coast.

The surface layer cools by 1-2°C during southwest monsoon due to the monsoonal cooling (Colborn, 1975). A bunch of isotherms surfaces during December to January due to severe winter cooling. Thermal field at the subsurface levels reveals bimodal oscillation for the coastal waters and for the offshore waters at depths below 100 m. But, the upper 100 m water column in the offshore region shows a unimodal oscillation. The sesonal effects in this region appear to penetrate to a depth of about 200 m.

2.1.3 Off Bombay(Fig.2.2)

The thermal field of the deep waters off Bombay is situated at about 500 km off the coast. Similar to Kandla region, the inshore waters are associated with slightly less annual SST range (~ 3°C) compared to the deep (~ 4°C). The temperature extremes occur during May (~ 29°C) and February (25/26°C) correspondiong to pre-monsoon heating and winter cooling. The annual cycles of SST and MLD in the shelf waters display a prominent bimodal (sometimes referred to as double modal) signal similar to that at Kandla, with secondary maximum occuring by October (September for off Kandla). The processes, governing the annual cycle of SST at this place are same as those at Kandla region, but the signal off Bombay appears to be more distinct because of higher depth of the shelf. On the other hand, the annual signals of the SST and MLD in the offshore waters show unimodal oscillation, as in Kandla, but the conditions represent a mirror image. The mixed layer in the deep waters extends to around 100 m (against 40 m off Kandla) during southwest monsoon under the influence of anticyclonic gyre and maintains merely a steady value of about 55 m (against 40 to 100 m off Kandla) during the rest of the year. In deep waters, the shallowing of the mixed layer during winter indicates the domination of upwelling over winter cooling. During southwest monson the deepening of the mixed layer might also be influenced by the strong monsoonal winds (8 to 12 m/s) and the associated heat losses (0 to -80 W/m^2) (Hasternath and Lamb, 1979).

As in Kandla, isotherms descend in the upper 70 m during March to May/June due to downward flow of heat as a result of warming of surface waters. An interesting feature in the deep water during

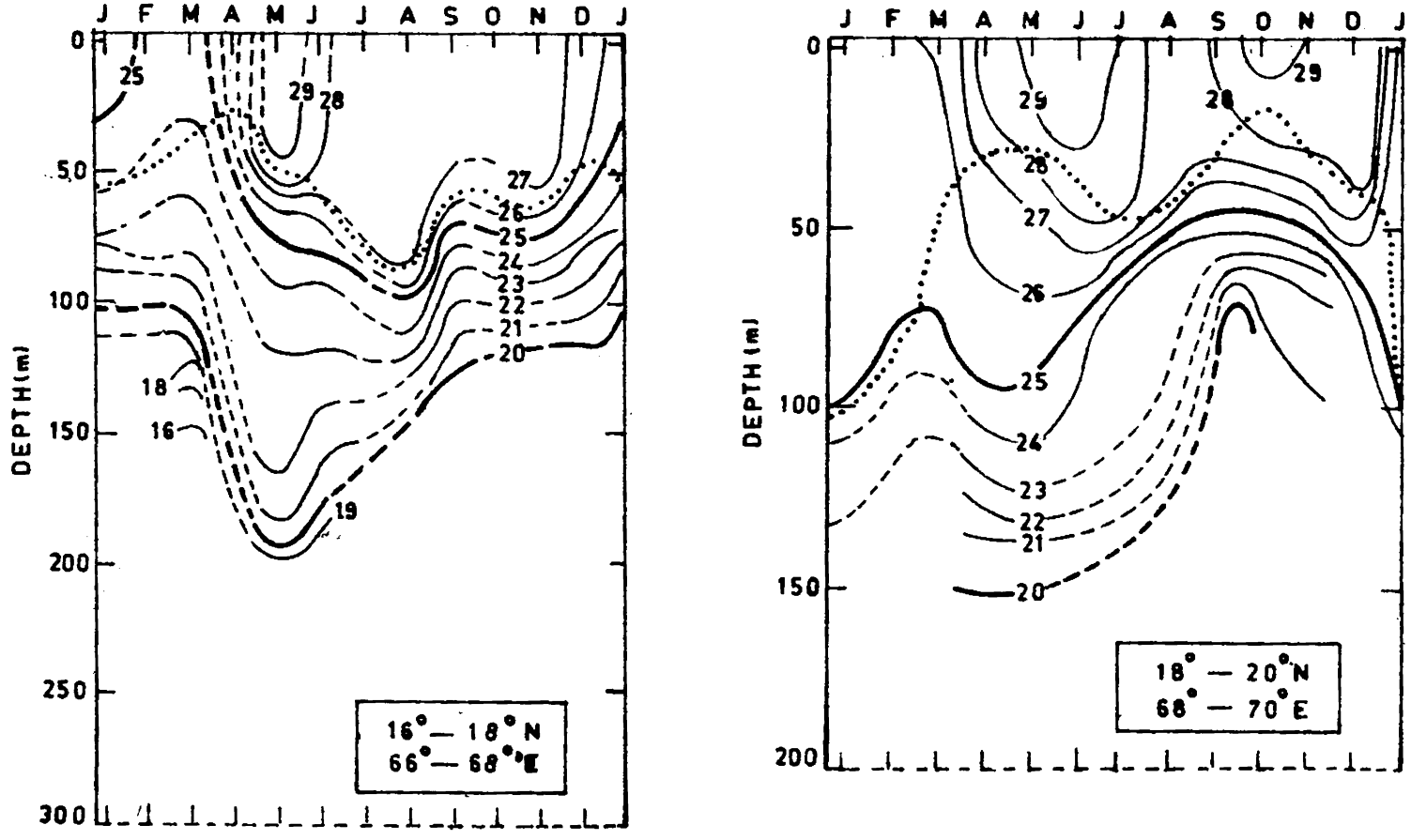

FIG 2.2 SEASONAL VARIATION OF THERMAL STRUCTURE OFF BOMBAY

(i) Coastal waters (ii) Deep waters

——— Isotherms (°C) ..... Mixed Layer Depth

June to August is the coexistence of sinking in the upper 100 m and upwelling down below. The coupling of these two mechanisms increases the thermal gradients in the thermocline during this period. A similar phenomenon can be noticed during April to June in the upper 70 m of the shelf waters. Upwelling in the shelf waters starts at subsurface layers in April and extends upto October with intensities of about 15-20 m/month. It is slowly replaced by sinking and winter cooling during November to February.

The warming of surface layer can be, strikingly, seen during primary (March-June) and secondary (October-November)warming periods. A gradual temperature drop ($\sim$ 1.5°C) in this layer during July to August reflects the influecne of monsoonal cooling . It is then followed by a rapid winter cooling (2.0 to 3.5°C) during November to February. The thermal structure as a whole exhibits a bimodal oscillation in the shelf and a unimodal in the deep waters. Similar to Kandla region, the sesonal influence can be seen upto about 200 m.

2.1.4 Off Karwar (Fig.2.3)

The temperature section of the deep waters is located at about 300 km off the coast. The annual range of SST in the shelf and deep waters is around 2.5°C (27.5 - 30.0°C) which is lower compared to northern regions, possibly, due to mild winter cooling. The maximum and minimum SSTs are recorded in May and July respectively. Analogous to northern regions, the annual cycle of SST in the shelf waters shows a double modal oscillation, with a reduced amplitude. Contrary

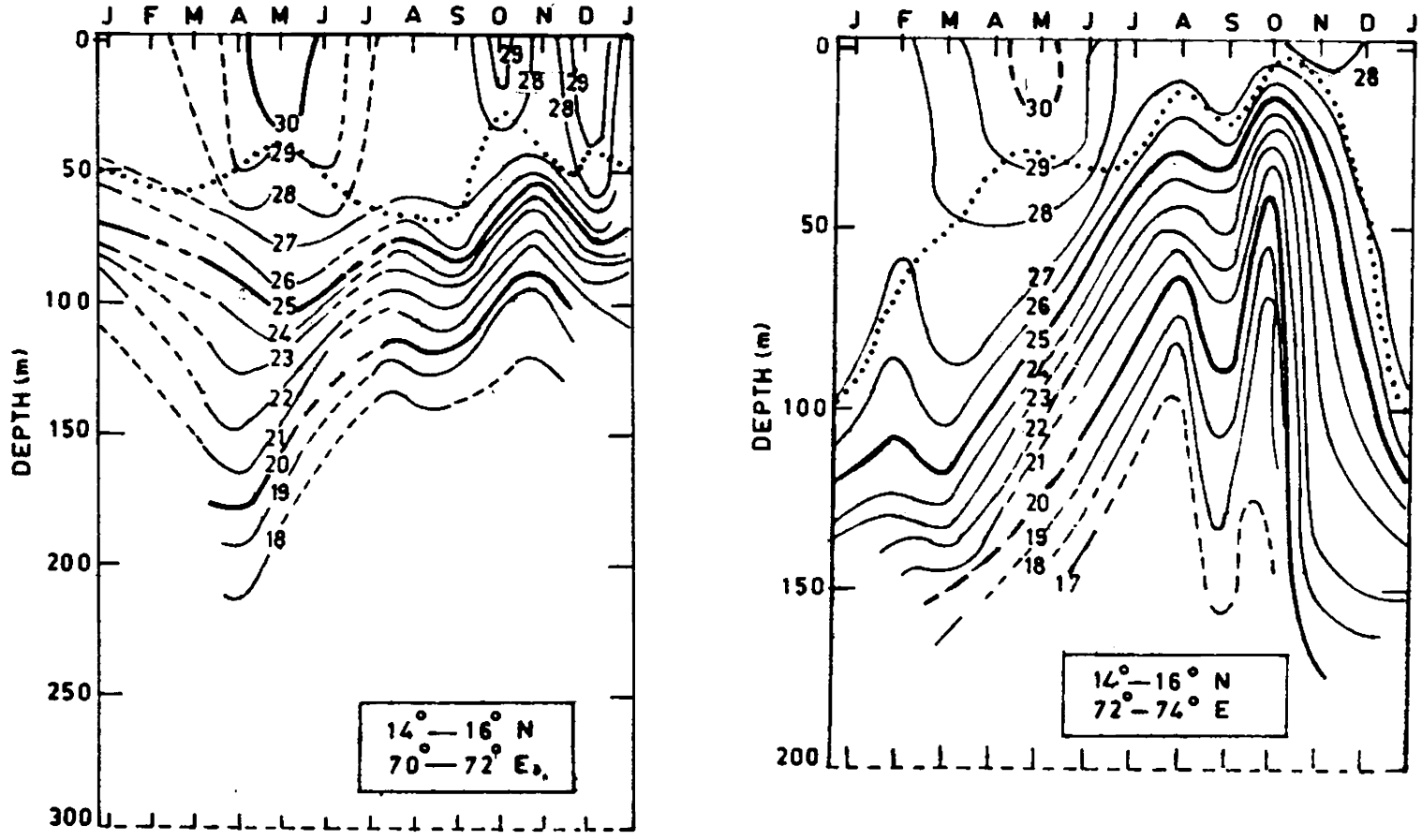

FIG 2.3 SEASONAL VARIATION OF THERMAL STRUCTURE OFF KARWAR

(i) Coastal waters (ii) Deep waters

——— Isotherms (°C) ..... Mixed Layer Depth

to these features, the annual SST variation in deep waters shows a trimodal oscillation with maxima in May, October and December and minima in January, August and November.

The annual variation of MLD indicates features different from the other two regions. It exhibits a trimodal oscillation in the shelf waters with maxima in January, June and September with corresponding minima in April, August and October. The additional minimum in August and maximum in September might be associated with the changes in the intensity of upwelling. On the other hand, the annual cycle of MLD in the offshore waters exhibits the usual bimodal signature.

The downward sloping of the isotherms in the shelf waters from November to February might be related to sinking, occurring due to northerly currents in this area. The winter cooling, although not severe in this area, also contributes to this downward trend of isotherms. The upwelling in shelf waters is initiated at subsurface levels during March under the influence of south-southeast currents and the upwelled waters reach the surface layer (10 m) by August as they are subdued by summer heating during March to May. In offshore waters, upwelling commences in May and extends upto August with upwelled waters reaching about 50 m. The descending and ascending isotherms in the thermal structure in the inshore and offshore waters occur during August to September and September to October respectively. Such features are reported by Basil Mathew (1982) and attributed to the weakening of upwelling due to reduced strength of the winds and currents during August to September and to the resonance between the poleward propagating baroclinic waves and local wind field during

September to October. The coexistence of sinking in the shelf waters and upwelling in the offshore waters and vice versa, as noticed off Bombay, is not clearly reflected in this region. Probably, the deep water temperature section taken may not be representative of offshore region. Such features may occur still farther off Karwar.

The monsoonal cooling during the southwest monsoon accounts for a temperature drop of 2.5°C in the shelf and offshore waters. The upwelling rates in offshore waters are weak (10-15 m/month) compared to shallow waters (15-20 m/month).

Thermal structure in the upper 150 m in this region shows a bimodal annual oscillation. Similar to that in the other regions, the sesonal influence at this place is felt upto a depth of about 200 m.

2.1.5 Off Cochin (Fig.2.4)

The temperature section of the deep waters off Cochin is at about 150 km far from the coast. The annual range and bimodal oscillation of SST in this area are similar to those off Karwar. The winter cooling is practically insignificant in this region due to its proximity to the equator, where the sesonal influence on SST variation is minimum. The annual cycle of MLD in shallow waters depicts the general bimodal oscillation, with a shift in the occurrrence of maxima and minima. The secondary maximum occurs in April in shelf waters and in September for deep waters. Similarly, the primary mimimum for these areas occurs in October and August respectively. The waters in the upper 50m are heated during the two warming seasons. A mild

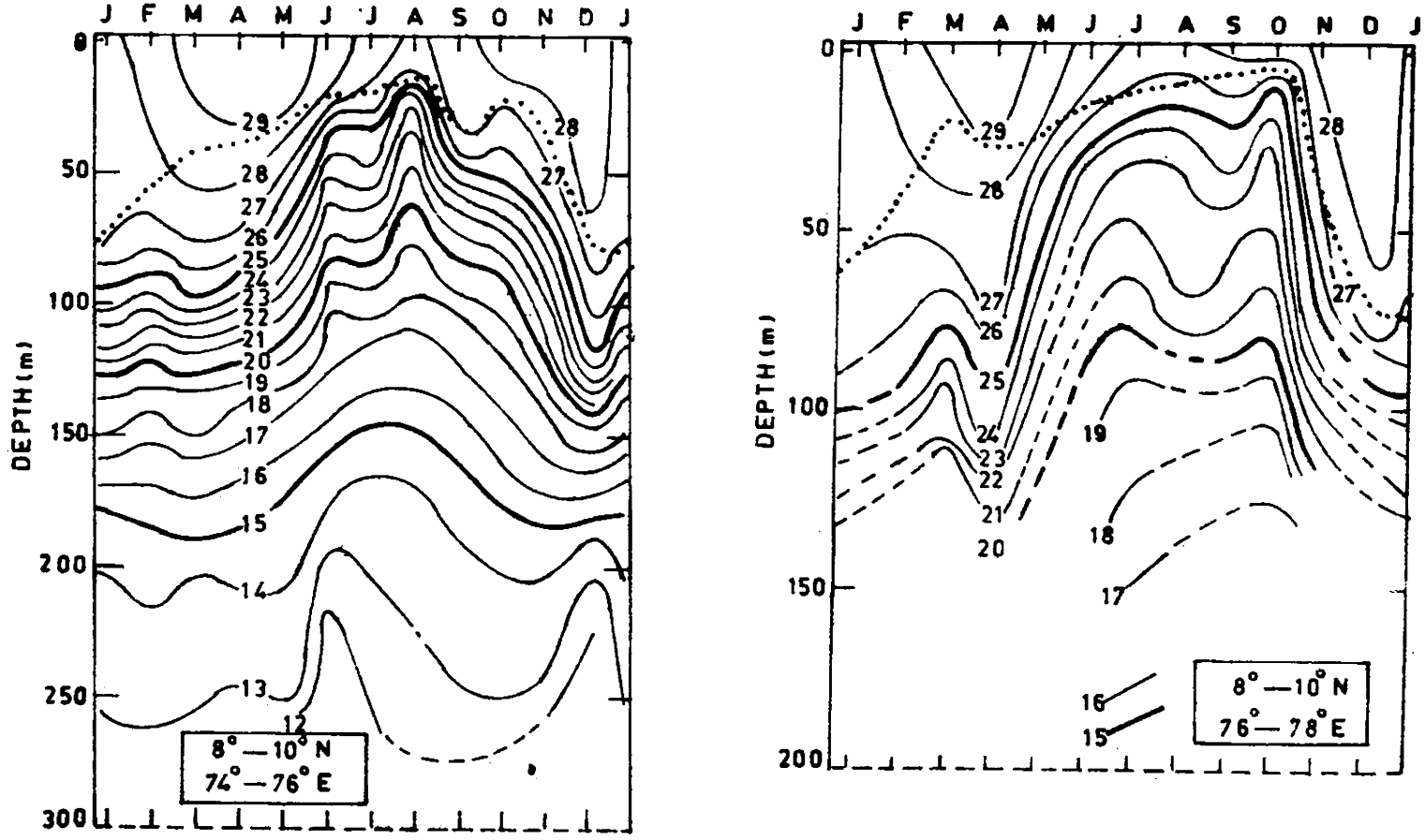

FIG. 2.4 SEASONAL VARIATION OF THERMAL STRUCTURE OFF COCHIN

(i) Coastal waters (ii) Deep waters

——— Isotherms (°C) .....Mixed Layer Depth

cooling of about 0.5°C is noticed in the surface layer between December and January, possibly evolved out of the inflow of Bay of Bengal waters, as explained in Chapter IV [Fig.4.1].

Many similarities exist in the thermal structure of inshore waters off Cochin and Karwar and the explanations offered for shelf waters off Karwar are equally applicable to this region. But, the thermal features of the deep waters off Cochin deviate from the other regions covered so far. The thermal field in the upper 150 m during October to January shows a downward trend of isotherms under the influence of sinking and not by winter cooling, as in the northern regions. The north-northwest surface flow (Wooster et al., 1967) during this period supports sinking in this region.

The upslope of isotherms suggests the commencement of upwelling in the deeper levels by March, with upwelled waters surfacing in June, while in the northern regions they seldom cross 30 m level. The upwelling extends to farther regions in the deep waters off Cochin (400 km) compared to the northern regions ($\sim$ 200 km). During June to August, the intensity of upwelling off Cochin (20-30 m/month) is higher than at any other region covered so far. The influence of monsoonal cooling in this period is masked by dominant downwelling.

Thermal structure in the upper 150 m of deep water exhibits unimodal oscillation, while it maintains a bimodal signal in shallow waters. The seasonal effects are conspicuously seen even upto a depth of 250 m.

2.1.6 Off peninsular India (Fig.2.5)

Out of the three vertical sections of the thermal field in the deep waters representing the influence of Arabian Sea, Bay of Bengal and equatorial Indian Ocean, the first two are located south of Cape Comorin, slightly, near the coast and the last section south of Sri Lanka, a little far from the coast. For convenience of discussion, they are respectively named as A, B and E.

The section A (Arabian Sea) records the maximum annual range of SST (3.8°C) compared to section B (Bay of Bengal : 2.5°C) and section E (equatorial waters : 2.0°C). The higher annual range for section A results out of intense upwelling ($\prec$ 26.0°C) during July to August. Similar to other areas, the annual cycle of SST in this area displays the double modal oscillation with the maxima and minima occurring at the times as reported for the other regions.

The annual march of MLD in these areas exhibits the bimodal oscillation with the primary maximum occuring during December/January (80-100 m) due to sinking, while the secondary maximum occurs at different periods. It occurs in August for section A due to weakening of upwelling, June for section E because of strong monsoonal winds (6-7 m/s : Hasternath and Lamb, 1979) and May in section B, although less prominent. The minima are accounted during the two warming seasons with exception to section A, where the primary minimum occurs in June during the active period of upwelling. The seasonal heating in these areas extends to depths 30-50 m. The surfacing of 28°C isotherm about July and its reappearance in October in section E are related to monsoonal cooling and secondary warming respectively.

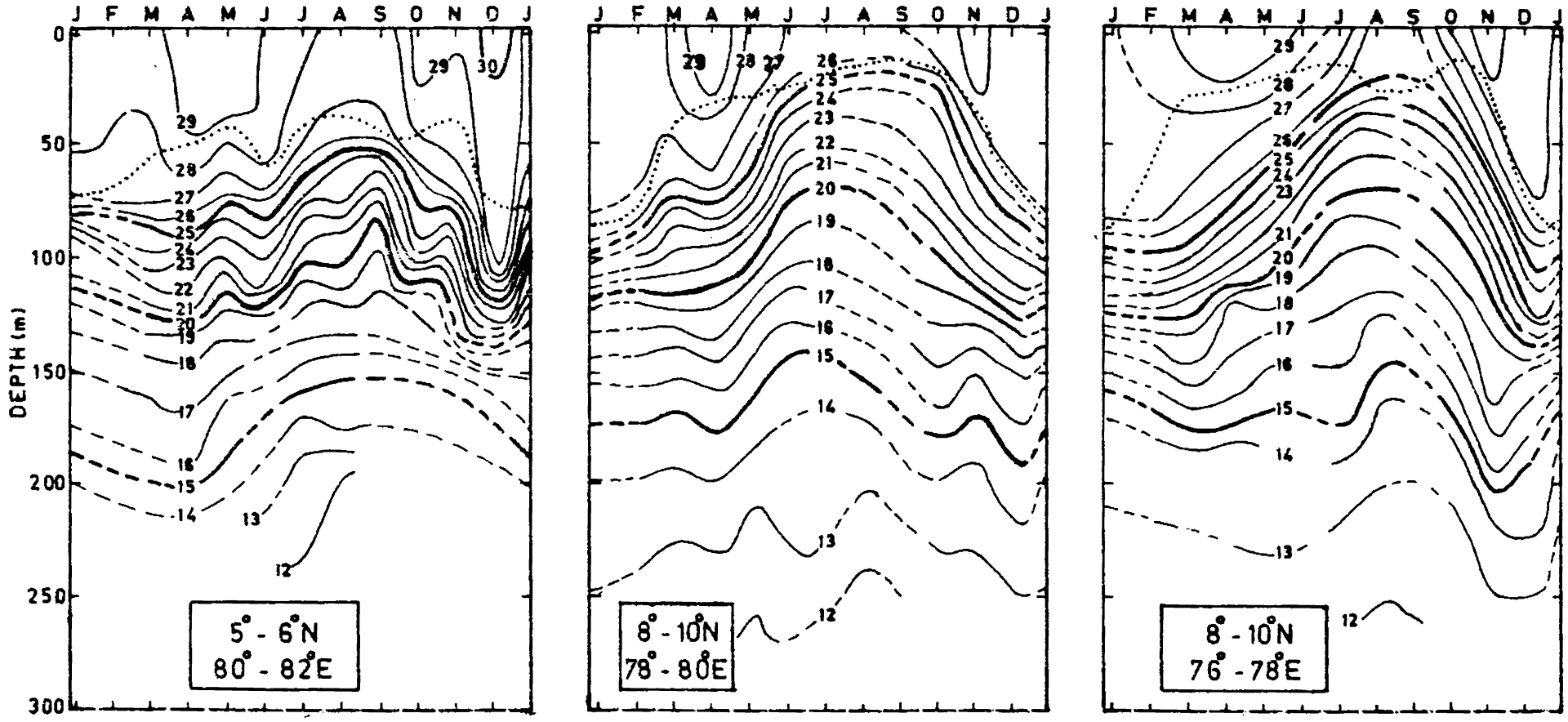

FIG 2.5 SEASONAL VARIATION OF THERMAL STRUCTURE OFF PENINSULAR INDIA

Influence of (i) Arabian Sea waters

(ii) Bay of Bengal waters

(iii) Equatorial Indian Ocean waters

——— Isotherms (°C) ..... Mixed Layer Depth

The annual march of the thermal field displays a striking dome structure for section A and B during February to September in these areas and wavy pattern with periods of 2 to 4 months for section E. The dome structure, more conspicuous in section A, shows a remarkable shoaling of the isotherms in the upper 150 m during February to September and deepening during the rest of the year. These two features might be the results of upwelling and sinking, as explained in the anomaly conditions [Figs.4.3 (i)and (ii)]. The intensities of upwelling in these areas are 15 m/month (section A) and 10 m/month (section B) with the upwelled waters reaching the surface during June to August. A closer examination of the thermal field in section E may reveal the subdued activity of upwelling, starting at deeper depths around April and extending to about 50 m by September and sinking during October to December.

The orientation of isotherms in section E indicates a possible flow of opposite currents around a depth of 150 m during November to January. Further, the waters in the upper 50 m of section E are warmer throughout the year compared to the remaining regions, mainly because they are not influenced by upwelling in this layer. A similar feature prevails at depths below 150 m. The wavy pattern in the section E may be related to either non-filtering of the internal waves from the medium due to inadequate data or to the propagation of Rossby/ Kelvin waves (Wunsch, 1977; Knox, 1981; Luyten and Roemmich, 1982; and McPhaden, 1982a). The annual cycle of thermal fields reflects unimodal oscillation in the upper 150 m and bimodal oscillation down below for sections A and B. Its counterpart in section E depicts a broad unimodal oscillation in the upper 150 m superimposed by other waves.

2.1.7 Southwest Bay of Bengal (Fig.2.6)

The vertical thermal fields representing the typical southern Bay of Bengal and equatorial waters of the Indian Ocean are located at 430 and 220 km east of Sri Lanka and designated for convenience as section B and E respectively.

Contrary to the thermal conditions in the other areas covered so far, the annual variation of SST in this region shows two different features viz. a lower annual range of 1.0 to 1.5°C against 2.0 to 5.0°C and unimodal oscillation against bimodal oscillation in other areas. Both these features emerge owing to their proximity to the equator. The maximum temperature ($\sim$ 29°C) occurs around April due to seasonal heating and minimum temperature ($\sim$ 27.5°C) in July because of monsoonal cooling. The annual variability of MLD in section E exhibits bimodal signal with maxima in February and July and minima in January and March, while it shows multimodal oscillation in section B. In both these sections, the annual cycles of MLD and subsurface thermal field are synonymous.

The prominent feature in both these sections is the distinct wavy pattern in the thermal structure at depths below 50 m with periods of 2-4 months in section B and about 6 months in section E. They may be the extensions of Rossby and Kelvin waves, as discussed under 'off Peninsular India'.

2.1.8 Meridional variation of thermal structure

It is attempted to report the meridional changes of the thermal

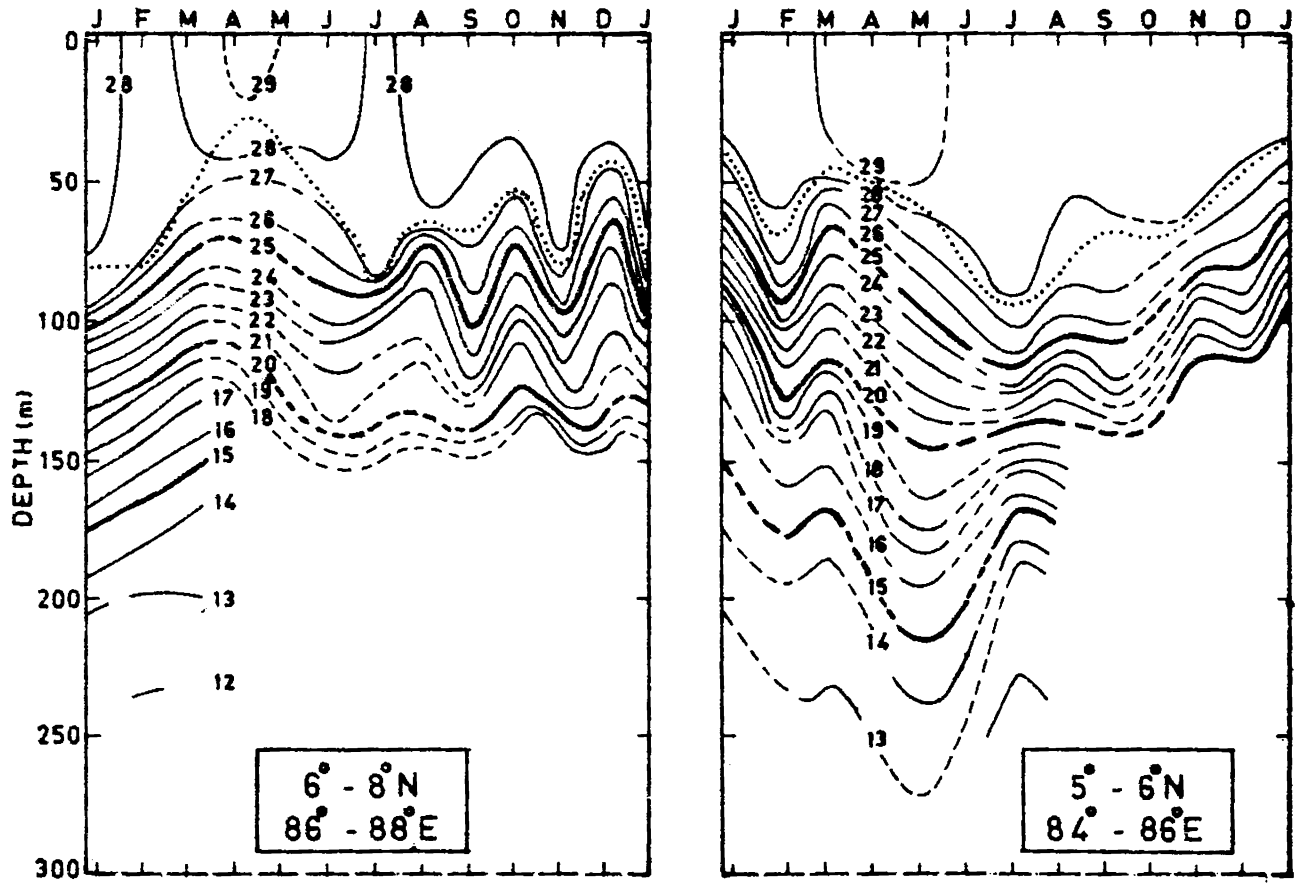

FIG.2.6 SEASONAL VARIATION OF THERMAL STRUCTURE IN THE SOUTHWEST BAY OF BENGAL

Influence of (i) Bay of Bengal waters
(ii) Equatorial Indian Ocean waters

——— Isotherms (°C) ..... Mixed Layer Depth

structure in the eastern Arabian Sea.

The annual range of SST gradually reduces from north (5.5°C) to south (1.5°C) [Figs.2.1 (ii) and 2.5 (iii)]. The higher range in the northern regions is due to dominant winter cooling. During southwest monsoon, the surface waters record a cooling of about 2°C in the northern regions caused by the fall in the insolation rates and entrainment. This cooling increases to about 2 to 4°C in the southern regions due to strong upwelling. Such a condition further gives rise to relatively larger temperature change during the secondary heating — October-November/December, in the south ($\sim$3°C) compared to north ($\sim$1°C).

The bimodal variation of the mixed layer, observed in the eastern parts of the Arabian Sea is replaced by a multimodal oscillation in the south, off the peninsular India. During November to February, the general descent of isotherms in the upper 150 m is controlled by winter cooling as well as sinking in the north, whereas it is mainly governed by sinking in the south. However, a mild cooling of 0.5°C occurs in the southern sector during December to January due to inflow of Bay of Bengal Water which is cooler by 1°C compared to the Arabian Sea Water. This water may not extend to regions beyond 15°N. During March to June, the water in the upper 50 to 70m warms up due to heating in the northern areas, while it is cooled during May to June in the south under the influence of upwelling. During the active period of upwelling the waters rarely cross 30 m depth in the northern region, while they surface in the south. In the south, the isotherms descend from August to September due to relaxation in local winds and ascend from September to October due to resonance

between baroclinic waves and wind field. No such features are observed in the north. The intensity of upwelling is higher in the south (20-30 m/month) compared to that in the north (10-20 m/month).

In the southernmost zones, thermocline exhibits the propagation of Rossby/Kelvin waves which may be a typical feature in the equatorial Indian Ocean.

2.2 DISCUSSION

The annual range of SST records a maximum value (5.5°C) in the northern regions under the influence of intense winter cooling and minimum value (1.0°C) in the southernmost areas due to proximity to the equator where the seasonal variations are minimum. The pre-monsoon heating and upwelling/monsoonal/winter cooling form the effective mechanisms to produce maximum SST in May and minimum SST in July in the south and around January in the north. The annual cycle of SST indicates the bimodal oscillation except in the offshore regions north of Bombay and south of Sri Lanka. The two temperature maxima, generally, occur around May and October respectively, associated with seasonal heating and minima in February and August. The winter cooling in the northern region and inflow of Bay of Bengal Water in the south cause temperature minimum in February, while the general monsoonal cooling in the northern areas and upwelling in the south create the secondary minimum temperature in August. Such bimodal signal appears more prominent between Karwar and Cochin because of pronounced cooling during June to August and secondary heating during October to November [Figs.2.3 and 2.4].

The seasonal variation of MLD closely follows the bimodal oscillation of SST but, generally, the occurrence of mixed layer maxima coincide with the minima of SST and vice versa. The larger thickness of the mixed layer during December to February in the north is caused by the combined effect of winter cooling and sinking, while it is produced in the south by sinking alone. During this period, in certain offshore regions, the sinking is replaced by upwelling following the prevailing circulation. Consequently, the mixed layer shallows during December to February but penetrates to maximum depth during southwest monsoon due to offshore downwelling, exhibiting unimodal oscillation in its annual cycle.

The isotherms in the upper 150 m of the nearshore regions during December to February, in general, show a downward trend under the influence of sinking and winter cooling, which is in accordance with the results of thermal anomalies [Fig.4.3 (i)]. In far off regions from the coast under the influence of offshore upwelling, isotherms in the upper 150 m shoal. During March to May, the strong seasonal heating warms the water in the upper 50-70 m. Along the west coast of India in the coastal waters, upwelling dominates during March-September/October commencing at the subsurface levels either in February or March in the south and gradually extending to north by either May or June. The upwelled waters seldom cross 30-40 m levels in the north [Fig.2.1], while they surface in the south around June [Fig.2.4]. The intensity of upwelling is higher in the south (20-30 m/month) compared to the north (15-20 m/month). The higher rates are probably caused by the combined action of the winds and the currents in the southern region. In the region between Cochin and Karwar, the upwelling weakens in August due to relaxation of winds, while

it rejuvenates in September owing to the resonance between winds and poleward propagating baroclinic waves [Fig.2.3]. Thermal structure in the coastal waters exhibits a bimodal oscillation. However, the deep waters indicate, in general, a unimodal oscillation, excepting for a few sections [Figs.2.3, 2.4 and 2.5]. Thermal structure in the upper 250 m appears to respond to the seasonal effects. Thermocline in the region south of Cape Comorin and Sri Lanka exhibits oscillations of periods 2-4 months, induced probably by Rossby/Kelvin waves.

The present analysis is based on the mean monthly temperatures in a two degree quadrangle. As such, point to point comparison can not be made with the values of the atlases, which are also based on similar analyses but differ in the spatial resolution or in the data points. However, a general comparison is done between these works and the similar studies made from mean monthly temperatures or synoptic temperatures having annual coverage in specific areas.

From the monthly hydrographic conditions, for the first time, Ramasastry (1959) reports bimodal and multimodal oscillations in the annual cycle of SST off Quilon and Kasargod. The present study confirms the bimodal signature in this area, besides suggesting a trimodal oscillation in SST off Karwar. Panikkar and Jayaraman (1966) point out an anuual range of SST of 6.0°C in the Arabian Sea against the present value of 5.5°C. Wooster et al. (1967) reveal a bimodal signature in the annual cycle of SST at several places in the Arabian Sea, as revealed in this study and the SST ranges closely agree with the present values. The bimodal oscillation and the times of occurrence of maxima and minima of the present study are in conformity with the results of several earlier works (Sharma, 1968; Noble, 1968;

Lonkar, 1971; Wyrtki, 1971; Colborn, 1975; Robinson et al., 1979; Hasternath and Lamb, 1979; Anjaneyulu, 1980; Narayana Pillai et al., 1980). This study also brings out the bimodal oscillation of SST in the shelf waters off Bombay and north of it, which is not reflected in the works of Wooster et al. (1967) and Colborn (1975). The difference in the data sets and mode of averaging might be responsible for such deviations. The trimodal oscillation of SST off Karwar in this analysis supports a similar observation of Narayana Pillai et al.(1980) off Ratnagiri. But, against the present SST range of 4.0°C they report a value of 10.0°C between Ratnagiri and Tuticorin. Their study, although based on mean monthly conditions, is restricted to the shelf waters for specific areas. But the present method of obtaining mean temperature in a larger area (two degree grid) might have created this discrepancy. Same logic can be extended to the difference in the annual range of SST of 3.5°C off Cochin, from the results of Basil Mathew (1982). A similar difference of 6.5°C is noticed from the work of Qasim (1982) in the northern Arabian Sea (north of 15°N).The western limit of 53°E in his study and the averaging in 1 degree quadrangle are expected to create this deviation.

The present study is also compared with the findings of some earlier works based on synoptic conditions. A rise in SST of 3.0°C is found against 3.5°C noticed by Rao et al.(1974) during January to April between Karwar and Vengurla. Such a difference between mean and synoptic conditions is quite common. Ramesh Babu et al. (1980) and Varma et al. (1980) observe a general increase of temperature towards north during February to March/April along the west coast of India. Since the winter cooling gradually weakens from north to south and presummer heating commences in the entire area after March,

such a trend appears to be unusual and the reverse trend, as obtained in this analysis, appears to be logical. The penetration of seasonal heating to depth of 50-70 m confirms the earlier results of Sharma (1968), Sastry and D'Souza (1970), Colborn (1975) and McPhaden (1982b).

The monsoonal cooling of 2°C in the north due to heat losses from the sea and entrainment, and 3 to 4°C in the south, mainly due to upwelling are compared with some earlier works in the Arabian Sea and Bay of Bengal. In the present study, it is not possible to isolate the individual influence of these processes and hence, an overall comparison is made. The present figures of monsoonal cooling compare with the value of 1.0 to 4.5°C reported by Rao et al.(1976), who attribute to one of these processes, that used to dominate regionally. Similar temperature drops (1.0 to 2.5°C) at the surface are reported by Ramesh Babu et al. (1976) and Ramam et al.(1979) in their studies at a few zonal sections in the eastern Arabian Sea. A similar cooling of 1.0 to 2.0°C in the surface layer in the Arabian Sea and Bay of Bengal is related by Anjaneyulu (1980) and Joseph and Pillai (1986) to heat losses and upwelling. An equivalent fall of 1 to 2°C is noticed by Rao et al.(1981, 1983), Ramesh Babu and Sastry (1984), Sastry and Ramesh Babu (1985) and Rao (1986) at some fixed points in offshore waters of the Arabian Sea and Bay of Bengal and is related to the processes outlined above. The characteristics of upwelling and sinking like commencement, duration etc., gradual extension of upwelled waters towards surface and northwards, and coexistence of upwelling and sinking support the earlier results of Sharma (1966 1968, 1978). The present analysis also agrees with the results of Banse (1971) who points out the occurrence of upwelling off Bombay during southwest monsoon. The upwelling rates in the north (15-20 m/month) and south (20-30 m/month) compare with the rates of 19-26 m/month reported by Narayana Pillai et al. (1980). The extension of upwelling to about 400 km off Cochin, revival of upwelling activity between Cochin

and Karwar during September to October, and onset of sinking agree with the reports of Basil Mathew (1982) who infers upwelling from vergence and curl of wind stress. Upwelling rates of about 30 m/month off Cochin are comparable to the present values. According to him and Shetye (1984) the higher upwelling rates in the southern region are produced by the combined action of the currents and equatorward component of wind. The results of the present study endorse the same views.

The present results broadly agree with the earlier upwelling studies based on synoptic conditions for one or two seasons at specific areas. The active periods of upwelling and sinking between Cape Comorin and Cochin are in agreement with the periods reported by Ramamirtham and Jayaraman (1959), Banse (1959) and Ramasastry and Myrland (1959). The present study shows a general agreement with the subsequent works by Sastry and D'Souza (1970), Lonkar (1971), Sankaranarayanan and Qasim (1968), Ramamirtham and Rao (1973) and Rao et al. (1974) who have interpreted upwelling and sinking from the variations of hydrographic conditions at different places off the west coast of India in different seasons.

The bimodal oscillation of the thermal structure at the subsurface levels in the coastal waters confirms the results of Wooster et al. (1967). However, they suggest bimodal oscillation for the deep waters at several places against present unimodal oscillation. The additional data and mode of averaging in this work probably, can account for the deviation.

The wavy pattern of the thermal structure in the thermocline with periods of 2-4 months south of Cape Comorin and Sri Lanka are perhaps induced by Rossby/Kelvin waves. Such waves with semi-annual periods in current and wind at Addu Atoll in the equatorial Indian Ocean are reported by Wunsch (1977) and Luyten and Roemmick (1982) from the time series records of 2-8 years. From a 2 year time series record of temperature and surface meteorological parameters at Gana Island, McPhaden (1982a) reveals a 6 month period wave in the thermocline superimposed by wind forced response with periods of 1-2 months. However, the wavy nature of the thermocline noticed in this study can also be generated by internal waves, if they are not smoothened in the average picture. However, further investigation in this area based on intensive data network can enlighten these features.

CHAPTER III

CHAPTER III

MIXED LAYER TOPOGRAPHY

The buoyant motions due to heat losses across the air-sea interface, the turbulent motions associated with winds, waves and currents can individually or collectively produce a nearly isothermal surface layer of the ocean, normally referred to as 'mixed layer'. The changes in the scales of these factors, together with the stability of water column just below the base of the mixed layer govern the vertical extension of the mixed layer. Since the water column of the mixed layer is characterised by least stratification, the vertical exchange of heat content extends sufficiently deep within it. The effects of seasonal extremes (intense heating and severe cooling), meteorological systems (monsoon/depressions) and eddies are primarily absorbed in this mixed layer. Thus, the mixed layer acts as a thermal buffer, shielding the interior of the ocean considerably.

As the mixed layer in the sea extends to a few tens of metres, the heat potential of mixed layer becomes an important factor in controlling the changes of weather and formation of monsoons as well as depressions in the initial stages. The bottom of the mixed layer approximately forms as a boundary of thermal discontinuity and acts as a barrier for the vertical motions across it. A knowledge on the mixed layer is also useful for predicting the thickness of the sound duct in regions of weak vertical salinity gradient and to account for the mobility of marine life.

In the present study, the Mixed Layer Depth (MLD) is considered as a depth where the temperature drops by 1.0°C from SST in the mean monthly temperature profile. The topography of the mixed layer in the area under investigation is depicted in Figs. 3.1 to 3.6 for all 12 months. Such maps are not attempted for the area bounded by 10 -22°N and 80 -90°E due to paucity of data on the annual cycle. Although, the MLD and top of thermocline are not identical, invariably they tend to coincide. It becomes, therefore, possible to interpret the topographic charts of mixed layer in terms of topography of thermocline with certain limitations, which are spelt out in the course of discussion. The values of MLD need to be cautiously considered in certain regions where remarkable salinity gradients exist within the mixed layer and where the internal waves are not smoothened from the medium.

3.1.2 January [Fig.3.1(i)]

The MLD during January varies from 50 to 130 m. The general topography and its orientation indicate a clear shoaling to 50 m in the offshore belt (68 -71°E) and deepening to 90-130 m on either side. The values of MLD tend to decrease from north (130 m) to south (60 m). However, in the eastern region (southwest Bay of Bengal - east of 80°E) under investigation the reverse conditions prevail. It is probable that the extension of the mixed layer is restricted by the sea bottom in the nearshore region - off Kandla and Bombay. In such regions the exact depth of mixed layer can not be delineated.

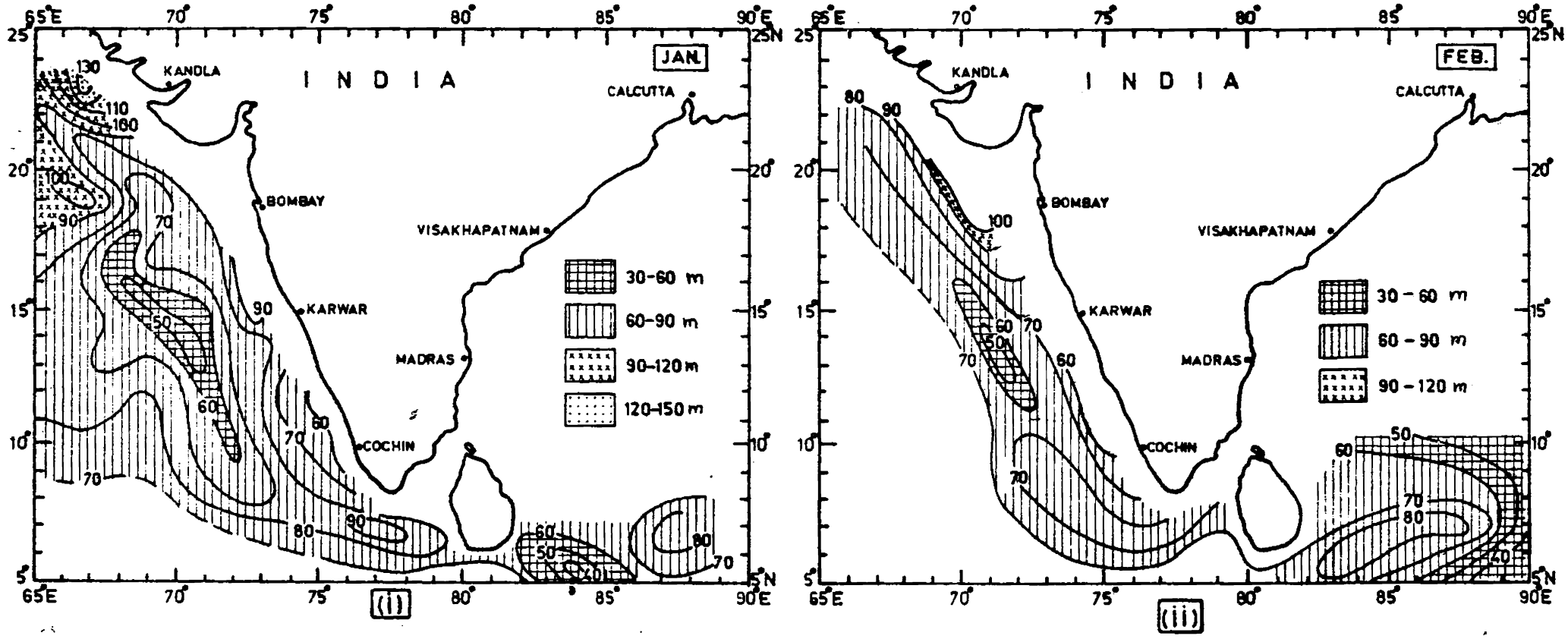

FIG.3.1 TOPOGRAPHY OF THE MIXED LAYER

(i) January

(ii) February

As this month represents the typical winter conditions, the influence of cooling is more in the north compared to the south, thereby producing a deeper mixed layer in the north. Besides winter cooling, the downwelling in the inshore waters, as seen in Chapter IV, might have deepened the mixed layer, particularly south of Karwar. The shallow mixed layer (50 m) in the offshore region bounded by 10°-20°N, 68°-71°E with its lateral shoaling of 40 m (90-50 m) is developed due to upwelling in this area as explained in Chapter IV [Fig.4.2(i)]. Thus, in the coastal waters the larger thickness of mixed layer (80-130 m) in the northern region might be linked to the combined action of winter cooling and downwelling, while the mixed layers of 60-80 m south of Karwar might emerge out of downwelling alone.

3.1.3 February [Fig.3.1 (ii)]

Although, the general pattern of topography of mixed layer remains more or less the same as in January, an overall fall of 10-30 m is noticed in the northern region. It may be related to weakening in downwelling as a result of reversal of surface current (Varadachari and Sharma, 1967). The ridge of MLD in the offshore area (along 71°E) shifted towards the coast from its position in January. Off Sri Lanka, the MLD decreases offshore (80-40 m), which shows a reverse trend of the one in January. Besides, the zonal gradients strengthen, probably, due to advective transfer of heat from the southern hemisphere to the north of the equator. Although, such

advective transfer is possible in January, it is, perhaps, masked under the influence of downwelling.

3.1.4 March [Fig.3.2 (i)]

The topography of mixed layer displays significant deviation, both in magnitude and orientation. MLD varies over a wide range of 20-90 m, with low values of 20 m off Kandla. In the northern part, the isobaths of mixed layer are oriented more or less parallel to the latitudes, while they run parallel to the longitudes in February. The abrupt changes in the topography are, probably, influenced by the transition conditions from northeast monsoon to southwest monsoon. Further, the mixed layer topography depicts a series of troughs and ridges. These cellualar structures are likely to be caused by the unsteady conditions in the wind field. Contrary to February conditions, a ridge structure appears off Sri Lanka. The ridge and trough structures located around 15°N, 67°E; 10°N, 75°E and 17°N, 70°E ; 8°N, 70°E respectively are the manifestations of the circulation pattern. In fact, the surface flow reveals two anticyclonic gyres with their centres approximately coinciding with the troughs (Wooster et al., 1967). The ridge structure around 15°N, 67°E might be associated with the interfacial zone between these two gyres. The low MLD values off Kandla and the ridge off Cochin emerge, possibly, out of commencement of pre-summer heating. Such features are also reflected in the thermal structures (Figs. 2.1 and 2.4) and thermal anomaly patterns [Figs. 4.1 (i) and 4.2 (i)].

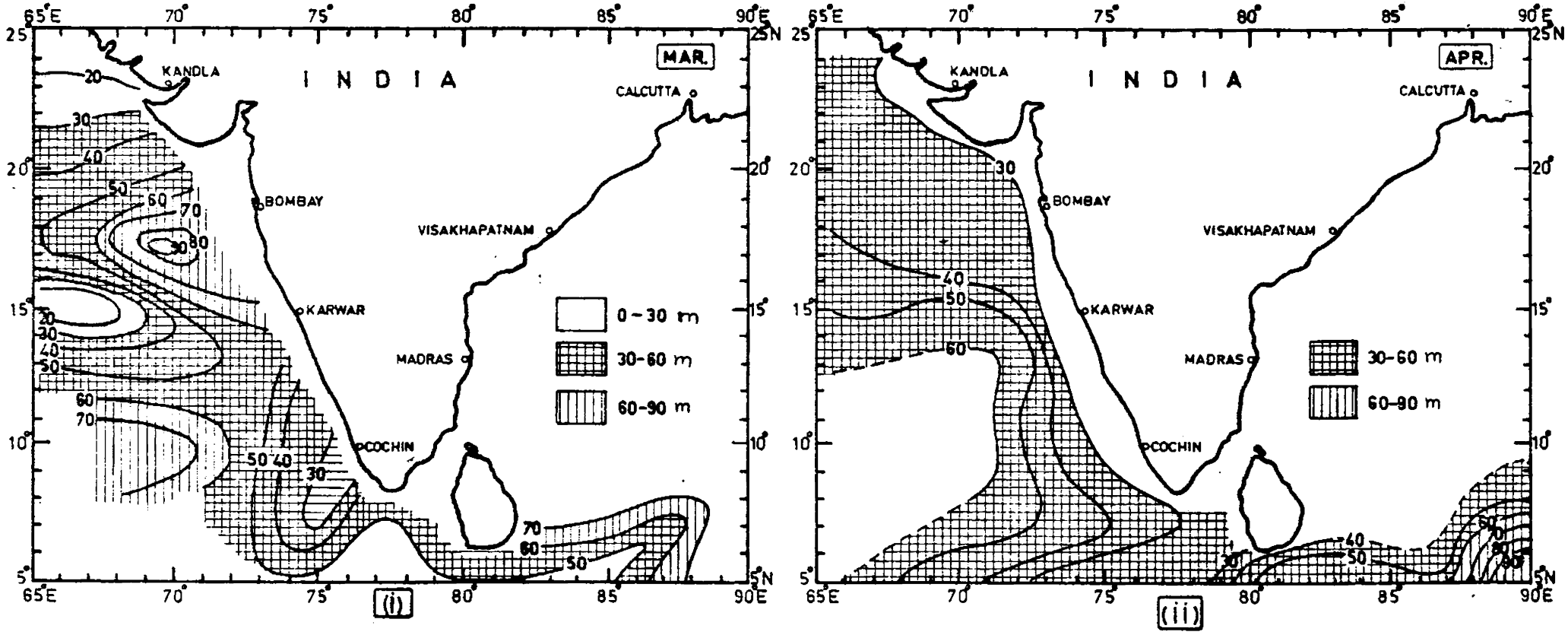

FIG.3.2 TOPOGRAPHY OF THE MIXED LAYER

(i) March

(ii) April

3.1.5 April [Fig.3.2 (ii)]

The isopleths of the mixed layer run parallel to the meridians. There is an overall drop in the values of MLD by about 30 m (30-60 m, against 30-90 m in March) with a corresponding fall in its range from coastal to offshore regions (30 m, against 60 m in March). Unlike in the previous months, the offshore waters are characterized by deep mixed layers (50-60 m). The low MLD values in the coastal waters (30-40 m) can occur as an offshoot of seasonal heating as reflected in the seasonal thermal structures [Figs.2.1 to 2.6]. In response to these processes, the isobaths of mixed layer orient almost parallel to the coast, particularly along the west coast of India.

3.1.6 May [Fig.3.3 (i)]

The pattern of mixed layer topography in May closely resembles that in April, except for a well developed trough off Bombay. This distinct trough structure, appearing in April south of 15°N, though not so conspicuous, moved northward. In contrast to this, in the remaining area the progressive rise in the incoming heat fluxes and the flow of equatorial waters (Sastry and D'Souza, 1970) warm the surface layer thereby reducing the mixed layer thickness, as can be seen in the seasonal thermal structures [Figs. 2.1 to 2.3]. Further, the upwelling in the regions south of Karwar can also contribute to the general fall of MLD in this region, agreeing with the results of seasonal thermal sections [Figs. 2.4 to 2.6] and thermal anomalies [Fig. 4.2 (i)].

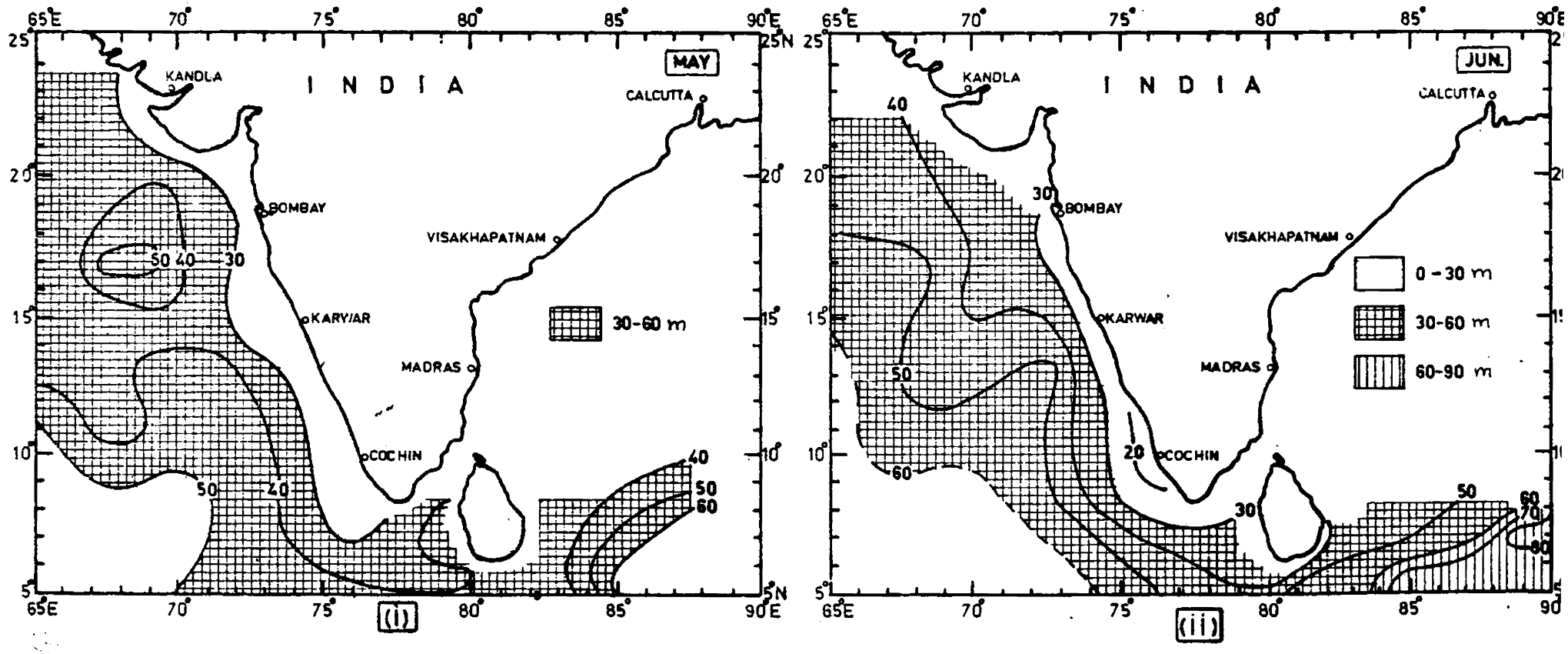

FIG.3.3 TOPOGRAPHY OF THE MIXED LAYER

(i) May
(ii) June

3.1.7 June [Fig.3.3 (ii)]

The mixed layer further shoals off the southwest coast of India with values less than 20 m. It is a clear reflection of the strong upwelling in this region. The mixed layer, normally, deepens due to reduced insolation under extensive cloud cover and increased amount of heat losses from the sea surface during summer monsoon. But, in this region, it is obviously dominated by upwelling. However, the low values of MLD (40 m) in the northern region are still maintained as a continuation of seasonal heating as reflected in the thermal anomaly pattern [Fig.4.1(i)].The offshore regions record deeper mixed layers (~ 60 m) resulting out of sinking. The tongue structure gets intensified from the previous month and moves towards north indicating the northward extension of upwelling, which is in accordance with the thermal anomaly pattern [Fig.4.2 (i)]. In the eastern region, the MLD increases from 40 to 50 m with a corresponding rise in its range from 20 - 30 m, probably, in response to the downward flow of heat of the previous season.

3.1.8 July [Fig.3.4(i)]

A striking feature of the mixed layer topography in July is the strengthening of its lateral gradients. Although the MLD in the nearshore regions is maintained at 20 m, it shows a deepening by 50 m, just in one month. This remarkable deepening of the mixed layer might have been produced either by monsoonal cooling or downwelling or by the combined effect of both, which is also supported by the

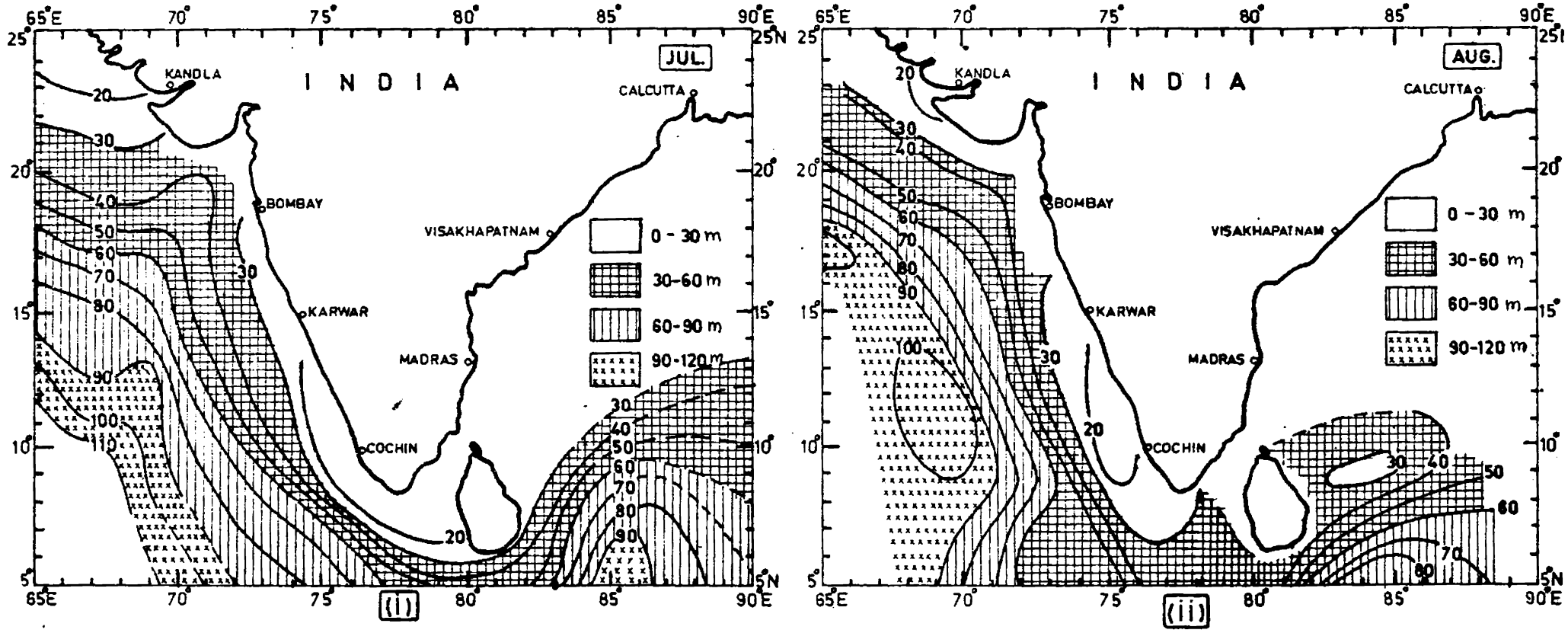

FIG. 3.4 TOPOGRAPHY OF THE MIXED LAYER

(i) July

(ii) August

thermal anomalies [Figs. 4.2 (ii) and 4.3 (ii)]. Normally, the mixed layer responds to the monsoonal force even in June. But, the pronounced deepening of the mixed layer during July might be due to the well set conditions of strong southwesterlies with speeds of about 12 m/s. (Hasternath and Lamb, 1979) and predominant sinking. The coexisting nearshore upwelling and offshore sinking developed under the influence of a broad anticyclonic gyre in the offshore regions might be responsible for the observed mixed layer topography (Varadachari and Sharma, 1967; Sastry and D'Souza, 1970). Further, the trough structure 14°N, 70°E) with the depths exceeding 80 m becomes more prominent and shifts westward under the influence of sinking. Even in the eastern region, the lateral gradients of the mixed layer got built up, with the mixed layer shallowing towards the coast, indicating upwelling off the east coast of Sri Lanka due to southerly currents (La Fond,1954a; Murty and Varadachari, 1968; Basil Mathew, 1982).

3.1.9 August [Fig.3.4 (ii)]

The general pattern of mixed layer in August is similar to the one in July. The mixed layer trough in the Arabian Sea moves northeastward, thus increasing its lateral gradients. The MLD in the nearshore regions is almost the same as in July, indicating the quasi-stationary nature of upwelling off the west coast of India in August. The features in the eastern region, as observed in July, continue with a southward shift of the trough.

3.1.10 September [Fig.3.5 (i)].

A major deviation in the mixed layer topography in September compared to August is the westward shift of the trough in the Arabian Sea, probably associated with the receding of the southwest monsoon. The isobaths of mixed layer in the offshore regions are oriented parallel to the longitudes in the nearshore waters following the broad anticyclonic gyral circulation in this area. While the mixed layer in the offshore regions remains same as in August, very near the coast it shoals further by about 10 m. This may be a consequence of rejuvenation in upwelling compared to August conditions or the flow of warm coastal current in the surface layer.

3.1.11 October [Fig.3.5 (ii)]

In this month the pattern of the mixed layer suggests the initiation of deepening in the coastal waters against a remarkable shoaling to 50-60 m in the offshore waters of the west coast of India, indicating a fall of 40 m just in one month. This behaviour can be linked to the transition of upwelling to sinking in the shelf waters and sinking to upwelling in the offshore regions.

3.1.12 November [Fig 3.6 (i)]

The mixed layer topography in November is characterized by a series of troughs and ridges - a typical feature during the transition period. This behaviour is similar to the one in March - another transition month - but the patterns are reversed. During this month, the coastal waters are associated with shallow mixed layers ($\sim$ 30

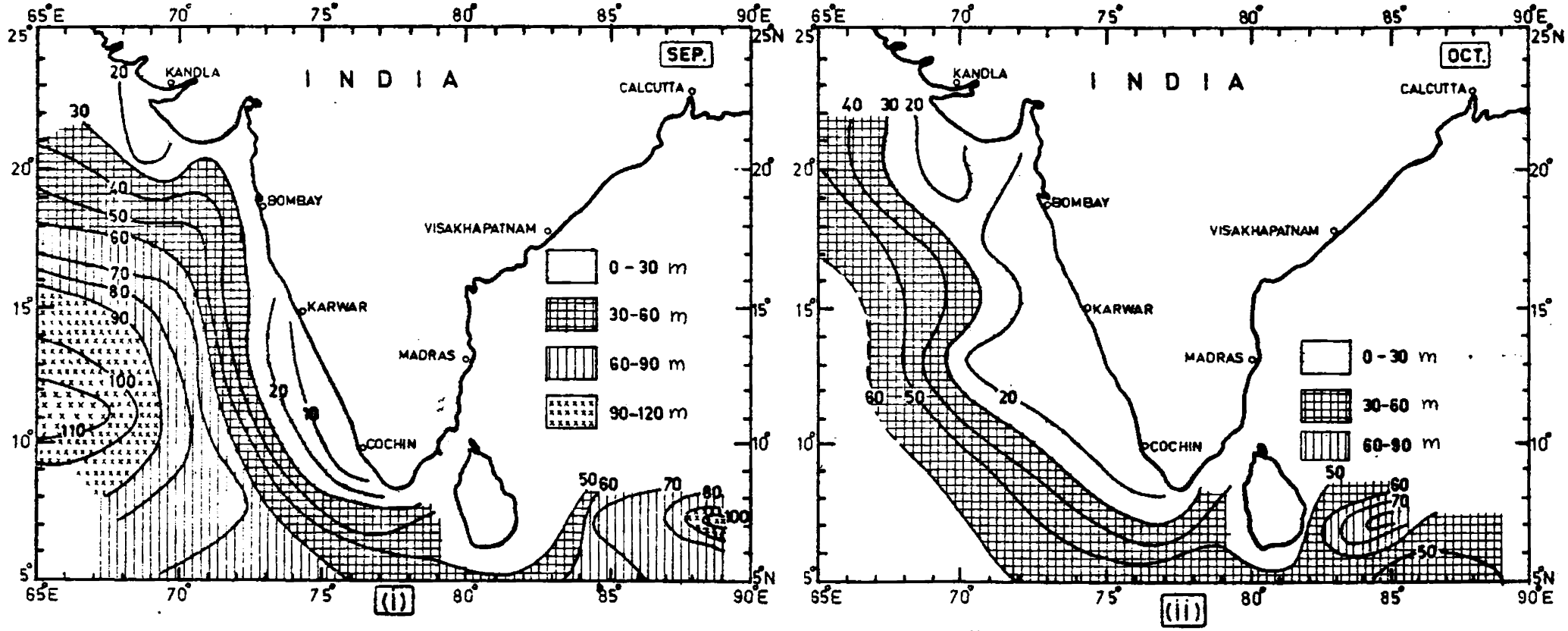

FIG. 3.5 TOPOGRAPHY OF THE MIXED LAYER

(i) September

(ii) October

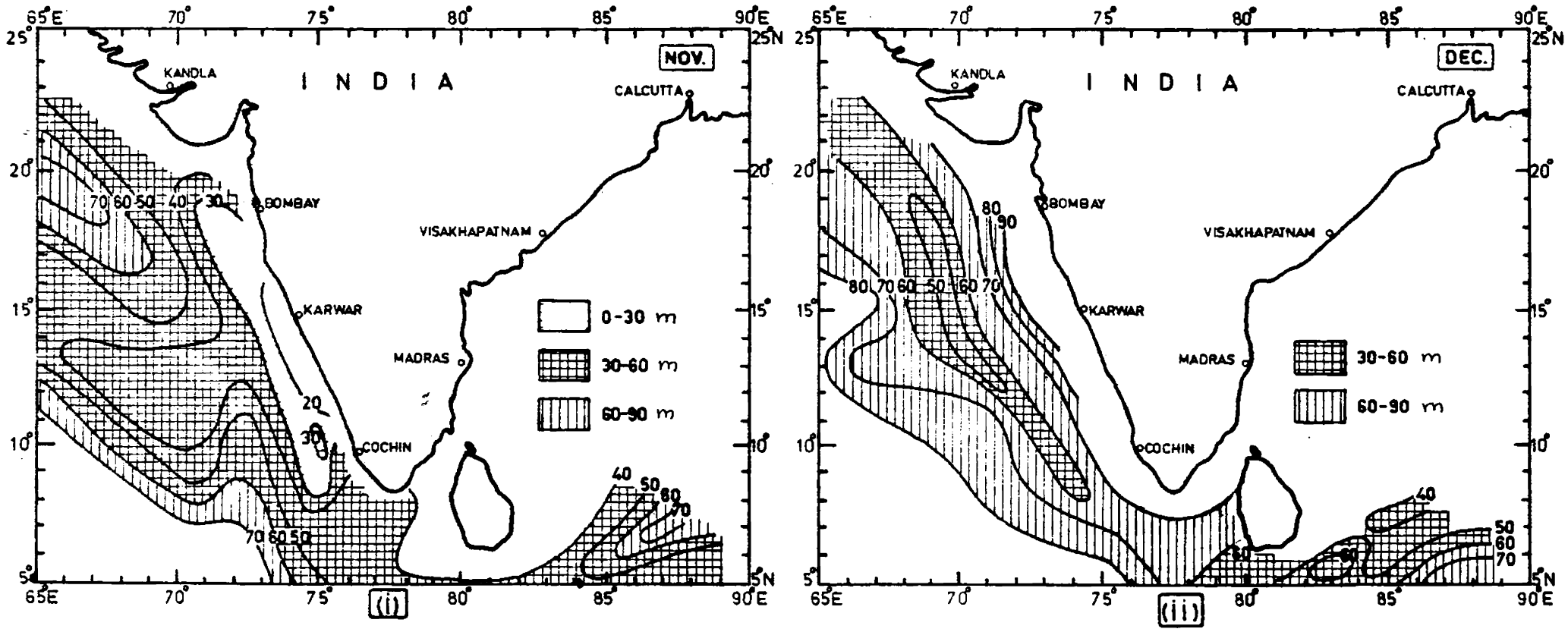

FIG. 3.6 TOPOGRAPHY OF THE MIXED LAYER

(i) November

(ii) December

while offshore waters record deep mixed layers (~ 70 m). The opposite conditions prevail in March. This is understandable, as November acts as the transition month from summer to winter, while March is the transition from winter to summer. Besides, there is a general reversal in the surface circulation between October and November. In this month a prominent ridge is formed at the central region in the offshore waters of the eastern Arabian Sea, with its axis following 40 m isobath. This ridge structure can emerge out of the broad cyclonic gyre that can induce upwelling (Varadachari and Sharma, 1967; Wooster et al., 1967). This is further supplemented by a hyperbolic point. The low MLD values along the coastal belt off the west coast of India might also evolve out of secondary seasonal heating. A ridge structure exists off Sri Lanka, probably, due to a cyclonic circulation cell in this region (Varadachari and Sharma, 1967).

3.1.13 December [Fig. 3.6 (ii)]

The topography of the mixed layer in December, a typical winter month, closely resembles the pattern of January. The coastal waters are associated with deep mixed layer (70 - 80 m) in contrast to the shallow mixed layer (~ 50 m) in the offshore regions. These conditions might be related to the downwelling in the coastal waters and upwelling in the deep waters, as shown in the temperature anomaly pattern [Figs. 4.1 (ii) to 4.2 (ii)]. In the coastal waters the low MLD values off Saurashtra (40-50 m) apparently exist because of shallowness of this area. Alternatively, it can be a manifestation of secondary upwelling due to northeast winds (Jayaraman and Gogate, 1957; Carruthers and Gogate, 1959). The higher MLD values in the northern regions

might be due to the influence of commencement of winter cooling. The ridge structure off Sri Lanka, appeared in November, still persists.

3.2 DISCUSSION

During December to February, the sinking and upwelling produce deep (70-120 m) mixed layers in the coastal waters and shallow layers marked by a well defined ridge (50 m) in the deep waters respectively [Figs. 3.1 and 3.6 (ii)]. In the northern region, winter cooling causes further deepening of the mixed layer. In March, the topography exhibits a series of troughs and ridges. The anticyclonic cells around 8°N and 17°N along 70°E might have developed the troughs, producing a ridge in the interfacial zone [Fig.3.2(i)].

During April-May,the broad anticyclonic gyre accounts for relatively deeper mixed layer in the offshore regions and shallow mixed layer in the southern region. However, the seasonal heating also reduces the layer thickness north of Bombay [Fig.3.3(i)]. In June,the upwelling and sinking interchange their positions and modify the layer accordingly. In the subsequent three months the coastal upwelling and offshore downwelling get strengthened due to strong currents and monsoonal winds, shoaling the layer to 10 m in the coastal waters and deepening to $>$ 100 m in the offshore regions [Fig.3.4 (i)]. The monsoonal cooling, resulting out of heat losses, also contributes to the deepening of the mixed layer. In October, the downwelling weakens and reduces the thickness of the layer, especially, in the offshore waters (from 100 to 60 m). This change is also influenced by current reversal [Fig.3.5 (ii)]. November forms the transition period for interchanging of the positions of upwelling and sinking from coastal to offshore

regions thereby creating cellular features in the topography. [Fig.3.6 (i)].

The mean monthly temperatures in a two degree quadrangle of the present analysis enables only a general comparison with earlier works but not a point to point comparison. Very few works cover monthly conditions of mixed layer in the Arabian Sea. Wyrtki (1971) presents bimonthly mixed layer maps. Direct comparison can not be made because of large grids used by Wyrtki and smoothening by clubbing the data of two months. There is a general agreement of his maps with the present ones. However, during peak winter and southwest monsoon the extreme values of the mixed layer differ by 30-50 m. Further, many ridges and troughs are not depicted in his maps. Several contrastive inshore and offshore features of the mixed layer are not apparent due to coarse spatial resolution. Robinson et al. (1979) depicts monthly maps of the top of thermocline (1.1°C fall from SST) which are in general agreement within 20 m. Although the annual trend agrees, the ridge and trough structures are not clear due to difference in data densities. On a wider spatial coverage,Colborn (1975) documents the seasonal features of thermal structure. There is a broad agreement in the overall annual ranges of mixed layer but the topographies can not be directly compared due to average conditions in 5 degree grid.

Some investigations cover the complete annual cycle but confine to specific regions. From the monthly thermal conditions in the area

7 -14°N, 73.5 -77.5°E, Sharma (1966) utilises the top of the thermocline to identify upwelling and sinking and reports its range from 40-130 m during November to February and 100-10 m during March to August against the present figures of 20-90 and 90-20 respectively. The deviations might be due to different criteria adopted for the top layer and average conditions in a two degree latitude-longitude quadrangle in contrast to his synoptic picture. He relates them to inshore sinking and offshore upwelling and interchange of these processes during these two periods. He confirms these results with his subsequent works (1968, 1978). The present results supplement these features. Narayana Pillai et al. (1980) document the top of the thermocline in the coastal waters between Tuticorin and Ratnagiri recording 40-80 m during the period of sinking and 10-30 m during upwelling, which deviate generally by 10-20 m from this analysis. However, shallow mixed layers of ~40 m reported by them are unusual during winter and might have resulted out of the shallowness of some regions near the coast. Basil Mathew (1982) examines the thermal structure variability in relation to upwelling and sinking between Quilon and Ratnagiri and reports similar trends in the mixed layer.

Apart from these works some studies report MLD values in different regions based on synoptic conditions. Patil and Ramamirtham (1962) point out MLD values of 65-80 m off Laccadive Islands in December, which agree with the present values. However, Patil et al.(1964) suggest low MLD values of 20-30 m between Cape Comorin and Veraval during January to May. They can be considered as underestimates since such low values during winter are unusual.

In the region between 5 -20°N and 50 -75°E during southwest monsoon, Sastry and D'Souza (1970) report mixed layers of 100-20 m with depths decreasing east of 60°E. They attribute low values in the coastal regions to upwelling and high values in the central regions to a clockwise gyre, which are in agreement with the present results. Rao et al.(1976) document a rise in MLD values from 15 m (70 -75°E) to 50 m (65 -70°E) in the zonal belt of 10 -15°N during May to July, attributing it to wind activity, which is nearly confirmed by the present values. Ramesh Bau et al.(1976) indicate a deepening of about 15-40 m around 20°N and 71° 30'E during May to July and attribute to strong winds. Ramam et al.(1979) find a similar deepening at 11° 30'N and 16°N in the eastern Arabian Sea during the same period and relate to wind mixing. These results generally agree with the present study.Ramesh Babu et al.(1980) indicate mixed layers of 75-100 m decreasing towards south off the west coast of India in early March. These values differ by about 20 m because of present method of averaging in 2 degree grid. Analysing the thermal characteristics in the northern Arabian Sea (north of 17°N), Varma et al.(1983) attribute the deep mixed layer of about 125 m during winter to winter cooling, which is in accordance with the present analysis.

Some studies (Rao et al.,1981, 1983; Ramesh Babu and Sastry,1984) document the deepening of mixed layer by 20-40 m at selected points in the central Arabian Sea and Bay of Bengal through MONEX data sets and attribute to convective turn over and curl of wind stress. Sastry and Ramesh Babu (1985) report shallow mixed layer in the coastal regions and deep mixed layer in the central Arabian Sea under the

influence of anticyclonic gyre, producing coastal upwelling and offshore sinking. Rao (1986) supplements the deepening of the mixed layer by 25-35 m in the offshore waters off Bombay and Mangalore during southwest monsoon and relate it to the heat losses from the sea. Similar results are obtained in the present study also.

CHAPTER IV

CHAPTER IV

THERMAL ANOMALY

In this analysis, the thermal/temperature anomaly is considered as the deviation of monthly mean temperature from the annual mean temperature at each grid point. The depiction of such anomalies for different spatial grids at a depth for a month gives the departure of that month's mean temperature from the annual mean temperature at that depth. Such presentation can not be achieved from the conventional isotherm plotting at a particular surface or from the time series vertical temperature section. The sequence of monthly temperature anomalies at a depth delineates the regions of heat sources and sinks. A comparison of such maps at different depths provides a qualitative estimate of the vertical circulation, like intensity and persistence of upwelling and sinking.

The temperature anomaly maps are prepared for 3 different depths viz. 0, 50 and 100 m and presented in Figs. 4.2 and 4.3. It may be noted that the positive temperature anomalies represent warming of the waters and negative anomalies, cooling.

4.1.2 Sea surface [Figs. 4.1 (i) and (ii)]

In January, negative temperature anomalies at the sea surface prevail throughout the area under study. The negative anomalies decrease from north (-3°C) to south (0°C) due to gradual weakening of winter

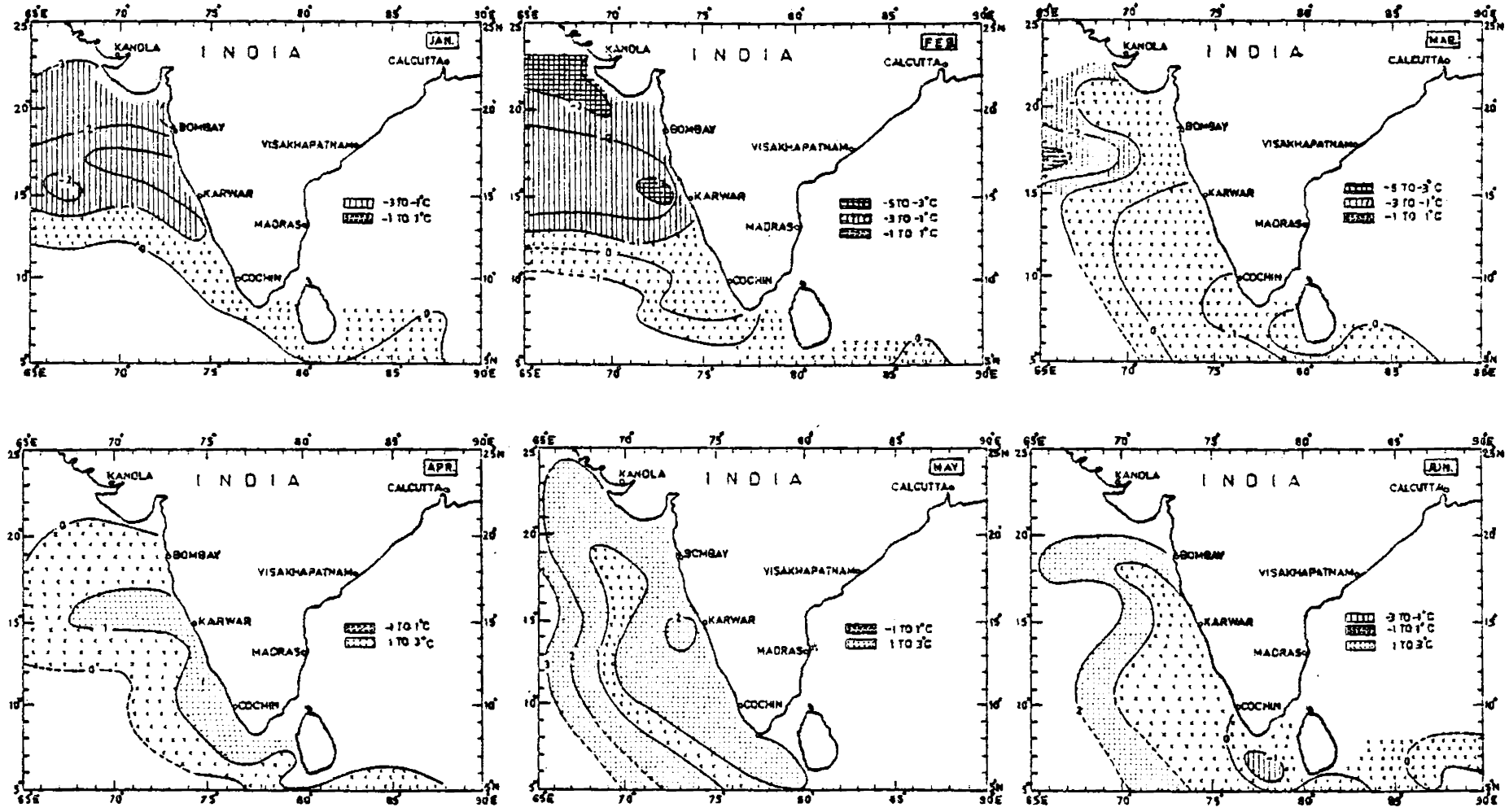

FIG. 4.1(i) THERMAL ANOMALY DISTRIBUTION AT 0 m (January to June)

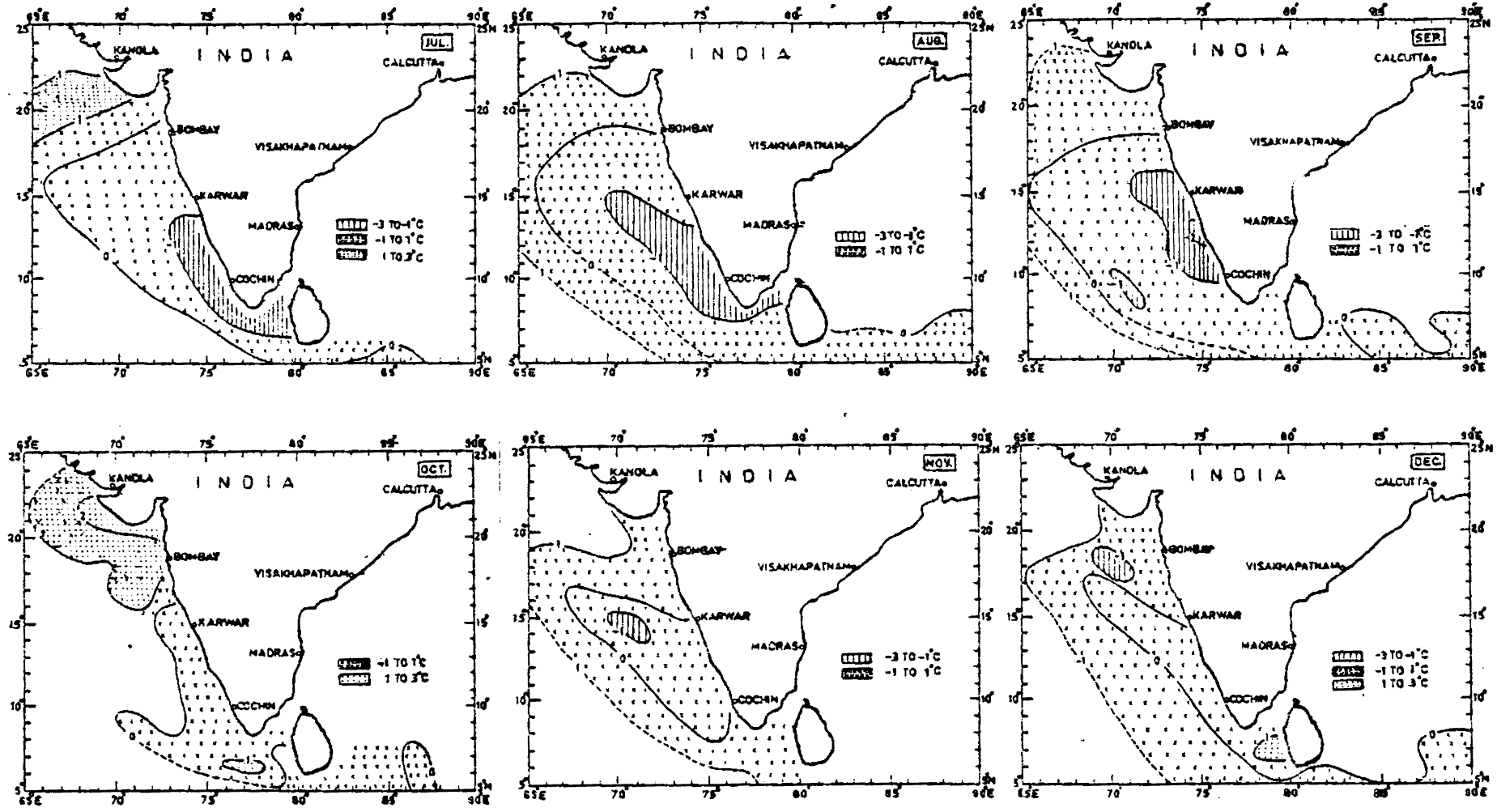

FIG. 4.1 (ii) THERMAL ANOMALY DISTRIBUTION AT 0 m (July to December)

cooling towards south. The anomaly of 0°C appears south of Mangalore as a result of intrusion of Bay of bengal waters into this region. Such flow, normally, sets in during November and continues upto February (Varadachari and Sharma, 1967). During this period, along the east coast of India, the southerly current brings cool and less saline waters from the north and the flow of this water into southeastern Arabian Sea reduces the temperature, producing the anomaly of 0°C. Similar flow is reported by Ramamirtham and Jayaraman (1960). Subsequently, such an inference is supported by several authors. This flow of water reduces the temperature and along with the north equatorial current produces the anomaly of 0°C. A similar anomaly pattern continues in February. The appearance of -1°C in the southeast Arabian Sea might be associated with the retreat of the warm equatorial current (Varadachari and Sharma, 1967). The tongue-like structure (-2 to -3°C) off Ratnagiri might have developed due to the inflow of southerly current (Varadachari and Sharma, 1967) bringing the cold waters from the north. The winter cooling also contributes to the negative anomaly. By March, there is a general fall in the negative anomalies in the entire area under study, indicating the initiation of pre-monsoon heating. The tongue structure off Ratnagiri shifts offshore and disappears by April. The progressive warming of the waters in the eastrn Arabian Sea and southwest Bay of Bengal during March to May is clearly seen by positive anomalies of 1 to 3°C. The seasonal vertical thermal structure (Figs. 2.1 to 2.6) also indicates similar heating. In June, the anomaly pattern, in general, reveals the cooling of the surface water by about 1°C due to monsoonal cooling. But the temperature anomalies around peninsular India dropped to $<$0°C as a result of upwelling. In this month, south-

southeast currents of 0.5 - 0.8 m/s (Varadachari and Sharma, 1967) and west northwesterly winds of 4-5 m/s prevail in this region (Hasternath and Lamb, 1979). Such a flow regime favours upwelling and the upwelled waters surface in this region. The negative temperature anomalies further increase from -1 to -2°C and extend upto Karwar in the subsequent three months due to the northward extension of upwelling and the monsoonal cooling.

There is a significant change in the anomaly pattern in October. The isopleths exhibit closed cells in October in response to the transition conditions from southwest to northeast monsoon. The anomalies increase in the eastern Arabian Sea due to several factors, like cessation of upwelling, retreat of monsoonal cooling and commencement of secondary heating. In November, the positive anomalies decrease from 2 to 1°C in the northern region, particularly off Saurashtra and Bombay coasts, due to winter cooling. In the southern region, the negative anomalies disappear because of the commencement of sinking. By December, the winter cooling produces negative anomalies of about -1°C in the northern region. Further, the cooling observed in the southern region might result out of inflow of Bay of Bengal waters as discussed under the January conditions.

4.1.3 50 m depth [Figs. 4.2(i) and (ii)]

Thermal anomaly conditions in January reveal positive values (0 to 2°C) in the coastal belt south of Bombay and negative (-1°C), in the remaining areas. The isopleths of anomaly run almost parallel to the coast, indicating warming near the coast and cooling in the offshore waters. The northwesterly current flows at the surface along

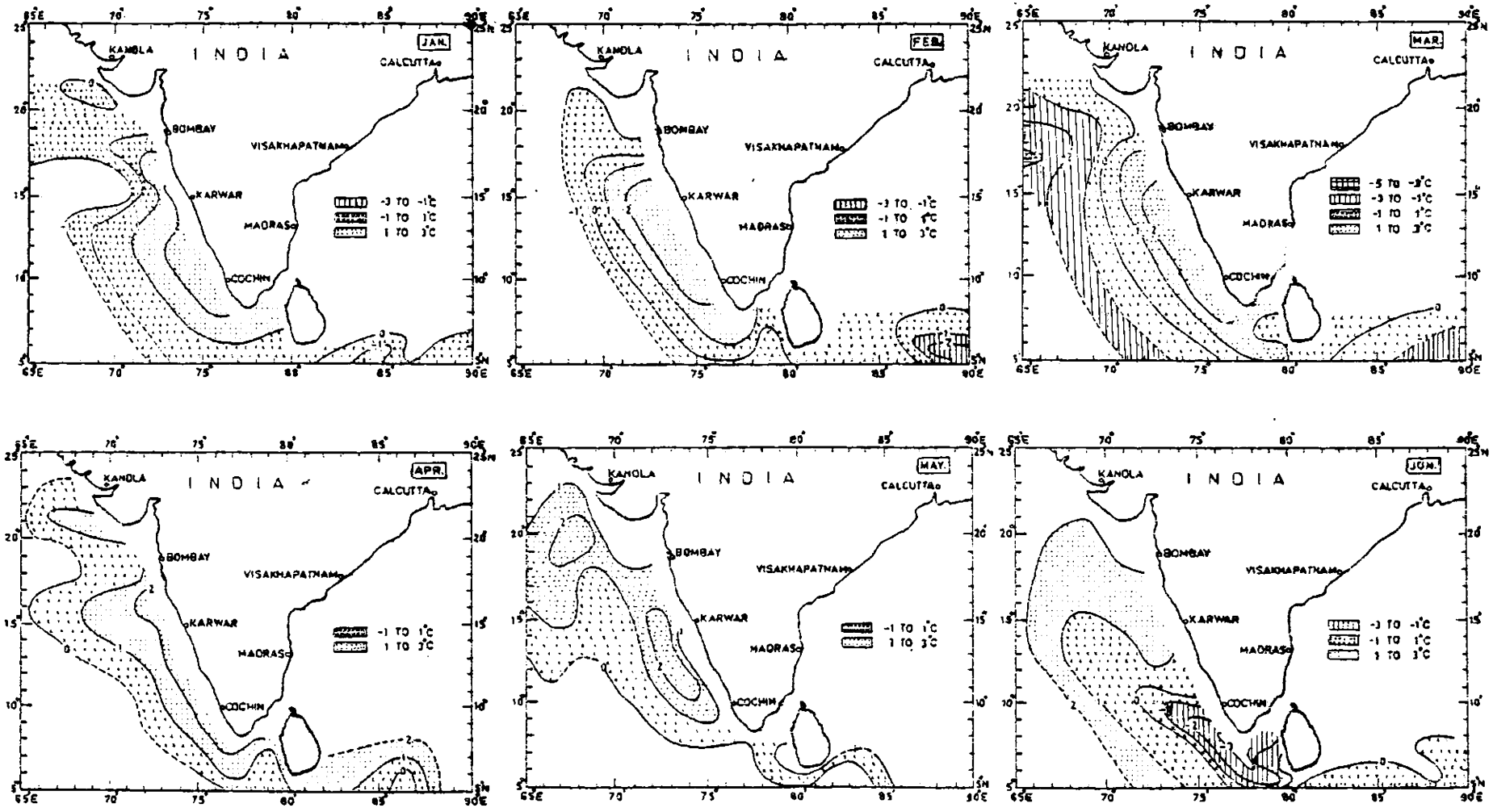

FIG. 4.2 (i) THERMAL ANOMALY DISTRIBUTION AT 50 m (January to June)

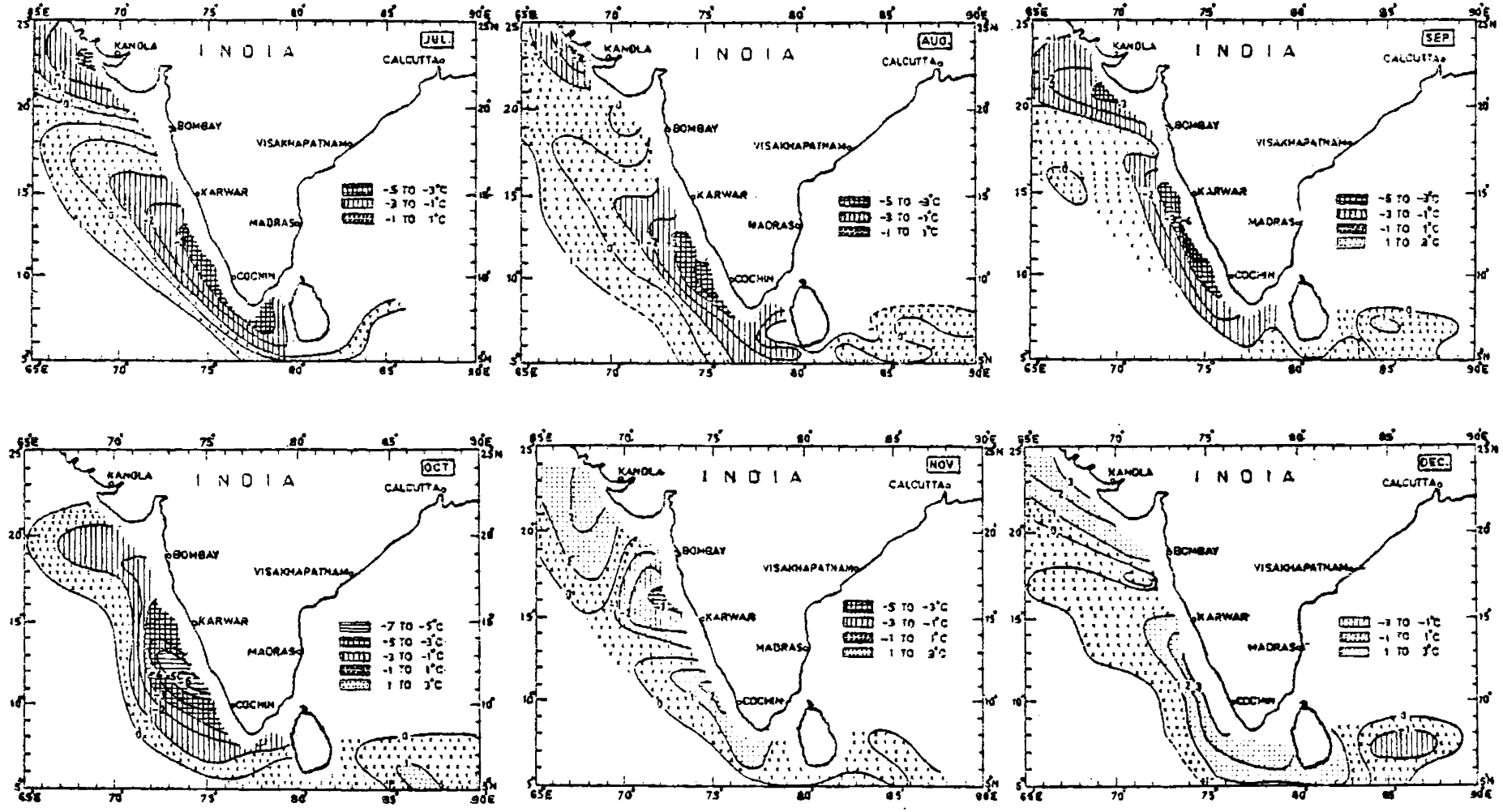

FIG. 4.2 (ii) THERMAL ANOMALY DISTRIBUTION AT 50 m (July to December)

the west coast of India in this month, causing sinking in the coastal regions (Sharma, 1966, 1968, 1978; Banse, 1971; Narayana Pillai et al., 1980; Basil Mathew, 1982) and upwelling in the offshore regions, which can account for the observed anomaly pattern. The low anomalies ($\sim$ 0°C) off Saurashtra coast might be associated with the upwelling (Carruthers and Gogate, 1959; Jayaraman and Gogate, 1959). The anomaly pattern in February is almost similar to that in January. In March, the lateral gradients of anomaly strengthen (-3 to 3°C). On comparison of the anomaly values of earlier months, February appears to be the cessation time for offshore upwelling. It is probable that the mass readjustment follows the cessation of upwelling and the horizontal gradients of the anomaly might build up in this process. By April, the negative anomalies in the northern region are replaced by positive values. Such conditions reveal warmer waters at this depth compared to February/March, which may arise out of seasonal heating (Colborn, 1975). The vertical seasonal thermal structure (Figs. 2.1 to 2.6) also reveals the seasonal heating during April to May at this level. Further, in the southwestern Bay of Bengal, higher positive anomalies appear at this depth compared to surface values. But, the same analogy can not be applied here as seasonal changes are less in this region. An easterly surface flow (Varadachari and Sharma, 1967) brings warm saline Arabian Sea Waters which sink in this area giving rise to positive anomalies.

By May, a fall in the anomaly values by about 1°C can be noticed in the coastal regions south of Mangalore. The southerly flow at the surface in the coastal region (Varadachari and Sharma, 1967) is conducive for upwelling. But, its non-extension to regions north of Karwar in May confirms the early onset of upwelling in the south and its graudal extension to north (Sharma, 1968; Narayana Pillai et al., 1980; Basil Mathew, 1982). Although the surface flow is southerl

even in April, the expected cooling due to upwelling at this level is probably masked by seasonal heating. The increase in the positive anomalies north of Bombay compared to previous month may result out of the seasonal heat penetration (Colborn, 1975). The anticyclonic flow (Varadachari and Sharma, 1967) in this area can also increase the positive anomalies, through sinking. The topography of the mixed layers [Fig 3.3 (i)] also supports this inference.

By June, the negative anomalies increase along the southwest coast of India revealing an active upwelling in this region. Compared to May conditions, a fall in the positive values of the anomaly (from 2 to 1°C) in the coastal region between Karwar and Bombay occurs due to northward extension of upwelling. However, there is a further increase of positive anomaly north of Bombay, resulting out of a heat source as reported by Wooster et al.(1967) and other investigators. The anomaly pattern in July exhibits significant deviations compared to June. The negative anomalies prevail all along the west coast, including the northern region. Along the west coast of India, the coexistence of inshore upwelling (-ve anomalies) and offshore downwelling (+ ve anomalies) is prominently observed in this month. During July, the southerly surface current strengthens in the entire coastal belt, intensifying the upwelling off the west coast of India. However, such negative anomalies in the northern region are likely to be influenced by the flow of cold water off Somalia and Arabia coasts during the southwest monsoon. There is not much change in the pattern or in the values of thermal anomaly during August to September, except that maximum negative anomaly (-4°C) is recorded off the southwest coast of India in August, suggesting the peak intensity of upwelling in

this region. These features are well supported by the variability of thermal structure during the southwest monsoon (Figs. 2.1 to 2.6). In the Bay of Bengal, the anomaly exhibits similar pattern during June to July. The negative anomalies in August might have been developed owing to the inflow of upwelled waters from the western Arabian Sea into this region through easterly flow and also from the local upwelling (La Fond, 1954a).

In October, another typical transition month from the southwest to northeast monsoon, maximum lateral gradients of the anomaly are noticed. The situations in October and March are simliar, but the patterns are interchanged. Such pronounced gradients might have been produced by mass readjustment after the cessation of upwelling in coastal waters in September. November is marked by a differnt pattern with positive values in the coastal regions except between Karwar and Bombay, with a decrease towards offshore areas. The anomaly values between Karwar and Bombay, although negative, show warming tendency when compared to October. Such a situation reveals downwelling in the coastal regions caused by an anticyclonic gyre off Saurashtra coast along with the flow in the remaining areas (Varadachari and Sharma, 1967) and offshore divergence. The positive anomaly values in this month are likely to be affected by the secondary warming (Colborn, 1975) during this period as seen in the vertical thermal structures [Figs. 2.2 (i), 2.4 (i) and (ii)]. The anomaly conditions in December further confirm these processes, with positive anomalies prevailing even in the coastal waters between Karwar and Bombay.

4.1.4 100 m depth [Figs.4.3 (i) and (ii)]

The temperature anomalies at this depth exhibit a greater range of variation almost throughout the year compared to any other depth. A comparison of the monthly anomalies at various depths indicates that the 100 m depth is exposed to the maximum influence of upwelling and sinking by virtue of its location either in the upper part of the thermocline or within it throughout the year. Such large seasonal changes of temperature around this depth are reported by Sharma (1968), Colborn (1975), Narayana Pillai et al. (1980) and Basil Mathew (1982).

In the southwest Bay of Bengal, the anomaly pattern, in general, displays bands of alternate positive and negative anomalies except in some months, where there are data gaps. In this region, the mean monthly temperature profiles are evaluated from relatively less number of data points. Hence, the mean conditions might not have smoothened internal waves.Alternatively, they can be produced due to Rossby/Kelvin waves propagating usually in the equatorial belt, which are also noticed in the vertical temperature sections around 6°N (Figs. 2.5 and 2.6). But, their propagation through the same latitudinal belt in the Arabian Sea might have been prevented by Sri Lanka, which creates a shadow zone in its lee.

The negative thermal anomalies in the coastal waters and the positive anomalies in the offshore waters in January and February suggest the continuation of inshore downwelling and offshore upwelling, as noticed at 50 m depth. In February, south of peninsular India, a mild cooling is observed, probably due to the commencement of upwelling. Such cooling is not noticed at 50 m level, indicating the early onset of upwelling at deeper depths as mentioned earlier. Similar

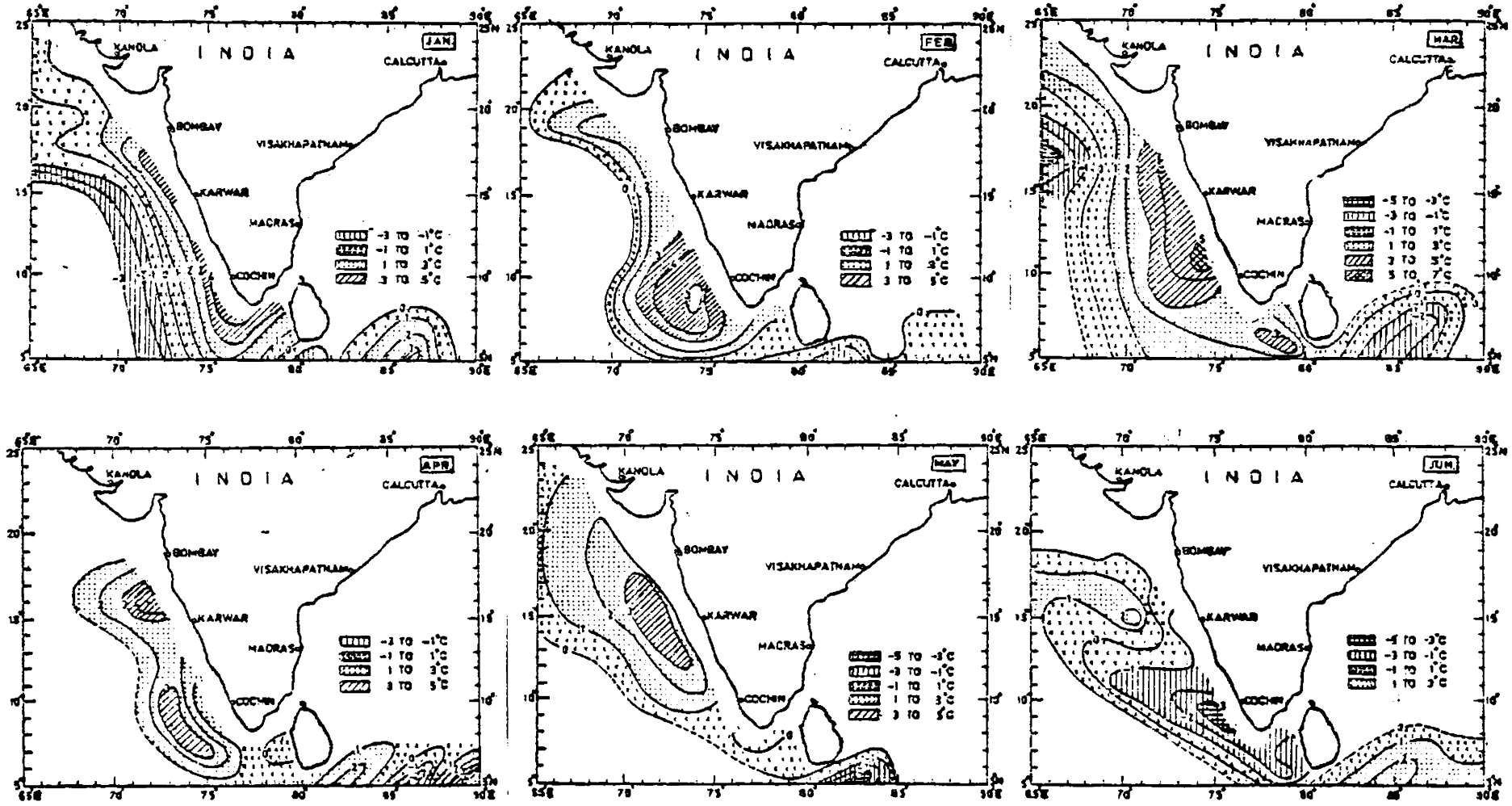

FIG. 4.3 (i) THERMAL ANOMALY DISTRIBUTION AT 100 m (January to June)

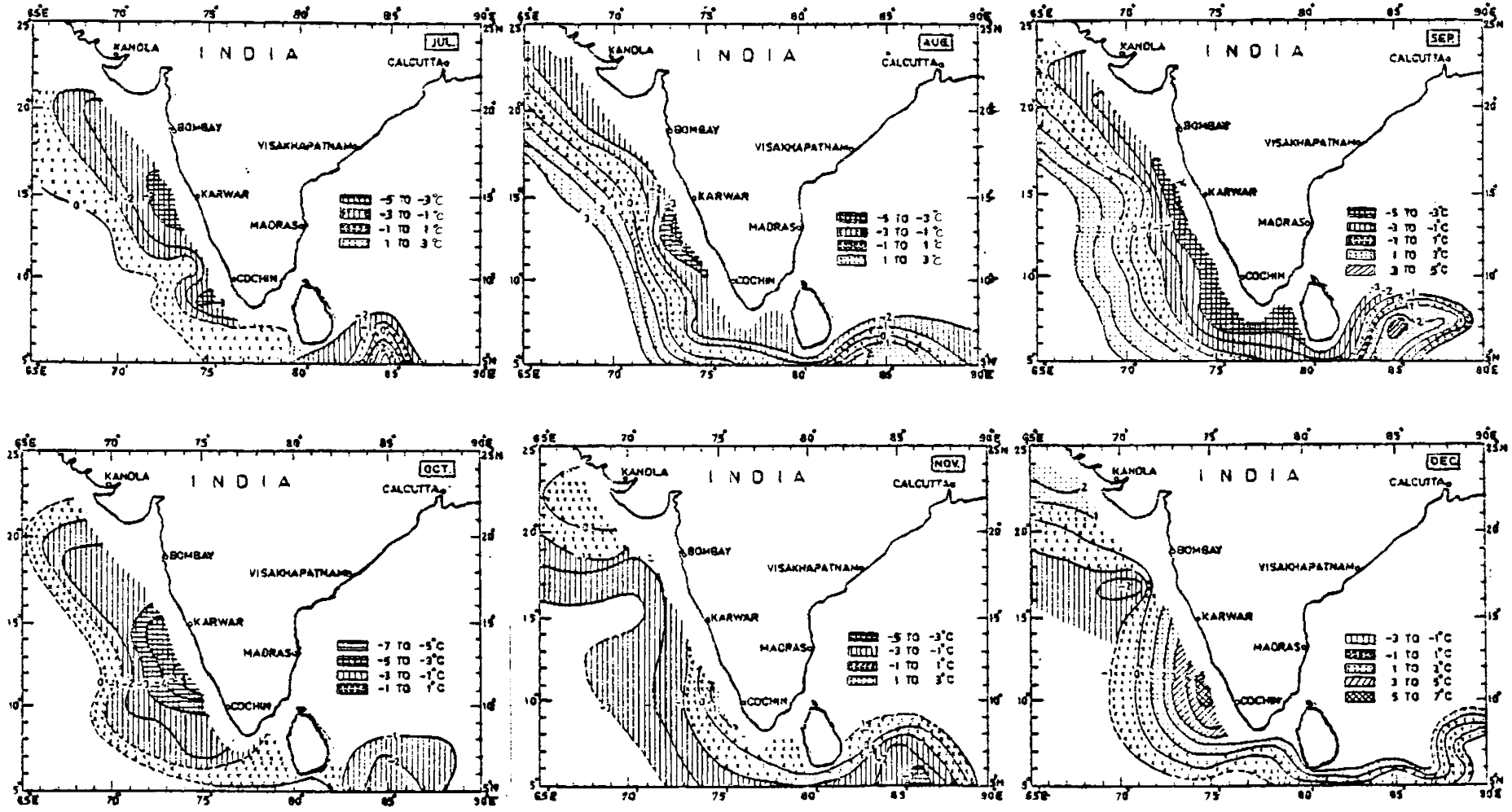

FIG. 4.3 (ii) THERMAL ANOMALY DISTRIBUTION AT 100 m (July to December)

anomalies prevail in March, except for a slight northward extension of the upwelled waters, compared to February. The sinking still continues in the coastal waters in the northern regions as shown by positive anomalies, because the flow in these areas has not completely reversed. A fall of about 1°C in the anomalies south of Karwar in April shows the gradual extension of upwelling towards north supporting the early occurrence of upwelling in the southern regions. By May, the upwelled waters reach Bombay as the anomalies indicate a cooling of about 2°C. A comparison of the anomalies with those at 50 m level in this region indicates the commencement of upwelling at 50 m in July. Therefore, the upwelled waters reach the 50 m depth within 2 to 3 months, suggesting the intensities of upwelling of 17-25 m/month, which agree with the values mentioned in Chapter II and those reported by earlier studies (Sharma, 1978; Narayana Pillai et al., 1980; Basil Mathew, 1982).

The anomaly map for June presents a different pattern compared to those for previous months. The positive anomalies in farther regions from the coast and the negative anomalies in the coastal regions are associated with divergence and convergence in these areas respectively. The situation continues upto September with slight fluctuations in the anomaly values which adjust according to the changes in the intensity of these processes. The anomalies between August and September indicate the cessation of upwelling in the coastal regions and sinking in the offshore regions at this level. However, these processes are still active at 50 m depth, indicating a time lag for their cessation at upper levels.

In October, the horizontal gradients in the anomalies strengthen in the nearshore waters, possibly due to the mass readjustment, as explained earlier. Normally, the transition periods of at least one

month are indicated in the upper levels, while at 100 m depth such conditions are not apparent. Probably, the transition period at this depth is less than a month.

In November, the anomaly pattern reflects an interchange in the vertical advections, and sinking appears in the coastal waters in a limited area. The temperature changes due to sinking at this level can be expected to be high, as the anomalies show a rise of 5°C between October and November. Similar features of smaller scales are observed at the 50 m level also. The gradual northward extension of sinking in the southern region is evident from the positive anomalies (2 to 4°C) in December.

4.2 DISCUSSION

In general, the mean monthly temperature anomalies in the eastern Arabian Sea are mainly governed by climatic conditions at the sea surface and advective processes at the subsurface levels. To be specific, the temperature anomalies at the sea surface north of Karwar are primarily governed by seasonal changes of heating and cooling (winter and monsoonal cooling) and by lateral and vertical advection processes, south of Karwar [Fig.4.1(i)]. During some parts of the year, the collective influence of these two types of processes is exerted for about 1 to 3 months in some regions. While documenting monthly thermal conditions at the sea surface off Bombay, Jayaraman and Gogate (1957) points out the importance of winter cooling and seasonal heating. In the northern regions of the Arabian Sea, these aspects are stressed by Colborn (1975), Anjaneyulu (1980), Narayana Pillai et al. (1980), Qasim (1982) and Joseph and Pillai (1986). In addition to these aspects, Sharma (1966, 1968, 1978), Narayana Pillai et al.(1980), Basil Mathew (1982) and

Joseph and Pillai (1986) suggest the importance of upwelling and sinking on the seasonal variations of SST and the associated thermal structure at subsurface levels in the southeastern Arabian Sea.

Unlike at the surface, the annual variations of the thermal anomaly at a depth of 50 m are chiefly controlled by lateral and vertical advection processes. The influence of winter cooling and pre-summer heating at this level are confined to 1-3 months. The coexistence of coastal sinking and offshore upwelling during November to March and interchange of these processes during May to September are mainly responsible for the anomaly variations at this depth [Figs.4.2 (i) and (ii)]. Winter cooling in the northern regions during December to February and pre-monsoon heating during April to May influence the conditions at 50 m level [Figs 4.2 (i) and (ii)]. Some of the north-south contrastive features at 50 m, derived from this analysis, are as follows. In the regions south of Karwar, the effect of sinking dominates from November to March, while in the north the winter cooling also influences the anomaly during December to February. The effect of pre-monsoon heating is observed upto April, but the northern region it extends upto June. The upwelling in the southern region sets in at this depth in May extends to the north gradually.

The temperature anomalies at 100 m seem to be governed by vertical advection processes. The sequence of these processes regarding onset/ cessation, duration etc., broadly follows that at 50 m depth with some marginal time shifts. Some of the additional features of the upwelling at this depth, are the onset in February, extension to northern regions by June and cessation by September [Figs.4.3 (i) and (ii)].

The upwelling is noticed to reach 50 m level after a delay of about 2-3 months with the upwelling rates around 17-25 m/month. The vertical velocity is weak in the initial stages of upwelling and it increases subsequently.

The simultaneity of coastal upwelling and offshore downwelling off the southwest coast of India is reported by Sharma (1966). The onset/cessation of upwelling and sinking in different regions, their duration and upwelling rates confirm the earlier investigations by Sharma (1966, 1968, 1978), Banse (1971), Narayana Pillai et al.(1980), Qasim (1982) and Basil Mathew (1982). Further, the periods and penetration of seasonal heating agree with the results of Sharma (1968), Colborn (1975), Narayan Pillai et al.(1980). In addition to these works, several studies (Ramasastry and Myrland, 1959; Banse, 1959; Ramamirtham and Jayaraman, 1959; Rao and Jayaraman, 1966 ; Lonkar, 1971; Sankara Narayanan and Qasim, 1968; Ramamirtham and Rao, 1973; Rao et al., 1974) are carried out on upwelling and sinking in the nearshore regions off the west coast of India confining to short durations and limited areas. The results of this study broadly agree with their findings.

The influence of the climatic conditions on SST variations is quantified in this analysis, based on relatively large data base on a wider spatial coverage. In addition to confirming the characteristics of upwelling and sinking, like onset/cessation, duration, intensity etc. south of Karwar, these are documented in the northern regions (Karwar to Okha) from a relatively large spatial network.

CHAPTER V

CHAPTER V

INTERNAL WAVES

Short-term variability in the upper layers of the ocean is known to be governed by a variety of physical processes, whose time scales vary from a few seconds to a few days. The surface waves, heat energy exchanges on a diurnal scale, internal gravity waves, double diffusion, fronts, strong local and lateral meteorological forcing etc. are all identified as important means in producing the observed short-term variability in the upper layers of the sea (Monin et al., 1974; Turner, 1981). In order to understand the nature of these processes, data sets with fine resolution in space and time are required. Unfortunately, such data sets in the Arabian Sea and Bay of Bengal are relatively few.

During the recent monsoon experiment and in some subsequent cruises, some short time series data sets at selected stationary positions are collected for the first time in an organised manner. These data sets can afford to study the short-term variability at these positions on time scales from diurnal to synoptic events. Utilising these data sets, some studies are made on the short-term variability, observed in the mixed layer, as mentioned in the previous chapters. The corresponding information on the variability in the thermocline is relatively meagre. Hence, it is attempted to study the variability in the thermocline with the aforementioned data sets.

These data sets provide a good opportunity to understand the nature of internal gravity waves and their contribution to the observed variability in the thermocline.

A knowledge of the internal waves is applicable in a variety of marine fields such as OTEC, underwater surveillance, offshore drilling operations, catch potential of certain types of fish, disposal of pollutants, etc. The time series data sets collected at a few stations [Fig. 1] in the Arabian Sea and Bay of Bengal are utilised to study the internal waves. For convenience, the internal wave fields are classified as long-period ($>$ 12 hours) and short-period ($<$ 12 hours) internal waves based on wave periods (Roberts, 1975). The time-depth thermal fields at these locations were presented in Figs.5.1 and 5.2 respectively. The temperature variations in the thermocline within the inertial periods of 41 and 70 hours (for the stations of three hourly sampling) are expected to be influenced by internal waves. The internal wave characteristics such as period, height, speed and wave length are evaluated as discussed in Chapter I.

The Brunt-Vaisala Frequencies (BVF) are evaluated [Eq. (2)] for the short-period internal waves and some of their typical profiles are shown in Fig.5.5. The spectra of long and short-period internal waves and spectra of some generating mechanisms viz. wind, atmospheric pressure and tide are subjected to Fast Fourier Transform (FFT) analysis to get the prevailing harmonics. The normalised spectral estimates against frequency/period of these spectra are depicted in Figs.5.3 and 5.4. Since various spectra of internal waves show similar harmonic

patterns, the presentation is restricted to some typical spectra for clarity. The computational details are given in Chapter I. The results are separately discussed for long and short-period internal waves.

5.2.1 Long-period internal wave characteristics [Fig.5.1]

The long-period internal waves in the sea are generated by various mechanisms like tidal forces (La Fond and Purnachandra Rao, 1954), the flow of water over an irregular bottom (La Fond 1966), atmospheric pressure fluctuations (Krauss, 1959), storms (Pollard, 1972) and current shears (Defant, 1961). Long-period internal waves are studied by La Fond and Purnachandra Rao (1954) off the east coast of India in February and Ramam et al. (1979) off Mahe in the Arabian Sea during May to July. In the Bay of Bengal, there is no information on these wave characteristics during southwest monsoon when the seasonal cycle shows maximum changes in the thermocline region. Hence, it is attempted to document long-period internal wave characteristics in the Bay of bengal and eastern Arabian Sea during southwest monsoon.

The internal waves in the Arabian Sea and Bay of Bengal vary with minimum periodsof about 9 hours and maximum periods of about 25 hours with an average period of 15 hours. These wave fields indicate that they are mainly composed of internal tides (La Fond and Purnachandra Rao, 1954) with periods of semi-diurnal and diurnal tides. The internal wave fields frequently superimpose over inertial oscillations with periods of 41 hours at 17°N and 71°E (Arabian Sea) and 50 hours at 40°N, 89°E (Bay of Bengal). The maximum wave heights at these stations

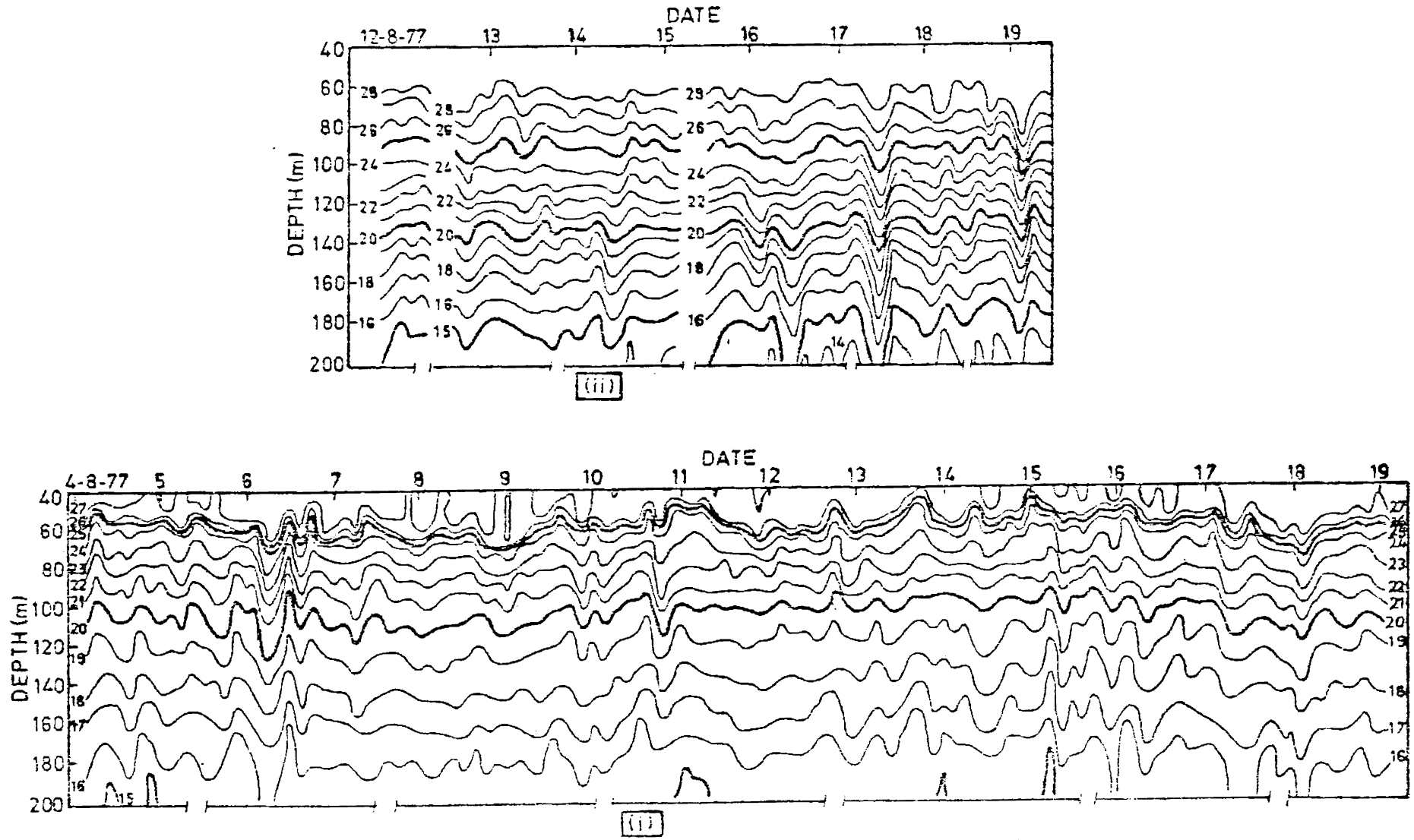

FIG.5.1 SHORT-TERM FLUCTUATIONS OF THERMAL FIELD

(i) Arabian Sea (17°N, 71°E)
(ii) Bay of Bengal (14°N, 89°E)

[Personal Communication, Dr. R.R. Rao]

correspond to 40 and 30 m with average heights of 16 and 13 m in the Arabian Sea and Bay of Bengal respectively. At both these stations the amplitudes of the internal waves show an increase below 100 m, suggesting the nature to be of first order internal waves (Roberts, 1975). At a depth of 50 m in the Arabian Sea and at 70 m in the Bay of Bengal, the internal waves propagate with speeds of 83 and 134 cm/s respectively. Higher speeds in the Bay of Bengal are attributed to greater density difference between the top and deeper layers (0.003218 g/cm^3) compared to that in the Arabian Sea (0.001253 g/cm^3). The wavelengths of the internal waves at these stations correspond to 45 and 77 km respectively.

5.2.2 Spectral characteristics [Fig.5.3]

The harmonics of internal waves correspond to the periods of 16.0, 8.0, 2.0/1.8, 1.0,0.5 and 0.3 days at both the stations in the Arabian Sea and Bay of Bengal, indicating almost a four hour mode oscillation. In both the regions, the dominant harmonic i.e., the harmonic having the maximum spectral level, concentrates around a semi-diurnal period. Generally, 10 to 15% of the energy is concentrated at the dominant harmonic of the internal wave spectra, with the rest of the energy distributed over the remaining harmonics.

The harmonics corresponding to semi-diurnal and diurnal periods are distinctly noticed in the spectra of atmospheric pressure and winds. The energy concentration at the dominant harmonic for the atmospheric pressure corresponds to about 60%, while it reduces to 20 to 35% for the winds, suggesting the distribution of energy over a wide range of harmonics of wind spectra. A secondary prominent peak at the harmonic of inertial period is noticed in the spectra

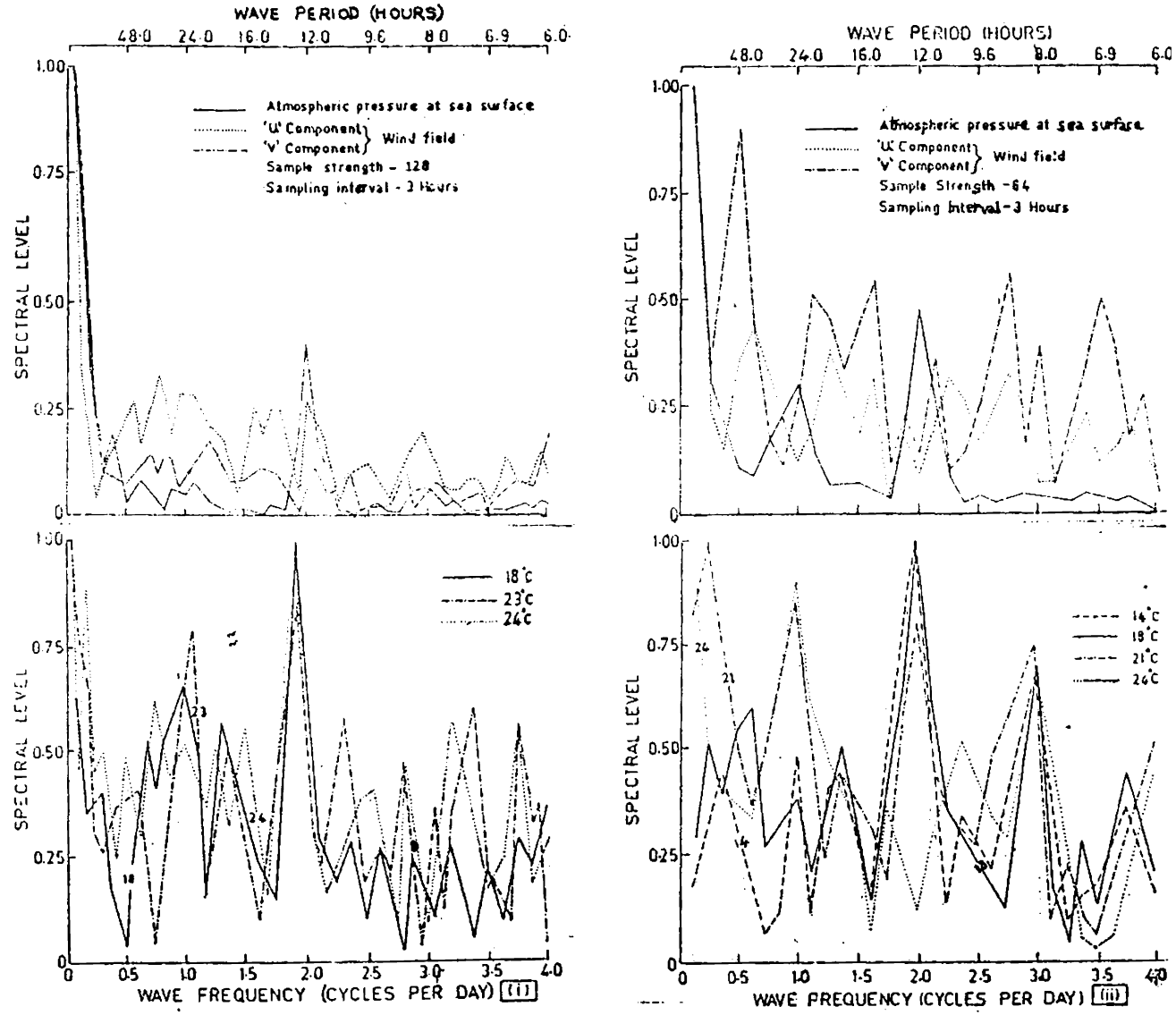

FIG.5.3 SPECTRAL ESTIMATES OF LONG-PERIOD INTERNAL WAVES, SURFACE WIND COMPONENTS AND ATMOSPHERIC PRESSURE
(i) Arabian Sea (17°N, 71°E)
(ii) Bay of Bengal (14°N, 89°E)

of internal waves and surface winds in the Bay of Bengal.

At semi-diurnal frequencies the harmonics of internal waves and atmospheric pressure are coherent, while at non-tidal frequencies, the internal wave and the wind spectra are coherent. The spectra of atmospheric pressure and the internal waves offer evidence that the internal waves of semi-diurnal and diurnal periods might have been generated by tides. The spectra of winds and of internal waves probably suggest that the internal waves of periods less than 12 hours are triggered by local wind force.

5.3.1 Short-period internal wave characteristics [Fig.5.2]

Several mechanisms produce short-period internal waves, like the motion of ship (Ekman, 1904), swell (Krauss, 1967), interaction of long-period internal waves amongst themselves (Gade and Erickson, 1969), storms (Larsen, 1969), the flow over sea mounts (Gade and Erickson, 1969; Zalkan, 1970), wind (Schott, 1971b), and submarine motions (Roberts, 1975). Some information is available on the characteristics of these waves in ther Bay of Bengal and adjacent areas (Perry and Schimke, 1965; La Fond and La Fond, 1968; Antony et al., 1985). But, there is no knowledge on the wave characteristics of these internal waves in the Arabian Sea. Hence, an effort is made to study the characteristics of these internal waves at a few stationary positions in the eastern Arabian Sea (off Cochin and Karwar) during September.

The internal waves in the shelf and deep waters off Cochin show periods ranging from 10 to 50 minutes with mean periods of 19 minutes and maximum heights of 8 to 11 m fluctuating around a mean

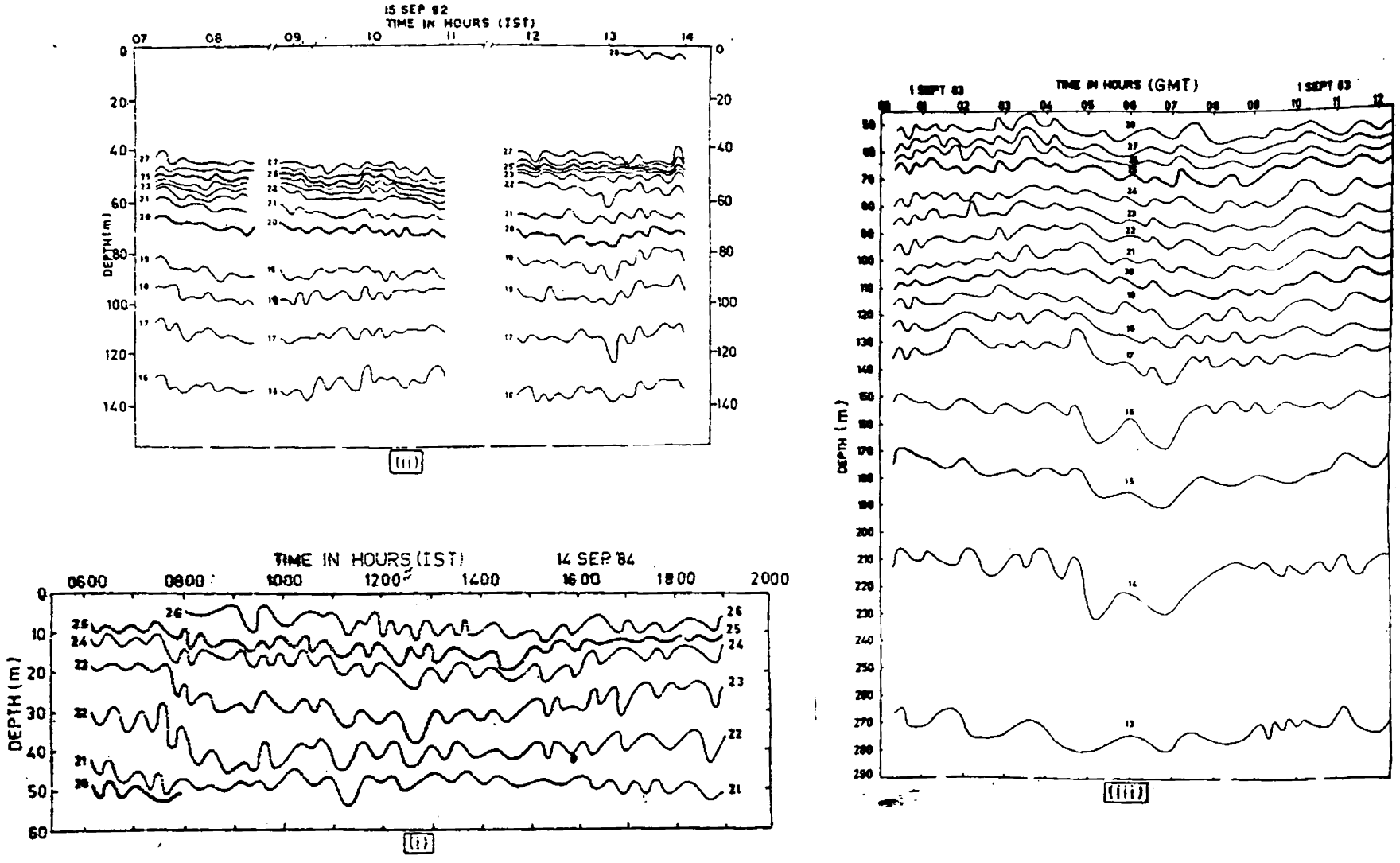

FIG.5.2 SHORT-TERM FLUCTUATIONS OF THERMAL FIELD (°C)

(i) Shelf waters off Cochin (10°00', 75°50'E)
(ii) Deep waters off Cochin (10°N, 73°E)
(iii) Deep waters off Karwar (15°N, 72°E)

height of 5 m. The corresponding values in the deep waters off Karwar are relatively high. The wave periods at this station have a range of 20-120 minutes with an average period of 55 minutes, and maximum wave height of 23 m with an average height of 7 m. The amplitudes of the internal waves increase with depth below 120 m. The energy levels from the generating source and the extent of stratification may be different at these stations giving rise to the observed difference in wave characteristics in the depth regime (La Fond and La Fond, 1968; Brekhovskikh 1975). The internal wave speeds at the top of the pycnocline occurring at 10, 40 and 50 m at these stations correspond to 38, 97 and 99 cm/s respectively, with maximum speed off Karwar and minimum speed in the shelf waters off Cochin. The internal wave speeds seem to be governed more by the density contrast between the top and bottom layers rathern than the thickness of the top layer. The wave lengths of the respective internal waves at these stations are 0.4, 1.0 and 3.0 km. A critical examination of thermal field at these stations reveals the superimposition of these waves over a component of internal tide. In the shelf waters off Cochin, a 25 m thick layer of weak temperature gradient persists in the depth range of 20-40 m. Generally, the internal wave fields are classified as first order, second order, third order, etc. according to the number of maxima (1, 2, 3 etc.) in the amplitudes occurring in the depth domain (Roberts, 1975). The nature of the internal wave fields at these places suggests second order internal waves in the shelf waters off Cochin and first order internal waves at the other two stations.

5.3.2 Special characteristics[Fig.5.4)

The spectral analysis of internal waves off Cochin and Karwar,

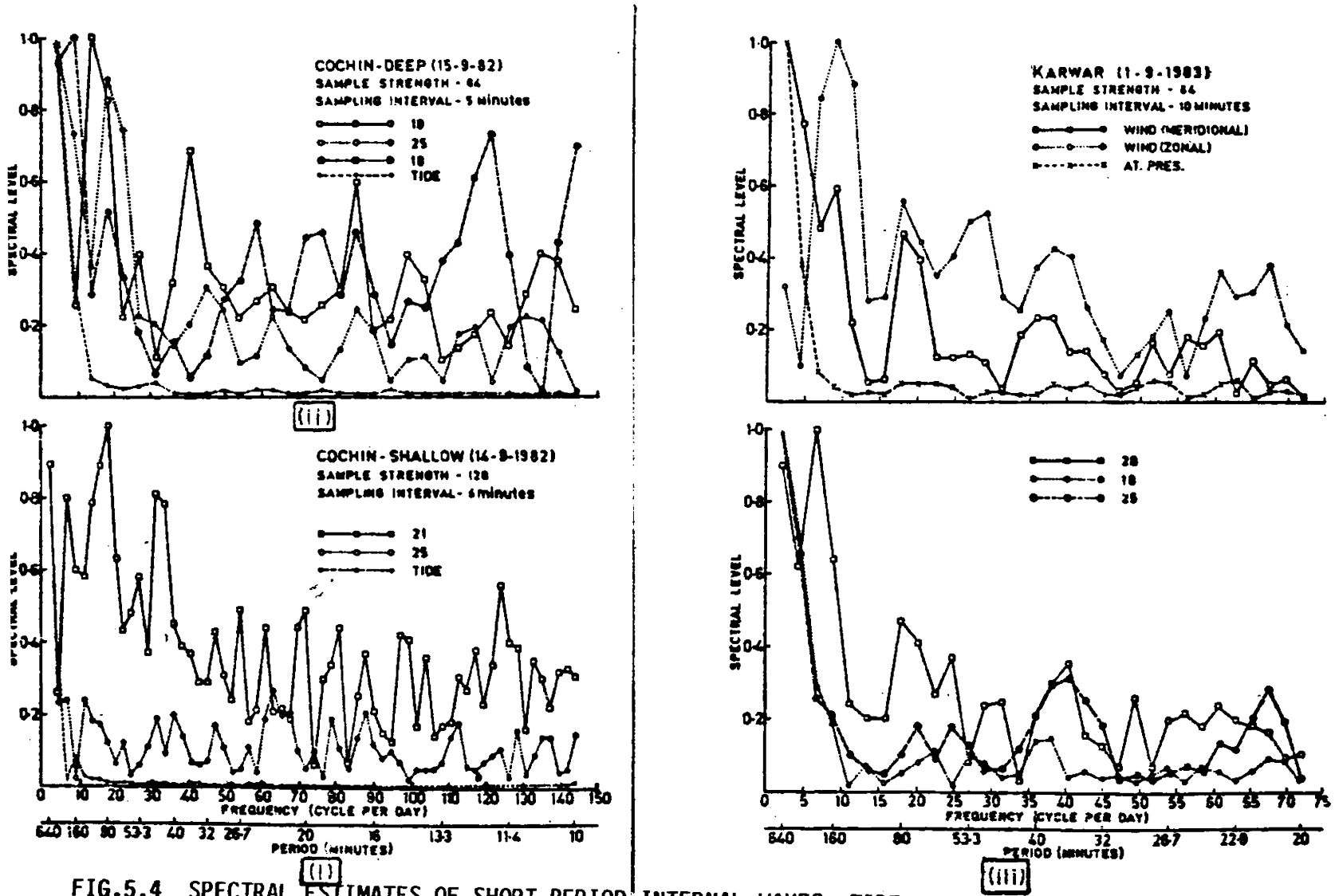

FIG.5.4 SPECTRAL ESTIMATES OF SHORT-PERIOD INTERNAL WAVES, TIDE , SURFACE WIND COMPONENTS AND ATMOSPHERIC PRESSURE

(i) Shelf waters off Cochin
(ii) Deep waters off Cochin
(iii)Deep waters off Karwar

in general, indicates prominent harmonics with periods of 640, 160, 80, 40 and 22 minutes suggesting a 20 minute mode of oscillation at these stations. The dominant harmonics show periods of about 640, 160 and 80 minutes at different depths. Such a mismatch among dominant peaks in the depth domain suggests the possibility of internal waves being produced by more than a single agency. The internal wave spectra in the deep waters off Cochin exhibit moderate fluctuations for harmonics of periods between 10 and 15 minutes. The energy content of the harmonics concentrates around semi-diurnal periods. For some spectra, about 50% of the energy concentrates at the dominant harmonic of period about 640 miniutes. For the remaining spectra, only 33% of the energy is available at the dominant harmonic of period about 80 minutes, indicating a significant energy level at higher frequencies.

The FFT analysis of atmospheric pressure and tide indicates a dominant harmonic of period around 640 minutes with energy concentration of 85 to 90% with virtually no other harmonics. On the other hand, the spectra of zonal and meridional components of the wind show dominant harmonics of periods around 160 and 640 minutes with energy concentration of 30-50% and fair amount of energy levels at harmonics of high frequencies. An examination of the harmonic patterns of the internal waves and winds reveals a striking resemblance in the harmonics at non-tidal periods at these stations. However, the harmonic pattrns of tide/atmospheric pressure and internal waves show similarity at harmonics of tidal frequencies. The similarity in harmonic patterns between the internal wave spectra and wind suggests that the local wind forcing might have acted as a possible generating agency in producing the observed internal waves.

5.3.3 Brunt-Vaisala frequencies (BVF) [Fig.5.5]

The Brunt-Vaisala Frequency (BVF) represents the frequency with which a displaced element of fluid oscillates (Turner, 1981). It can, therefore, be considered as a measure of the static stability of the water column. It sets the limit of the highest frequency (or the lowest period) for the internal waves in the sea.

The range of variation of BVF for the internal waves in the shelf waters off Cochin corresponds to 12-22 cycles per hour (cph), equivalent to periods of about 5 to 3 minutes. A similar range is noticed in BVF off Karwar too. However, the BVF in deep waters off Cochin records a maximum range of 10-28 cph corresponding to periods of about 6-2 minutes. The high range in this region occurs, mainly because of close packing of isotherms (6°C/15m) around a depth of 60 m [Fig.5.1(ii)]. In general, the BVF profiles indicate slightly higher value just below the top of thermocline due to the strong temperature gradient. The BVF profiles for the coastal waters off Cochin on the whole reflect a secondary maximum below 45 m depth and a lyaer of minimum changes (within 3 cph) in the depth region between 20 and 40 m. Such a situation represents a typical feature of second order internal waves. The high values of BVF (16-21 cph), associated with strong variations in the depth range of 50 to 100 m off Karwar indicate more stable medium, resulting out of sharp thermocline. These profiles in the deep waters off Cochin and Karwar below 80 and 100 m exhibit minimum variations with time due to weak changes in the temperature gradients in this depth range. The BVF profiles at these stations show a single maximum, depicting the typical nature of the first order internal waves.

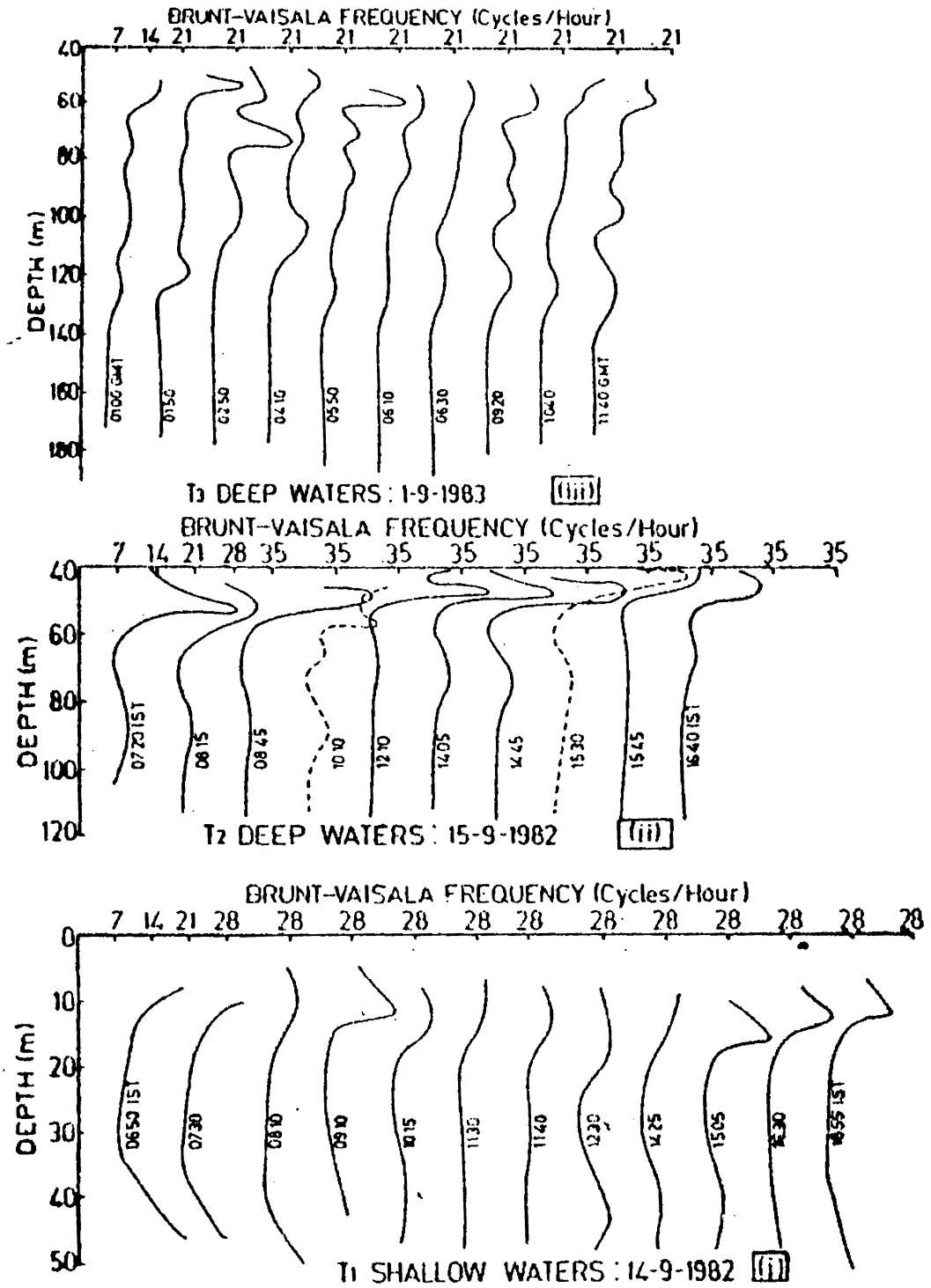

FIG.5.5 BRUNT-VAISALA FREQUENCY PROFILES OF SHORT-PERIOD INTERNAL WAVES

(i) Shelf waters off Cochin
(ii) Deep waters off Cochin
(iii)Deep waters off Karwar

5.4 DISCUSSION

So far, the results of various analyses of this study are discussed in relation to the past works conducted in the Arabian Sea and Bay of Bengal. Since, very few investigations are made in the field of internal waves in these areas, the characteristics of the observed internal wave fields are compared with similar works carried out in other seas also.

The characteristics of short-period internal waves correspond to mean periods of about 19 minutes (10-50 minutes) off Cochin and 55 minutes (20-120 minutes) off Karwar, with average heights of 5 m (maximum height : 11 m) and 7 m (maximum height : 23 m) respectively. They are found to propagate with speeds of 38 cm/s in the shelf waters off Cochin and about 98 cm/s in the deep waters off Cochin and Karwar with respective wavelengths of 0.4 km and 1.0 and 3.0 km. Short-period internal waves of similar order are reported by several investigators. From the time series BT operations Perry and Schimke (1965) near Sumatra region and La Fond and La Fond (1968) near Calcuttta and Thailand document similar waves. Internal waves of similar characteristics are noticed from moored thermistor chains by Ziegenbien (1969,1970) in deep waters of the Gibraltar Strait, Halpern (1971) in the shelf waters of the Massachusetts Bay, Maeda (1974) in the Sagami and Tachibana Bays, Brekhovskikh (1975) near Seyshells and Maldives and Midorikawa (1977) in the Sagami Bay. Through current meter moorings Briscoe (1975b) in Sargasso Sea and Antony et al.(1985) off Machilipatnam in the Bay of Bengal document similar waves.

Perry and Schimke (1965) report waves with amplitudes of 41 m due to shear in the frontal zone. The difference with the present amplitudes may be due to relative strengths of different generating mechanisms. Halpern (1971) observes waves of similar amplitudes but reports wave periods of 6 to 8 minutes, which could not be identified in the present study because of sampling limitation. Antony et al.(1985) suggest low wave speeds of about 13 cm/s against the present value of 38 cm/s, probably, because of the shallowness of the station ($\sim$ 25 m).

The present study reveals long-period internal waves in the Arabian Sea and Bay of Bengal with periods corresponding to semi-diurnal tide, diurnal tide and inertial oscillations with mean period around 15 hours (9-25 hours). Their average height is around 14 m (maximum heights of 40 and 30 m). They are found to move with speeds of 83 cm/s in the Arabian Sea and 134 cm/s in the Bay of Bengal with corresponding wave lengths of 45 and 77 km respectively. Internal waves of similar characteristics are reported by La Fond and Purnachandra Rao (1954) in the central Bay of Bengal, Maeda (1974) in the Sagami Bay and Ramam et al. (1979) off Mahe in the Arabian Sea. Both Maeda(1974) and Ramam et al. (1979) suggest higher speeds of 300 and 213cm/s. The bottom layer in the computation of Ramam et al. (1979) extends to 1930 m against the present values of 130 and 150 m. The difference in speeds can be attributed to the higher density difference between top and bottom layers in their study. The variation of the amplitude and period of the observed short-period internal waves with time might occur due to the interaction between short and long-period internal waves, as proposed by Maeda (1974) and Roberts (1975).

The short-period internal wave fields are superimposed on a tidal component. A layer of weak temperature gradient is sandwiched in the depth range of 20-40 m in the coastal waters off Cochin. As this weak temperature gradient persists throughout the observational period and not in the form of patches, the contribution from the internal wave breaking appears to be remote (Woods and Wiley, 1972). In this area, upwelling still persits in September. Under its influence, the opposing flows in the depth regime (Basil Mathew, 1982; Shetye, 1984) create shear (Federov, 1978) which can generate a layer of weak temperature gradient. Such layers of weak temperature gradient are reported by La Fond and La Fond (1971), Ramesh Babu et al.(1976), Ramam et al.(1979), and Turner (1981). The observed wave fields are of second order internal waves in the shallow waters off Cochin and of first order at the other stations. Similar first and second order internal waves are reported by Maeda (1974) in the Sagami Bay and Roberts (1975) as a general feature.

The spectral analysis of short-period internal waves suggest predominant harmonics with periods of 640, 160, 80, 40 and 22 minutes, indicating a 20 minute mode oscillation. The dominant harmonic for some spectra occurs at 640 minutes (about semi-diurnal period), while for other spectra, it shifts to 160 and 80 minutes. About 50% of the energy is concentrated at the harmonic of semi-diurnal period. Such energy concentration at tidal frequencies is reported by Fofonoff (1969), Halpern (1971), Schott (1971a) and Siedler (1971). Therefore, a significant content of energy is still available at other harmonics.

A wide scatter in the energy levels is noticed for harmonics of period 10-15 minutes too. Such energy peaks at relatively high frequencies corresponding to periods of 2-6 hours are reported by Schott (1971a) and of 1-12 minutes, by Brekhovskikh (1975) and Midorikawa (1977). However, in the present study, the energy contents for the harmonics of periods less than 10 minutes can not be accounted for due to sampling limitation.

The spectral characteristics of long-period internal waves reveal predominant harmonics of inertial, diurnal, semi-diurnal and 8 hour periods, suggesting a 4 hour mode of oscillation against a 20 minute mode in short-period wave field. In contrast to short-period internal waves, the energy concentration in the long-period internal waves at dominant harmonics is quite low i.e., 10-15% (30-50% in short-period waves) indicating that the energy is mostly distributed over a wide range of harmonics. Similar features are noticed by Briscoe (1975b) in Sargasso Sea. The energy concentration at inertial frequencies is suggested by Fofonoff (1969), but no such feature is indicated in this analysis.

The similarity in the harmonic patterns at high frequencies between short-period internal waves and winds suggests that the local wind force may generate these internal wave fields. Schott (1971b) and Roberts (1975) propose the winds as a possible generating mechanism for short-period internal waves. A good resemblance in the harmonic pattern of tides (or atmospheric pressure) and internal wave fields of tidal and inertial periods indicates that the tidal forces might have acted as a generating agency for the long-period internal waves.

La Fond and Purnachandra Rao (1954) attribute the genesis of internal waves of tidal periods in the central Bay of Bengal to tidal forces. Roberts (1975) supplements the same hypothesis.

The BVF values of the internal wave fields correspond to a general range of 10-28 cph equivalent to periods of 6-2 minutes. Similar values of BVF are reported by Maeda (1974), Midorikawa (1977) and Antony et al. (1985). Generally, the BVF profiles record a maximum value just below the top of thermocline due to strong temperature gradient. These profiles have shown the typical features associated with second order internal waves in the shelf waters off Cochin and first order internal waves at the other stations. Maeda (1974) documents similar first and second order internal waves in the shelf and deep waters of the Sagami Bay.

In this study, the internal wave characteristics are analysed at a few stations in the Arabian Sea and Bay of Bengal. However, these characteristics vary in spatial and temporal domains and as such, they can be regarded as local features only. The consistency of the internal wave characteristics could not be studied due to limitation on the operational duration. The present study is confined to the influence of two generating mechanisms. However, future investigations based on comprehensive time series data sets can lead to a better understanding on various generating mechanisms of the internal waves.

CHAPTER VI

CHAPTER VI

SUMMARY AND CONCLUSIONS

A comprehensive understanding of the regional thermal structure emerges from a combined study of the seasonal and short-term variations in the temperature field. With this objective, an attempt is made in the present study to document the nature of seasonal and short-term variability in the temperature field in the upper layers of the eastern Arabian Sea and southwestern Bay of Bengal, in relation to the physical and dynamical processes involved. Such processes constitute the seasonal changes in the surface climatic conditions, heat exchange processes at the sea surface, circulation regimes in the upper layers, and internal gravity waves. This investigation confirms some earlier results and brings out several new features.

The mechanical bathythermograph (MBT) data, pooled from various sources and expeditions/cruises, were grouped into two degree latitude-longitude quadrangles and the monthly mean temperature profiles were evaluated for the area under study.

The seasonal thermal structure in the upper 275 m water column for different two degree grids was prepared separately for coastal (depth $<$ 200 m) and offshore (depth $>$ 200 m) areas to compare and contrast the observed features in the shelf and deep waters. The presentation of thermal structure was restricted to a few selected places

representing the regional characteristics of the northern and southern regions.

The mixed layer depth, based on a temperature drop of 1°C from SST, was evaluated from the mean monthly temperature profile, for each two degree quadrangle. Monthly topography of mixed layer was presented for the area under study. The temperature anomaly in each two degree quadrangle was evaluated as the deviation of monthly mean temperature from its annual average. The mean temperature anomalies were depicted for each month for the area under study at three typical depths viz. 0, 50 and 100 m.

The seasonal variability of thermal field was examined from the seasonal thermal structure, mixed layer topography and thermal anomaly patterns.

The time series data sets of MBT, marine meteorological elements sampled at close intervals of time at some stationary positions in the Arabian Sea and Bay of Bengal, and tide data were utilised to study the short-term fluctuations of temperature caused by internal gravity waves. It is attempted to document the internal wave characteristics and discuss their possible generating mechanisms.

Along the west coast of India, the annual cycle of SST shows a bimodal oscillation upto Kandla (23°N) in the coastal waters (earlier studies documented upto Ratnagiri). Such a signal is prominently noticed in the offshore waters in the Arabian Sea south of 15°N.

In the other areas under study, a unimodal oscillation is noticed. The annual cycle in MLD distribution closely follows the bimodal or unimodal signal of SST, with a few exceptions. The annual range of SST records a maximum value of 5.5°C in the northern regions (north of Bombay - 19°N) and a minimum value of 1.0°C in the southern region (south of 8°N).

During winter, thermal field in the upper 150 m of the coastal waters is observed to respond to both sinking and winter cooling in the northern regions and to sinking alone in the southern regions. Such features are also reflected in the mixed layer topography and thermal anomaly patterns. The seasonal heating warms up the upper 50-70 m water column during March to May and October to November. Under its influence, the topography of the mixed layer shows a general shoaling. Such conditions are also seen in the thermal anomaly distribution at 50 m depth.

South of Cochin, the seasonal variation of thermal structure and temperature anomaly patterns at 100 m depth suggests the onset of upwelling around 100 m depth by February/March. They also indicate the upwelled waters reaching 50 m depth by May and at the surface by about July. The seasonal structure, mixed layer topography and thermal anomaly fields together indicate the onset of upwelling in the northern regions after a lag of about 3 months. During June to September, the surface waters in the southern regions are cooled by 3-4°C under the influence of upwelling, while in the northern regions

they are cooled by about 2°C due to summer monsoonal cooling. Between Cochin and Karwar, the upwelling is noticed to weaken during August to September and revive during September to October. Generally, upwelling is observed to cease by either September or October.

Upwelling rates are found to be 20-30 m/month in the southern regions and 17-25 m/month in the northern regions. Upwelling is noticed to extend to about 400 km off the shelf between Cochin and Karwar and to about 200 km, north of Ratnagiri.

The coexistence of coastal downwelling and offshore upwelling along the west coast of India during winter is clearly indicated in the mixed layer topography and thermal anomaly distribution. During southwest monsoon, they are found to interchange their positions. During the active period of these processes, the lateral gradients are strengthened.

During the active period of upwelling, a maximum cooling of 8 to 9°C is produced at 100 m depth, while during sinking a maximum warming of 7°C is noticed. Further, the mixed layer is confined to 10 m depth during upwelling, while it extends to 130 m during sinking. These two features indicate the strength of these processes. In the transition periods of these two processes i.e., March and October/ November, the mixed layer topography and thermal anomaly patterns depict a series of ridges and troughs.

In general, the thermal structure in the coastal waters suggests a bimodal oscillation, while that in the deep exhibits unimodal signature with a few exceptions. The thermocline regime south of Cape Comorin and Sri Lanka exhibits prominent oscillations with periods of 2 to 4 months, probably induced by Rossby/Kelvin waves.

The short-term thermal fields reflect the prominent long-period ($>$ 12 hours) and short-period ($<$ 12 hours) internal waves in the thermocline. The long-period internal waves show a range of periods from 9 to 25 hours with an average period of 15 hours, comparable to semi-diurnal period. These waves seem to have maximum heights of 40 m in the Arabian Sea (17°N, 71°E) and 30 m in the Bay of Bengal (14°N, 89°E) with a mean height of 15 m. They propagate with speeds of 83 cm/s at 50 m depth in the Arabian Sea and 134 cm/s at 70 m depth in the Bay of Bengal, with respective wavelengths of 45 and 77 km. The distribution of their amplitudes in the depth regime suggests the nature of first order internal waves.

The short-period internal waves exhibit periods from 10 to 120 minutes with an average of 20 minutes off Cochin and 55 minutes off Karwar. They are associated with wave heights upto about 10 m with a mean height of about 6 m. The internal wave speeds correspond to 38 cm/s in the shelf waters off Cochin and 98 cm/s in the deep waters off Cochin and Karwar. At these stations, the respective wavelengths are 0.4, 1.0 and 3.0 km. The Brunt-Vaisala Frequencies of these internal wave fields show a frequency range of 10-28 cph equivalent to periods of 6 to 2 minutes. These profiles suggest the nature of second order

internal wave fields in the shelf waters off Cochin and first order internal waves in the deep waters off Cochin and Karwar.

The Fast Fourier Transform (FFT) analysis of time series data at these places suggest a 20 minute mode of oscillations in the short-period, and a 240 minute mode of oscillations in the long-period internal wave fields. The similarity in the harmonic pattern among the spectra of the observed internal wave fields, winds, and surface atmospheric pressure/tide suggests the tidal force as a possible generating agency for the internal waves of tidal frequency, and local wind forcing for the internal waves of non-tidal frequencies.

The present study has certain limitations. The mean temperatures are based on an uneven distribution of data in space and time. Some of the areas, although having a full annual coverage, do not have adequate data for some months. Some portions in the area under study are having data gaps. The consistency and the coherence in the internal wave characteristics could not be examined due to non-availability of adequate data sets. The influence of generating mechanisms other than winds and tides on the observed internal wave fields could not be ascertained due to lack of data.

However, a comprehensive and intensive data collection can overcome these limitations. The deployment of moored buoys with arrays of sensors at different depths at some important locations for about

5 to 10 years can provide intensive and extensive data sets. This strong data base can afford to address the short-term and seasonal variability of thermal field and understand in detail the individual and collective influences of various physical and dynamical mechanisms responsible for such variability.

REFERENCES

Anjaneyulu, T.S.S. (1980). A study of the air and sea surface temperatures over the Indian Ocean. Mausam, 31 : 551-560.

* Anon., (1944). World Atlas of sea surface temperatures. US Navy Hydrographic Office, Hydrographic Office Publ. No.225.

* Anon., (1950). Atlas of surface currents - Indian Ocean. U.S.Navy Hyd. Office.

Anon., (1952). Koninklijk Nederlands Meteorologisch Instituut, Indische oceaan oceanographische on Meteorologische gegevens. 2nd Edn., Publ. No.135, 31 pp, 24 charts.

Anon., (1978). World Ocean Atlas. Volume 2, Atlantic and Indian Oceans. Pergamon Press, 306 pp.

Antony, M.K., C.S. Murty, G.V. Reddy and K.H. Rao (1985). Subsurface temperature oscillations and associated flow in the western Bay of Bengal. Estuarine, Coastal Shelf Sci., 21 : 823-834.

Banse, K. (1959). Upwelling and bottom trawling. J. mar. biol. Ass. India, 1 : 33-49.

Banse, K. (1971). Hydrography of the Arabian Sea shelf of India and Pakistan and effects of demersal fishes. Deep-Sea Res., 15 : 45-79.

Basil Mathew (1982). Studies on upwelling and sinking in the seas around India. Ph.D. Thesis, University of Cochin. 159 pp.

Brekhovskikh, L.M. (1975). Short-period internal waves in the sea. J. Geophys. Res.,80: 856-864.

Briscoe, M.G. (1975a). Internal waves in the oceans. Rev. Geophys. Space Phys., 13 : 591-598.

Briscoe, M.G. (1975b). Preliminary results from the trimoored internal wave experiment (IWEX). J. Geophys. Res., 80 : 3872-3884.

* Carruthers, J.N. and S.S. Gogate (1959). Shoreward upslope of the layer of minimum oxygen off Bombay : its influence on marine biology especially fisheries. Nature, 183 : 1084-1087.

* Chacko, P.I. (1956). Surface temperatures of the coastal waters of Madras state during 1949-'54. Science and Culture, 21 : 458-459.

Colborn, J.G (1975). The thermal structure of the Indian Ocean. The University Press of Hawai, Honolulu, 161 pp.

Defant, A (1961). Physical Oceanography - Vol. II. Pergamon Press, Oxford, 571 pp.

Duing, W (1970). The monsoon regime of the currents in the Indian Ocean. East-West Center Press, Honolulu, 67 pp.

Duing, W. and A. Leetma (1980). Arabian Sea cooling : A preliminary heat budget. J. Phys. Oceanogr., 10 : 307-312.

* Ekman, V.W. (1904), On dead water. Scientific results of the Norwegian North Polar Expedition, 1893-1896., 5 : 1-152.

Federov, K.N. (1978). The thermohaline fine structure of the ocean, Pergamon Press, Oxford, 168 pp.

Fofnoff, N.P. (1969). Spectral characteristics of internal waves in the ocean. Deep - Sea Res., 16 (suppl.) : 58-71.

* Gade, H.G. and E. Ericksen (1969). Notes on the internal tide and short-periodic secondary oscillations in the Strait of Gibraltar Universitetet i Bergen, Arbok Mat. Naturvit. ser., 9 : 24.

* Galle, P.H. (1924). Climatology of the Indian Ocean.

Ganapati,P.N. and V. S. Murty (1954). Salinity and temperature variations of the surface waters off Visakhapatnam coast. Andhra University Memoirs, 1 : 125-142.

Halpern, D. (1971). Observations on short-period internal waves in Massuchussets Bay. J. Mar. Res., 29 : 116-132.

Hasternath, S. and P.J. Lamb (1979). Climatic Atlas of the Indian Ocean. Part I - Surface Climate and Atmospheric Circulation; Part II - The Oceanic Heat Budget, University of Wisconsin Press, Wisconsin, 19 pp, 97 charts; 17 pp, 84 charts and 20 figures.

Jayaraman, R. and S. S. Gogate (1957). Salinity and temperature variations in the surface waters of the Arabian Sea off the Bombay and Saurashtra coasts. Proc. Indian Acad. Sci., 45 : 151-164.

John. R.A., H.M. Byrne, J.R. Proni and R.L. Charnell (1975). Observations of oceanic internal and surface waves from the Earth Resources Technology Satellite. J. Geophys. Res., 80 : 865-871.

Joseph, P.V. and P.V. Pillai (1986). Air-sea interaction on a monsoonal scale over North Indian Ocean - Part II: Monthly mean atmospheric and oceanic parameters during 1972 and 1973.Mausam, 37 : 159-168.

Knox, R.A. (1981). Time variability of Indian Ocean equatorial currents. Deep - Sea Res., 28 : 291-295.

* Krauss, W. (1959). Uber meteorologisch bedingte interne wellen auf einer dauerstation sudwestlich islands. Dtsch. Hydrogr. Zeit., Erganzungsheft Reihe B (4°), 3 : 55-58.

* Krauss, W. (1967). Interaction between surface and internal waves in shallow water. Navy Electronics Lab. Rept. 1432, 28.

Laevastu, T. and I. Hela (1970). Fisheries Oceanography. Fishing News (Books) Ltd., London : 238 pp.

La Fond, E.C. (1954a). On upwelling and sinking off the east coast of India. Andhra University Memoirs, 1 : 117-121.

La Fond, E.C. (1954b). Environmental factors affecting the vertical thermal structure of the upper layers of the sea. Andhra University Memoirs, 1 : 94-101.

La Fond, E.C. (1958). Oceanographic Studies in Bay of Bengal. Proc. Indian Acad. Sci., 46 : 1-46.

La Fond, E.C. (1961). Internal wave motion and its geological significance. Commemorative volume for Prof.C. Mahadevan. Publication in Osmania, Hyderabad, 61-77.

La Fond, E.C. (1966). Internal waves. The Encyclopedia of Oceanography. Reinhold Pub. Corp., New York, 402-408.

La Fond, E.C. and K.G. La Fond (1968). Studies on oceanic circulation in the Bay of Bengal. Bull. Nat. Inst. Sci. India, 38 : 164 -183.

La Fond, E.C. and K.G. La Fond (1971). Thermal structure through the California front, July 1971. NUCTP, 224.

La Fond, E.C. and C. Purnachandra Rao (1954). Vertical oscillations of tidal periods in the temperature structure of the sea. Andhra University Memoirs, 1 : 109-116.

*
Larsen, L.H. (1969). Internal waves and their role in mixing the upper layers of the ocean. The Trend in Engineering, University of Washington, Washington, 21 : 8-11 and 19.

Levine, M.D. (1983). Internal waves in the ocean. Rev. Geophys. Space Phys., 21 : 1206-1216.

Lonkar, S.D. (1971). Seasonal variations in the hydrographical conditions in the coastal waters of Ratnagiri. Mahasagar, 4 : 101-107.

Luyten, R.J. and D.H. Roemmich (1982). Equatorial currents at semi-annual period in the Indian Ocean. J. Phys. Oceanogr., 12 : 406-413.

Maeda, A. (1974). A description of short-period temperature fluctuations in the upper ocean. J. Oceanogr. Soc. Japan, 30 : 121-136.

McPhaden, M.J. (1982a). Variability in the central equatorial Indian Ocean Part I : Ocean dynamics. J. Mar. Res., 40 : 157-176.

McPhaden, M.J. (1982b). Variability in the central equatorial Indian Ocean Part II : Oceanic heat and turbulent energy balances. J. Mar. Res., 40 : 403-419.

Midorikawa, K. (1977). The effect of tidal currents on internal waves. J. Oceanogr. Soc. Japan, 33 : 311-319.

Monin, A.S., V.M. Kamenkovich and V.G.Kort (1974). Variability of the oceans. Wiley Interscience, New York, 237 pp.

Munk, W. (1981). Internal waves and small-scale processes. Evolution of Physical Oceanography, MIT Press, Massachusetts, 264-290.

Murty, C.S. and V.V.R.Varadachari (1968). Upwelling along the east coast of India. Bull. Nat. Inst. Sci. India, 38 : 80-86.

Murty, V.S.N., D.P.Rao and J.S. Sastry (1983). The lowering of sea surface in the east central Arabian Sea associated with a cyclone. Mahasagar, 16 : 67-71.

Narayana Pillai, V., P.K. Vijayarajan and A. Nanda Kumar (1980). Oceanographic investigations along the southwest coast of India (1976-'78). Field document by F.A.O of United Nations, Rome, 51 pp.

Noble, A. (1968). Studies on sea water off North Kanara coast. J. mar. biol. Ass. India, 10 : 197-223.

Panikkar, N.K. and R. Jayaraman (1966). Biological and oceanographic differences between the Arabian Sea and the Bay of Bengal as observed from the Indian Ocean. Proc. Indian Acad. Sci., 14-B : 231-240.

Patil, M.R. and C.P. Ramamirtham (1962). Hydrography of the Laccadives offshore waters - A study of the winter conditions. J. mar. biol. Ass. India, 4 : 159-169.

Patil, M.R., C.P. Ramamirtham, P. Udayavarma, C.P.A. Nair and P. Myrland (1964). Hydrography of the west coast of India during the pre-monsoon period of the year 1962. J.mar. biol. Ass. India, 6 : 151-164.

Perry, B.R. and G.R. Schimke (1965). Large amplitude internal waves observed off the Northwest coast of Sumatra. Geophys. Res., 20 : 2319-2324.

Pickard, G.L. and W.J. Emery (1982). Descriptive Physical Oceanography - Introduction. Pergamon Press, Oxford, 249 pp.

*
Pollard, R.T. (1972). Properties of nearsurface inertial oscillations. Woods Hole Oceanogr. Inst. Contrib., 2736, 44.pp.

Qasim, S.Z. (1982). Oceanography of the northern Arabian Sea. Deep - Sea Res., 29 : 1041-1068.

Ramam, K.V.S., P.G.K. Murthy and C.K.B. Kurup (1979). Thermal structure variation in the Arabian Sea (May-July 1973). Mausam, 30 : 105-112.

Ramamirtham, C.P. and R. Jayaraman (1959-60). Hydrography of the shelf waters off Cochin. J. mar. biol. Ass. India, 2 : 199-207.

Ramamirtham, C.P. and D.S. Rao (1973). On upwelling along the west coast of India, J. mar. biol. Ass. India, 15 : 306-317.

Ramasastry, A.A. (1959). Watermasses and the frequency of sea water characteristics in the upper layers of the southeast Arabian Sea. J. mar. biol. Ass. India., 1 : 233-246.

Ramasastry, A.A. (1963). Surface water characteristics in the Bay of Bengal off Madras. Indian J. Met. Geophys., 14 : 64-67.

Ramasastry, A.A. and P. Myrland (1959). Distribution of temperature, salinity and density in the Arabian Sea along the south Malabar coast (South India) during the post-monsoon season. Indian J. Fish., 6 : 223-255.

Ramesh Babu, V., L.V.G.Rao, M.J. Varkey and P. Udayavarma (1976). Temperature distribution of the upper layers of northern and eastern Arabian Sea during Indo-Soviet monsoon experiment. Indian J. Met. Geophys., 27 : 291-293.

Ramesh Babu, V., M.J. Varkey, V. Kesavadas and A.D. Gouvia (1980). Watermasses and general hydrography along west coast of India during early March. Indian J. Mar. Sci., 9 : 82-89.

Ramesh Babu, V. and J.S. Sastry (1984). Summer cooling in the east central Arabian Sea - A process of dynamic response to the southwest monsoon. Mausam, 35 : 17-26.

Rao, D.P., R.V.N. Sarma, J.S. Sastry and K. Premchand (1976). On the lowering of the surface temperatures in the Arabian Sea with the advance of the southwest monsoon season. Proc. Symp. on tropical monsoons, Pune, 106-115.

Rao, L.V.G. and R. Jayaraman (1966). Upwelling in the Minicoy region of the Arabian Sea. Curr. Sci., 35 : 378-380.

Rao, L.V.G. and R. Jayaraman (1968a). Hydrographical features of the southern and central Bay of Bengal during transition period between winter and summer. Bull. Nat. Inst. Sci. India, 38 : 184-205.

Rao, L.V.G. and R. Jayaraman (1968b). Vertical distribution of temperature, salinity and density in the upper 500 m of the north equatorial Indian Ocean during northeast monsoon period. Bull. nat. Inst. Sci. India, 38 : 123-147.

Rao, L.V.G., Thomas Cherian, K.K. Varma and V.V.R. Varadachari (1974). Hydrographical features of the inner shelf waters along the central west coast of India during winter, spring and summer. Mahasagar, 7 : 15-26.

Rao, R.R. (1986). On the thermal response of upper eastern Arabian Sea to the summer monsoonal forcing during Monsoon-77. Mausam, 37 : 77-84.

Rao, R.R., P.G.K.Murthy, M.G. Joseph and K.V.S. Ramam (1981). On the space-time variability of ocean surface mixed layer characteristics of central and eastern Arabian Sea during Monsoon-77. International Conference on early results of FGGE and large-scale aspects of its monsoon experiments, GENEVA, 9 : 20-27.

Rao, R.R., D.S. Rao., P.G.K.Murthy and M.X.Joseph (1983). A preliminary investigation on the summer monsoonal forcing on the thermal structure of upper Bay of Bengal during MONEX-79. Mausam, 34 : 239-250.

Rao, T.S.S. and V.C. Rao (1962). Studies on the diurnal variations in the hydrobiological conditions off Waltair Coast. J. mar. biol. Ass. India, 4 : 23-43.

Robert, P., (1981). On the use of Doppler sonar for internal wave measurements. Deep - Sea Res., 28 : 269-289.

Roberts, J., (1975). Internal gravity waves in the ocean. Marcel Dekker, Inc., New York, 263 pp.

Robinson, K., R.A. Bauer and E. H. Schroeder (1979). Atlas of North Atlantic-Indian Ocean monthly mean temperatures and mean salinities of the surface layer. Dept. of Navy, Washington, D.C., 20 pp 213 charts.

Sankaranarayanan, V.N. and S.Z. Qasim (1968). The influence of some hydrographical factors on the fisheries of Cochin area. Bull. Nat. Inst. Sci. India, 38 : 846-853.

Sastry, J.S. and R.S. D'Souza (1970). Oceanography of Arabian Sea during southwest monsoon - part I : Thermal structure. Indian J. Met. Geophys., 21 : 367-382.

Sastry, J.S. and V. Ramesh Babu (1985). Summer cooling of the Arabian Sea - a review. Proc. Indian Acad. Sci., 94 : 117-128.

Schott, F. (1971a). On horizontal coherence and internal wave propagation in the North Sea. Deep - Sea Res., 18 : 291-307.

Schott, F. (1971b). Spatial structure of inertial period motions in a two layered sea based on observations. J. Mar. Res., 29 : 85-102.

*
Sewell, R.B.S. (1929). Temperature and salinity of the surface waters of the Bay of Bengal and Andaman Sea with reference to the Laccadive Sea. Mem. Oceanogr. Soc. Bengal, 9 : 207-355.

Sharma, G.S. (1966). Thermocline as an indicator of upwelling. J. mar. biol. Ass. India, 8 : 8-19.

Sharma, G.S. (1968). Seasonal variations of some hydrographic properties of the shelf waters off the west coast of India. Bull. Nat. Inst. Sci. India, 38 : 263-276.

Sharma, G.S. (1978). Upwelling off the southwest coast of India. Indian J. Mar. Sci., 7 : 209-218.

Shetye, R.S. (1984). Seasonal variability of temferature field off southwest coast of India. Proc. Indian Acad. Sci., 93 : 399-411.

Siedler, G. (1971). Vertical coherence of short-periodic variations. Deep - Sea Res., 18 : 179-191.

Turner, J.S. (1981). Small-scale mixing processes. Evolution of Physical Oceanography, MIT Press, Massachusetts, 236-258.

Varadachari, V.V.R. and G.S. Sharma (1967). Circulation of the surface waters in the North Indian Ocean. J. Indian Geophys. Uni., 4 : 61-73.

Varma, K.K., V. Kesavadas and A. Gouvia (1980). Thermocline structure and watermasses in the northern Arabian Sea during February-April. Indian J. Mar. Sci., 9 : 148-155.

Woods, J.D. and R.L. Wiley (1972). Billow turbulence and ocean micro-structure. Deep - Sea Res., 19 : 87-121.

Wooster, S., M.B.Schaefer and M.K. Robinson (1967). Atlas of the Arabian Sea for fishery oceanography. University of California, California, 37 pp, 140 figures.

Wunsch, C. (1977). Response of an equatorial ocean to a periodic monsoon. J. Phy. Oceanogr., 7 : 497-511.

Wyrtki, K. (1971). Oceanographic atlas of the international Indian Ocean expedition, National Science foundation, Washington,D.C., 63 pp, 458 charts/figures.

Zalkan, R.L. (1970). High frequency internal waves in the Pacific Ocean. Deep - Sea Res., 17 : 91-108.

Ziegenbien, J. (1969). Short internal waves in the Strait of Gibraltar. Deep - Sea Res., 16 : 479-487.

Ziegenbien, J. (1970). Spatial observations of short internal waves in the Strait of Gibraltar. Deep - Sea Res., 17 : 867-875.

---

* Not referred in original.